ISSN 2433-2232(Online)
JAXA-SP-22-003

宇宙航空研究開発機構特別資料
JAXA Special Publication

Eighth Aerodynamics Prediction Challenge （APC-8）

開催日：2022年6月29日
開催場所：アイーナ いわて県民情報交流センター

2022年12月

宇宙航空研究開発機構
Japan Aerospace Exploration Agency

目次

Aerodynamics Prediction Challenge (APC) 企画趣意書

1983 年に初回が開催された航空宇宙技術研究所(当時)の航空機計算空気力学シンポジウムが，我が国の航空宇宙分野における計算空気力学技術の発展を牽引したことは論じるまでもありません。第 1 回のシンポジウム論文集(NAL SP-1)の巻頭言では，当時の武田峻所長が「各分野の研究者や技術者の皆様に研究発表と意見交換の場を提供し，それによって航空機設計技術の発展に寄与する」と記しています。その意思は 30 年以上経過した現在においても航空宇宙数値シミュレーション技術シンポジウム(ANSS)に引き継がれています。しかし，膨大な技術情報へのアクセスを容易に実現するインターネットの発達は，学生や研究者と民間技術者の交流の機会を減少させ，近年の計算空気力学研究が航空機設計開発現場の求める研究課題や方向性を見失う一因になっているのではないかと危惧されます。

今日の計算空気力学手法は，80 年代には想像できなかった計算機ハードウェアの著しい発展と数々の新しい計算技術に支えられ，航空機設計開発に不可欠なツールと認識されるまでに至りました。しかし一方，計算空気力学手法の成熟度が高まるに連れて，定常流れ場に対する計算空気力学手法はある種のスタンダードが認知浸透し，設計開発現場では宇宙航空研究開発機構(JAXA)の標準コードや商用コードの活用も進められるなど，計算空気力学研究に停滞感が出てきているのも事実です。計算空気力学の停滞は，空気力学研究のパートナーである風洞技術の高度化にも影響を与えかねません。この停滞感を打破し，いま一度新たな高みを目指すには，航空機設計開発現場の求める研究課題や方向性が具体的に示されることが重要だと思われます。

この APC と名付けられたワークショップでは，実機開発に活用されている計算空気力学課題や将来の利用が期待されるテーマを選定し，JAXA で取得された風洞試験データとの詳細な比較を行うことによって，計算空気力学ならびに風洞技術の発展に求められる新たな課題を抽出しその解決を共同で模索することを目指します。APC 参加者による新たな課題への挑戦は，計算空気力学研究や風洞技術開発を活性化させ，機会の減少が懸念される産官学交流を促し，最終的には我が国の航空宇宙産業の発展と欧米に次ぐ第 3 極としてのプレゼンス向上に貢献することが期待されます。産官学がそれぞれの立場から APC を活用していただくことを望んでいます。

澤田恵介，APC 有識者会議　前代表（全体）
今村太郎，APC 有識者会議　現代表（全体）
青山剛史，APC 有識者会議　代表（CFD）
浜本滋，　APC 有識者会議　代表（風洞試験）

Eighth Aerodynamics Prediction Challenge (APC-8) の開催について

APC-6 と APC-7 はコロナの影響でオンライン開催となりましたが、APC-8 は久しぶりの対面での開催となりました。現地で皆様にお会いできたこと、皆様の発表を聴けたこと、皆様と議論できたこと、コロナの前は普通にやっていたことですが、以前と同じように APC を開催できたことを大変うれしく思いました。

APC-8 では，JAXA，大学，産業界から 7 件の発表があり，約 90 人の方にご参加いただきました。APC-8 の開催にご協力いただいた関係者の方々に深く感謝申し上げます。APC-8 の課題は，高揚力装置形態の CRM-HL（Common Research Model – High Lift）における低速・高迎角流の予測を対象としました。航空機の認証では、飛行試験で高揚力装置形態の失速を証明することが求められます。理想的には、CFD で失速（最大揚力）を予測しながら形状設計を行い、想定通りに飛行試験で再現することが望ましいとされています。しかし、現状の CFD には、剥離流れの予測精度や複雑形状の取り扱いなどに課題があり、その課題解決に向けた取り組みが必要です。そこで、APC-8 では、参加者が解析した結果を分析することで、高揚力装置形態における CFD の評価を行うとともに、失速予測に向けた今後の方向性を議論することを目的として実施しました。

本資料では，APC-8 の成果を公開するため，JAXA 特別資料として出版します。JAXA，大学，産業界を含む All-Japan のチームで，CFD の難題に挑んだ成果です。参加者全員の発表資料と集計データを掲載しました。これらの成果が，今後の CFD や空気力学研究の発展に寄与することを期待しています。

APC 有識者会議

Aerodynamics Prediction Challenge 有識者会議　委員名簿

代表	今村太郎	東京大学大学院 工学研究科 航空宇宙工学専攻
代表	青山剛史	JAXA　航空技術部門　航空機ライフサイクルイノベーションハブ
代表	浜本滋	JAXA　航空技術部門　設備技術研究ユニット
委員	松島紀佐	富山大学　工学部 シニアアドバイザー
委員	佐々木大輔	金沢工業大学　工学部　航空システム工学科
委員	吉本稔	三菱重工業（株）総合研究所　流体研究部　流体第三研究室
委員	上野陽亮	川崎重工業（株）航空宇宙ｼｽﾃﾑｶﾝﾊﾟﾆｰ　技術統括部 技術開発部 空力技術課
委員	中北和之	JAXA　航空技術部門　航空環境適合イノベーションハブ
委員	村山光宏	JAXA　航空技術部門　航空プログラムディレクタ付
委員【事務局】	香西政孝	JAXA　航空技術部門　設備技術研究ユニット
委員【事務局】	橋本敦	JAXA　航空技術部門　航空機ライフサイクルイノベーションハブ

APC-8 プログラム

（2022 年 6 月 29 日第 54 回流力講演会／第 40 回 ANSS 内で開催）

14:40-15:00	APC-8 の課題説明 橋本 敦（JAXA）
15:00-15:20	Scale-resolving simulations of the CRM high-lift configuration at high angles of attack, ザウナー マルクス，小島 良実，サンシカ アンドレア（JAXA），林 謙司（菱友システムズ），橋本 敦（JAXA）
15:20-15:40	scFLOW による CRM-HL の低速高迎角条件における空力特性予測 中島 吉隆，武田 直哉，田口 誠一（Hexagon）
15:40-16:00	TAS による CRM-HL の RANS 定常空力解析 古谷 龍太郎（菱友システムズ），村山 光宏，伊藤 靖（JAXA），田中 健太郎（菱友システムズ）
16:00-16:20	休憩
16:20-16:40	Cflow による CRM-HL の検証解析 山内 優果，安田 英将，澤木 悠太，上野 陽亮（川崎重工）
16:40-17:00	階層型直交格子と埋め込み境界法を用いた CRM-HL の空力予測 船田 雅也，今村 太郎（東大），菅谷 圭祐（JAXA）
17:00-17:20	APC-8 の集計結果 橋本 敦（JAXA）
17:20-18:00	ディスカッション

The 54th Fluid Dynamics Conference/ The 40th Aerospace Numerical Simulation Symposium
29th June 2022

APC-8の課題説明
Test cases of Eighth Aerodynamics Prediction Challenge (APC-8)

橋本 敦 (JAXA)
Hashimoto Atsushi(JAXA)

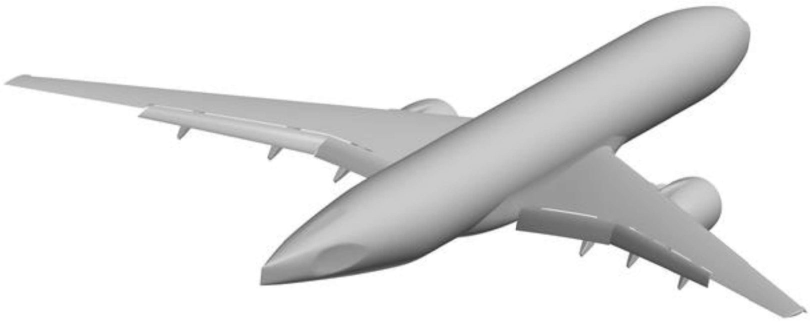

背景：デジタル認証（CbA）の研究

[1]CRM-HL資料 https://nari.arc.nasa.gov/tacp2021showcase/agenda/

- 新しい旅客機の認証取得には1～2千億円の費用が掛かっている[1]。飛行試験・地上試験を解析で代替することによって、機体の安全性と性能を向上しつつ、認証に必要な開発工数を削減することで、数百億円のコスト低下につながり、下記のような効果が得られる
  - 飛行試験期間の短縮（Boeingの目標：1年(現状)⇒半年(2023)⇒3か月(2026)）
  - フライト試験を経由しない新規技術/設計変更の導入
  - 飛行試験中の予期せぬ不具合の回避
  - 国際競争力の強化
- CbAにおける高揚力形態予測技術の重要性
  - エンベロープの中で認証取得に必要な項目の2/3は低速の飛行条件である。
  - 失速速度は低速特性の基本データであり、高揚力形態の最大揚力予測が最も重要であるが、流れの剥離現象が複雑なため予測が難しい。

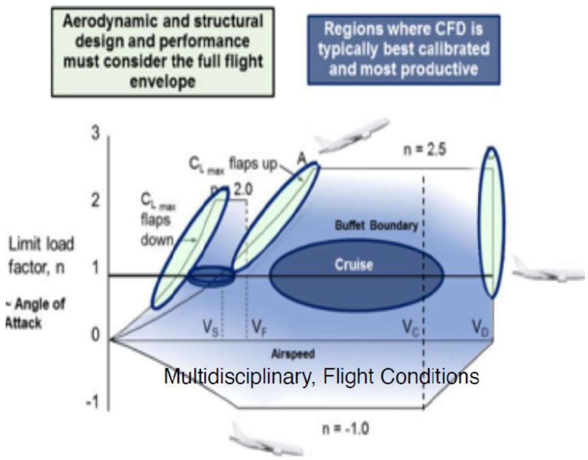

背景：デジタル認証（CbA）の研究

- 世界的に、安全で効率的な認証作業を推進するため、飛行試験を解析で代替する方向性が共有されており、AIAA等でCertification by Analysis(CbA)の国際コミュニティが形成され、認証に解析を使用する際のガイドラインを作成する活動が行われている。また、NASAにおいてもCbAに関する検討が行われ、その成果報告書が出版された。

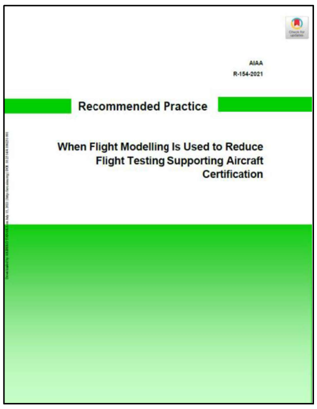
AIAA
R-154-2021
Recommended Practice
When Flight Modelling Is Used to Reduce Flight Testing Supporting Aircraft Certification

AIAAのCertification/Qualification by Analysis(CQbA) WGでは、航空機の適合性証明方法として、数値シミュレーションの活用を促進するため、製造メーカと認証機関の両方に使われるRecommended Practiceを出版（2021年4月）。Steering CommitteeはAirbus、Boeing、EASA、FAA、DLR、NASA。


Requirements for Aircraft Certification by Analysis
A 20-year Vision for Virtual Flight and Engine Testing

2021年5月にNASAが公開したCbAの報告書。BoeingとPratt & Whitneyの有識者により取りまとめられた。2040年におけるCbAのビジョン、それに向けたロードマップが示されている。

失速に関するレギュレーション

失速について耐空性審査要領では下記のように定められている
（米国の14 CFR Part25も同様）

□ 失速速度の選定

- 参照失速速度V_{SR}は、申請者が選定するものとする。(耐審2-3-2)

□ 失速の実証

- 失速は、直線飛行及び30度バンク旋回において行わなければならない。（耐審2-7-1）

□ 失速特性

- 飛行機が失速に達するまでは、異常な機首上げが起ってはならない。また、縦の操縦力は失速に至るまで及び失速中、正でなければならない。さらに操縦装置を通常に操作して失速をすみやかに防ぎ、また、失速から回復することができなければならない。（耐審2-7-2）

現状、飛行試験で実施しているこれらの証明を解析で代替するため、CFDで正確に失速を予測可能であることを証明する必要がある。その際に、世界的な標準模型であるCRM-HLで取得されたデータで風洞試験とCFDの信頼性を検証することが重要である。

※耐空性審査要領は下記からダウンロード可能です。
航空安全情報管理・提供システム https://www.asims.mlit.go.jp/

Grand Challenge

- AIAA CFD2030 Integration committeeでは、Low-speed wind-up turnをGrad Challengeとして設定。低速の高揚力装置形態で、高度を飛行速度を一定に保ったまま、迎角とバンク角を増やすマニューバであり、舵効きや操縦力の評価も必要になる。
- 高揚力装置形態における風洞試験による検証がファーストステップ。

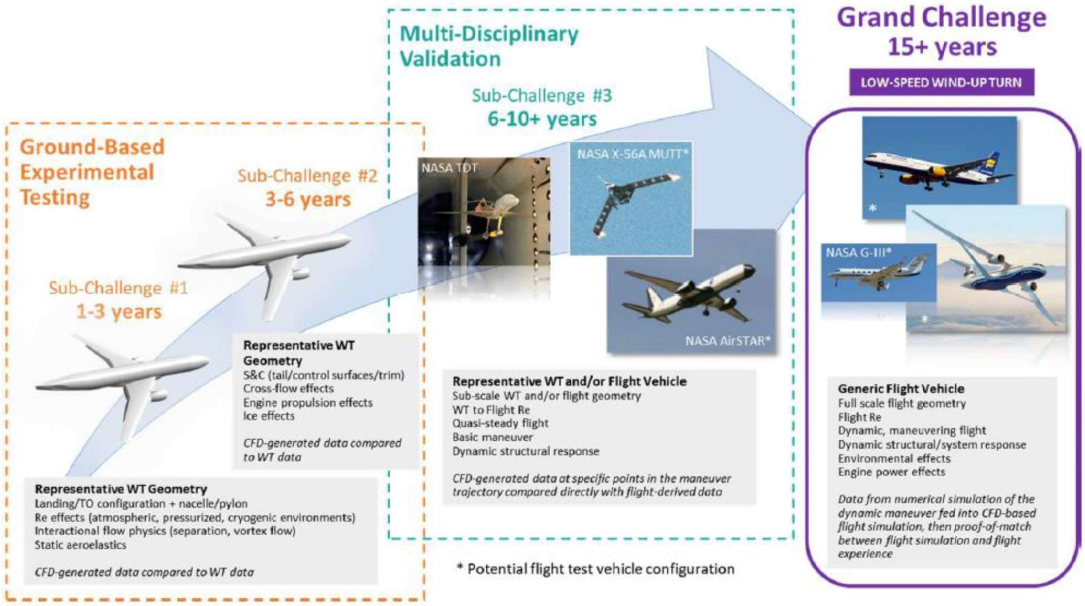

J. P. Slotnick, D. J. Mavriplis, "A Grand Challenge for the Advancement of Numerical Prediction of High Lift Aerodynamics," AIAA 2021-0955

5

Objective

- 航空機の認証では、飛行試験で高揚力装置形態の失速を証明することが求められる。理想的には、CFDで失速(最大揚力)を予測しながら形状設計を行い、想定通りに飛行試験で再現することが望ましい。
- しかし、現状のCFDには、剥離流れの予測精度や複雑形状の取り扱いなどに課題があり、その課題解決に向けた取り組みが必要である。
- そこで、APC-8では、参加者が解析した結果を分析することで、高揚力装置形態におけるCFDの評価を行うとともに、失速予測に向けた今後の方向性を議論することを目的とする。

6

Test cases of APC-8

- 課題1：3D CRM-HL、定常解析
- ~~課題2：3D CRM-HL、非定常解析~~
- 課題3：3D CRM-HL、フラップ舵角効果(任意)
- 課題4：2D CRM-HL、定常解析(任意)

※参加は上記の課題のうち一部のみでも可

7

Geometry

- 課題1～3：3D CRM-HL
  - 課題1～2： フラップ角 40°/37°(inboard/outboard)
  - 課題3： フラップ角 43°/40°(inboard/outboard)

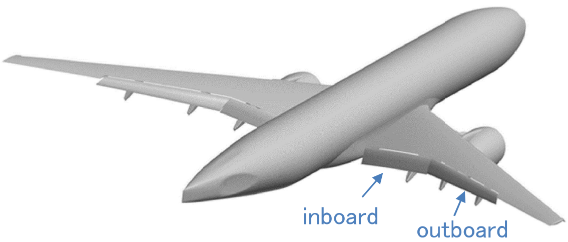

- 課題4：2D CRM-HL

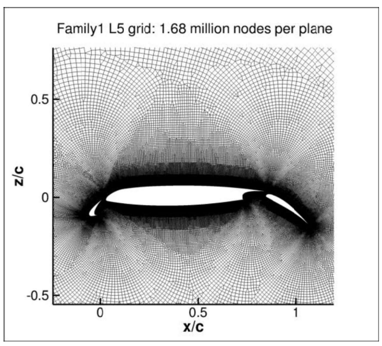

https://turbmodels.larc.nasa.gov/multielementverif_grids.html

8

Test cases of APC-8

- 課題1：3D CRM-HL、定常解析
  - M = 0.2, Re=5.49 × 10^6
  - AoA = 7.05, 17.05, 19.57, 21.47deg
- 課題2：3D CRM-HL、非定常解析
  - M = 0.2, Re=5.49 × 10^6
  - AoA = 7.05, 17.05, 19.57, 21.47deg
- 課題3：3D CRM-HL、フラップ舵角効果(任意)
  - M = 0.2, Re=5.49 × 10^6
  - AoA = 7.05, 17.05deg
- 課題4：2D CRM-HL、定常解析(任意)
  - M = 0.2, Re=5.00 × 10^6
  - AoA = 16deg

HLPW4
All Best-Practice Results
(03_GMGW3_HLPW4_RANS.pdf, p.17)

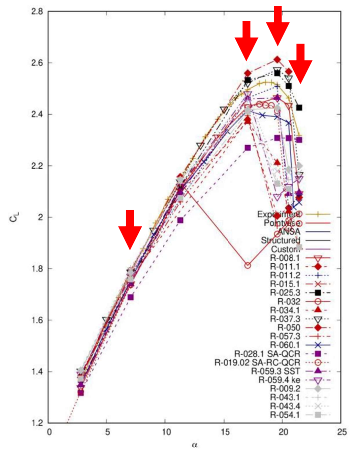

- 課題1-3はAIAA HLPW4の条件を参考に設定、課題4はNASA TMRの条件を参考に設定

格子、比較データ

- 課題1～3：
  - 格子は原則自由。HLPW4で公開されているを格子を使用可とし、JAXA格子（MEGG3D）を推奨。
  - 比較する実験データHLPW4で公開されているデータを使用。空力係数、圧力分布、オイルフローが公開されている。
- 課題4
  - 格子は原則自由。格子はNASA TMRで公開されているデータを使用可。
  - 実験データは無いので、NASA TMRで公開されている計算結果と比較

提出データ

課 題	項 目	迎 角	備 考
1	空力係数	全迎角	プロットデータ, 収束値 (圧力・摩擦で分解)
	表面C_p分布	全迎角	プロットデータ, 収束値 Slat,Main,Flap 8断面（位置はHLPW4参照）
	表面C_fコンター図	全迎角	画像データ, 収束値 視点2つ(HLPW4のVIEW1,5)
2	空力係数	全迎角	プロットデータ, 平均値 (圧力・摩擦で分解)
	表面C_p分布	全迎角	プロットデータ, 平均値 Slat,Main,Flap 8断面（位置はHLPW4参照）
	表面C_fコンター図	全迎角	画像データ, 平均値 視点2つ(HLPW4のVIEW1,5)
3	空力係数	全迎角	プロットデータ, 収束値 or 平均値 (圧力・摩擦で分解)
	表面C_p分布	全迎角	プロットデータ, 収束値 or 平均値 Slat,Main,Flap 8断面（位置はHLPW4参照）
	表面C_fコンター図	全迎角	画像データ, 収束値 or 平均値 視点2つ(HLPW4のVIEW1,5)
4	空力係数	16deg	F1～F7の格子収束 プロットデータ, 収束値 (圧力・摩擦で分解)
	表面C_p分布	16deg	F1～F7の格子収束 プロットデータ, 収束値 Slat,Main,Flap

11

まとめ

- CbAに関する動向及びCRM-HLを紹介した。
- APCの課題について、条件、形状/格子、比較データ、提出データを説明した。

12

謝辞

- 本資料を作成するにあたり、APC有識者会議の皆様には、課題設定に関するご助言をいただきました。菱友システムズの林謙司氏にはWebページ作成作業のご支援をいただきました。上記の関係者の皆様に、ここに感謝の意を表します。

13

APC Website

- Please see the APC website for more information
  - https://cfdws.chofu.jaxa.jp/apc/

14

Scale-resolving simulations of the CRM high-lift configuration at high angles of attack.

Zauner M., Kojima Y., Sansica A., Hayashi K., and Hashimoto A.
JAXA - Aircraft Lifecycle Innovation Hub

APC-8 Workshop

RANS ~~Scale-resolving~~ simulations of the CRM high-lift configuration at high angles of attack.

M. Zauner, Y. Kojima, A. Sansica, K. Hayashi, and A. Hashimoto
JAXA - Aircraft Lifecycle Innovation Hub

APC-8 Workshop

Agenda

- Introduction
- Methods
- Convergence
- Sensitivity of RANS simulations to initial conditions
- Sensitivity of RANS simulations to turbulence model

- Conclusions

Introduction

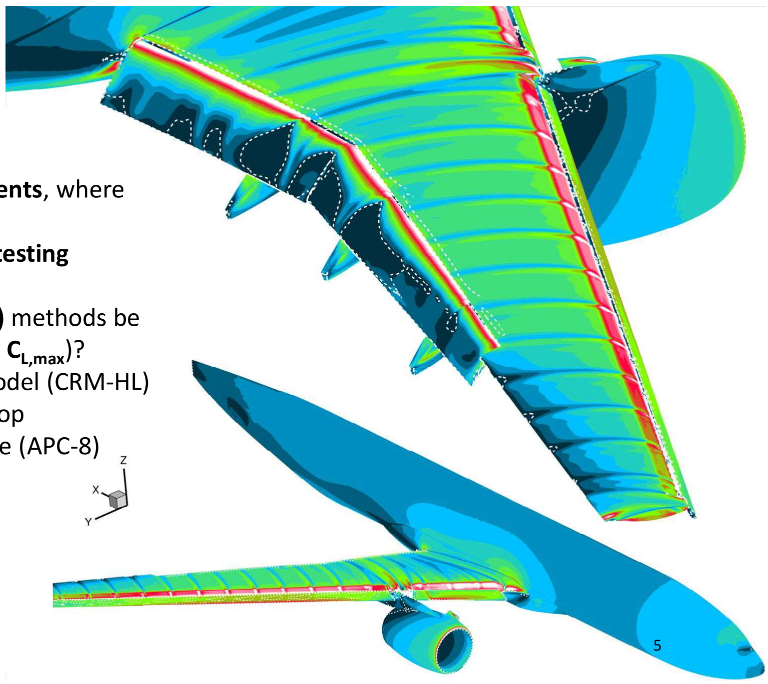

- **Low-speed** flight envelope **critical for safety.**
- More than **50% of commercial airplane accidents**, where high-lift devices are engaged.
- Status: Certification requires **extensive flight testing**
  - ➢ **EXPENSIVE!!!**
- Can **Reynolds-averaged Navier-Stokes (RANS)** methods be used to predict low-speed flight envelope (i.e. $\mathbf{C_{L,max}}$)?
  - ➢ High-lift version of Common Research Model (CRM-HL)
  - ➢ Fourth NASA High-Lift Prediction Workshop
  - ➢ Eighth Aerodynamics Prediction Challenge (APC-8)
- Nominal CRM-HL configuration
  - Flap/Slat angles:
  - AoA: varied
  - M = 0.2
  - Re = 5.5 million

Methods

Code: **JAXA's in-house code FaSTAR**

Set-up based on successful contribution to Drag-Prediction Workshop:

- Finite volume, unstructured
- HLLEW for inviscid fluxes
- U-MUSCL reconstruction
- GLSQ for gradient computation
- Limiter: van Leer type Hishida
- LU-SGS for time integration
- Turbulence models:
  - Submitted results: SA-noft2 and SA-noft2-R-QCR2000
  - Additional preliminary results: SA-noft2-R, SA-noft2-QCR2000, SST k-omega variants

Convergence Characteristics

Residuals in our case:
1) Compute L2-norm of residuals
2) Pick maximum value of entire domain

In case of no "perfect" convergence (machine-precision zero residuals):
Residuals can depend on numerical schemes and regions with maximum residuals do not necessarily coincide with the those relevant for industrial application. Also, residuals usually only compare two consecutive iterations, which **could understate the total change of results** over longer run times.

As an **alternative** we propose to assess **fluctuations** of **aerodynamic coefficients**, which are often used for evaluating simulation performances.

Definition of **convergence parameter ConvP**:

-> Statistics (root-mean-square and time average) of aerodyn. coefficients computed over 50000 iterations

-> ConvP= $\log([(C_{D,rms}/C_{D,avrg})^2 + (C_{L,rms}/C_{L,avrg})^2 + (C_{M,rms}/C_{M,avrg})$^2 $]^{0.5}$)

ConvP~-7 CL-jumps of 10-5

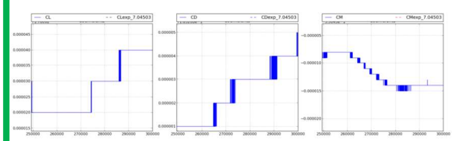

ConvP~-6 CL-oscillations of 10-4

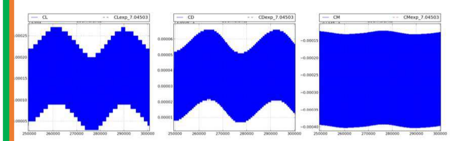

ConvP~-5 CL-oscillations of 10-3

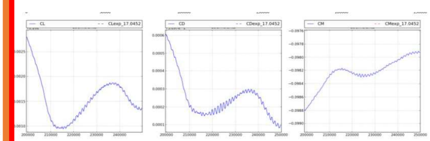

Convergence Characteristics

This convergence parameter allows us for the present test case to
- **separate convergence characteristics** of simulations for the current test case **more clearly**
- **evaluate convergence based on physical quantities**, which are of main interest for practical application

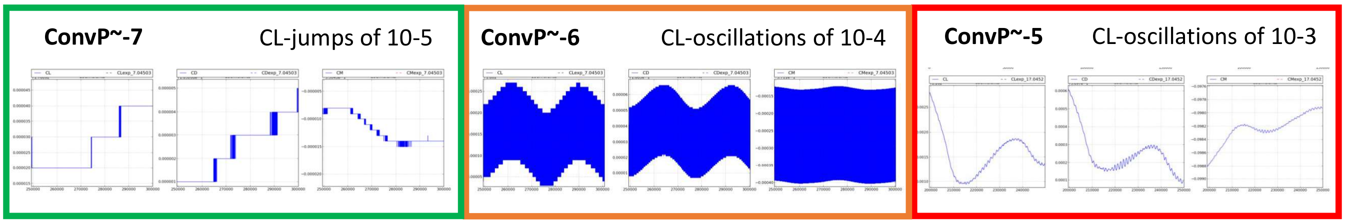

Cold-started RANS simulations

- Testing **different RANS turbulence models** (SA & SST), starting from uniform flow conditions
- **Lift** was significantly **underpredicted** for all simulations **near $C_{L,max}$**.
- **Poor performance** of our simulations compared to HLPW-4 results even at low AoA
- **SST models** show **no improvement**, but are **more expensive**

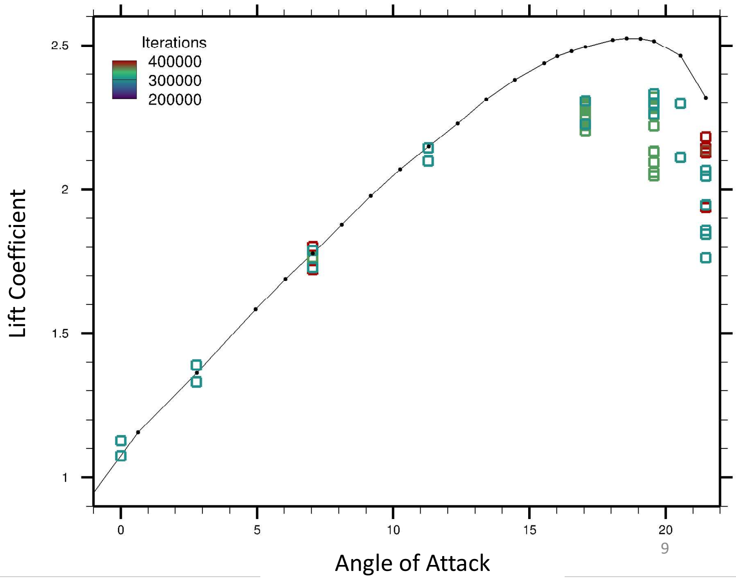

Warm-started RANS simulations

- **Selected RANS SA turbulence models**:
  - SA-noft2
  - SA-noft2-R-QCR2000
- Simulations were **restarted** from a solution obtained at AoA = 0 degrees, run for 10,000 iterations.
- **Significant improvement** compared to cold-started simulations. Results now compare well with HLPW-4 results.

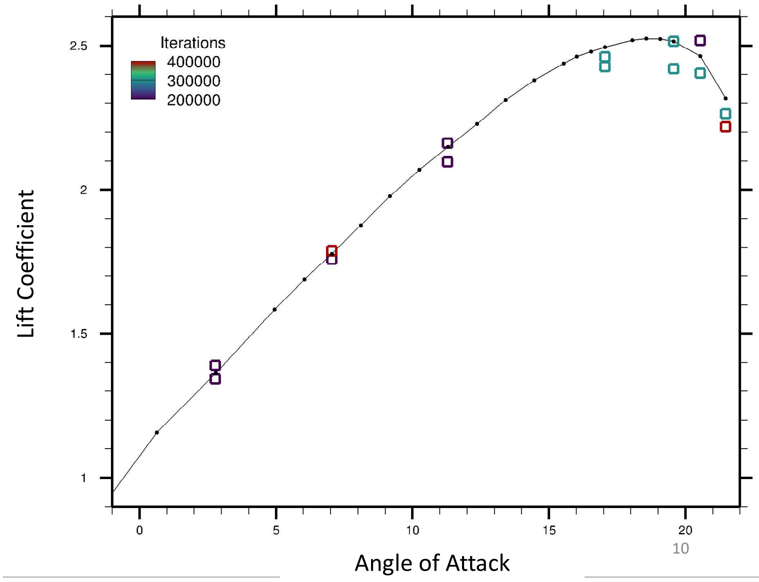

10

Results for SA-noft2

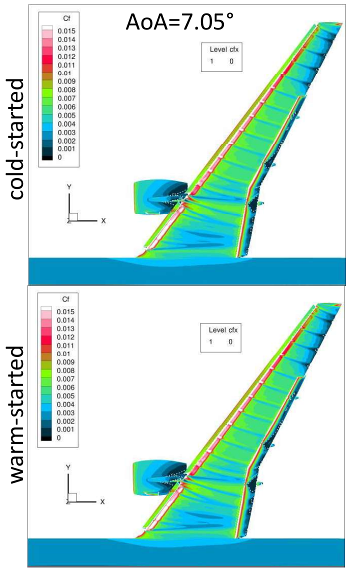

- Showing contours of skin-friction coefficient **Cf** for **cold- and warm-started** solutions using a **SA-noft2** model
- At low angles of attack results look qualitatively similar

11

Results for SA-noft2

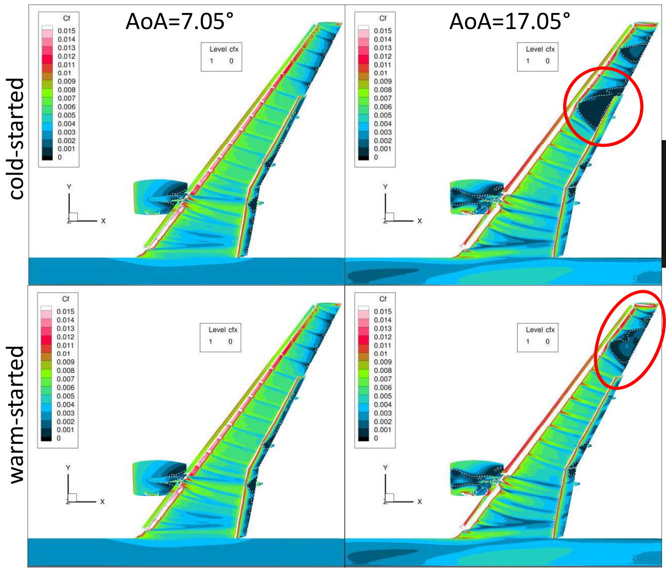

- Cold-start:
  Two regions of un-physical outboard flow separation

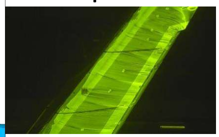

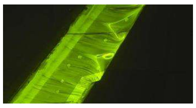

- Un-physical separation region near wing tip larger for warm-started simulation.

12

Results for SA-noft2

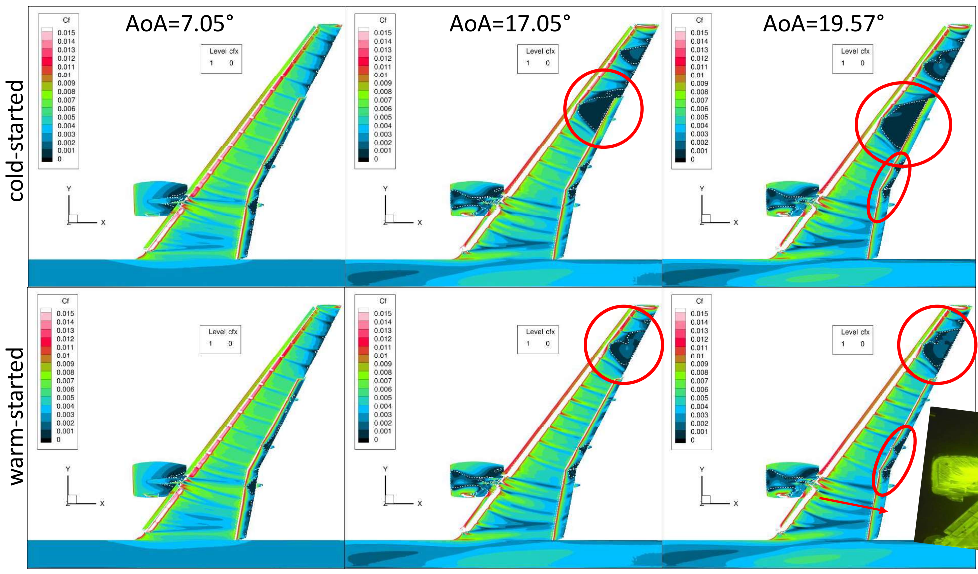

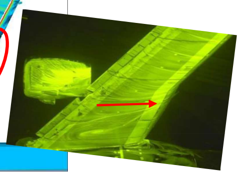

- **Cold-start**: **Un-physical flow separation** grows for further increasing AoA
- **Warm-start**: Out-board flow separation does not change much
- Both cases seem to **over-predict flow separation at the bend** of the wing
- **In-board flow is deflected towards the root**

13

Results for SA-noft2

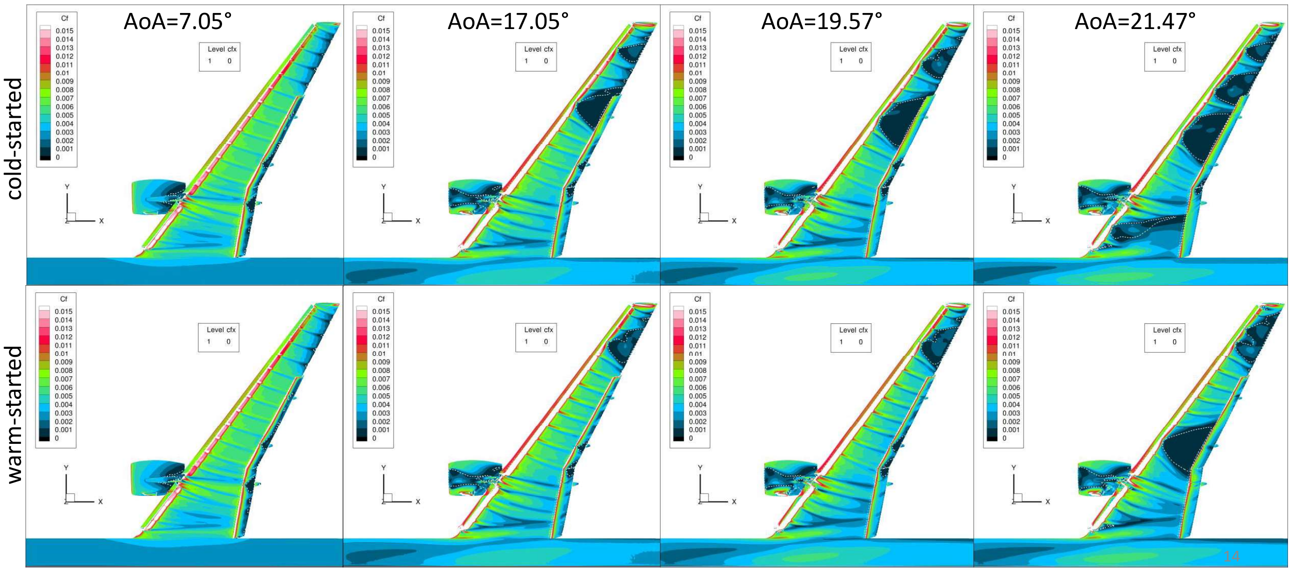

Results for SA-noft2

- **At 21.47°**, also warm-started simulations shows flow separation near bend.
- Large separation regions promote reattachment at the flaps.

- **Cold started** solutions show an **additional** region of out-board **separation.**

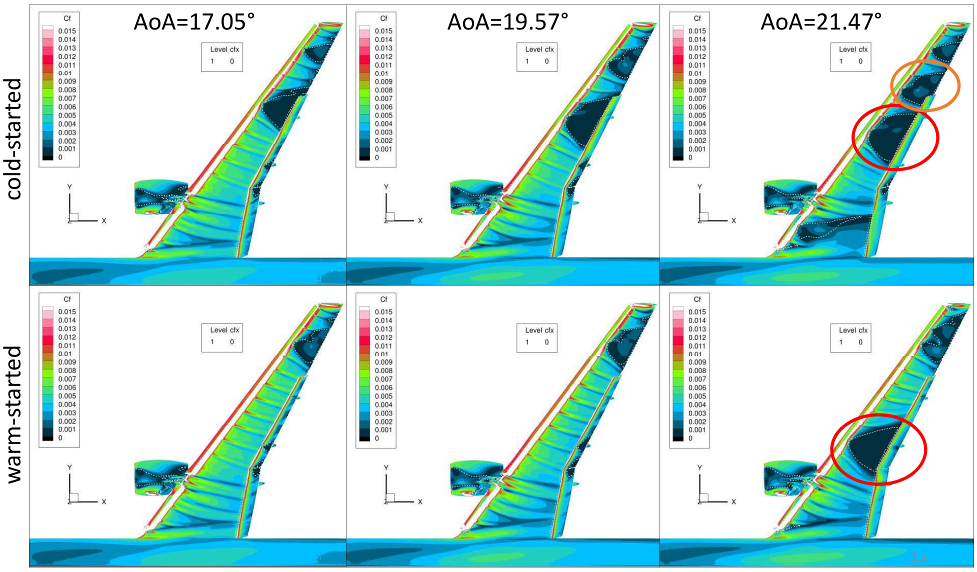

Cold vs Warm Start using SA-noft2

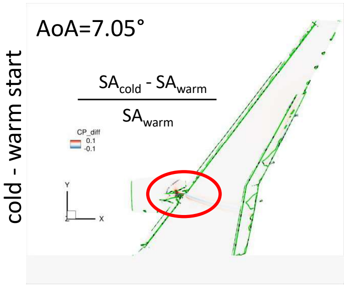

- Plots show relative **differences between Cp contours** of cold- and warm-started RANS simulations:
  - ❖ Blue: Cp of cold-started solutions < Cp of warm-started solution
  - ❖ Red: Cp of cold-started solutions > Cp of warm-started solution
  - ❖ Lower Cp -> increased velocities -> reduced separation
- **Green solid curves: warm-started**
- **Black dashed curves: cold-started**

- Minor differences near nacelle at 7.05°

16

Cold vs Warm Start using SA-noft2

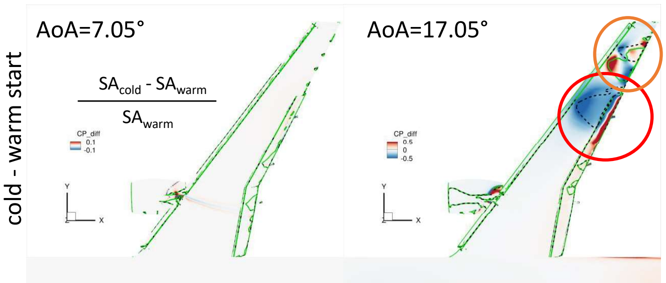

- **Additional separated flow** region for **cold-started** simulation well pronounced.
- Cp on out-board part of flap increased for cold-started case
- Reduced separated flow near wing-tip for cold-started simulation

- **Black dashed curves: cold-started**
- **Green solid curves: warm-started**

17

Cold vs Warm Start using SA-noft2

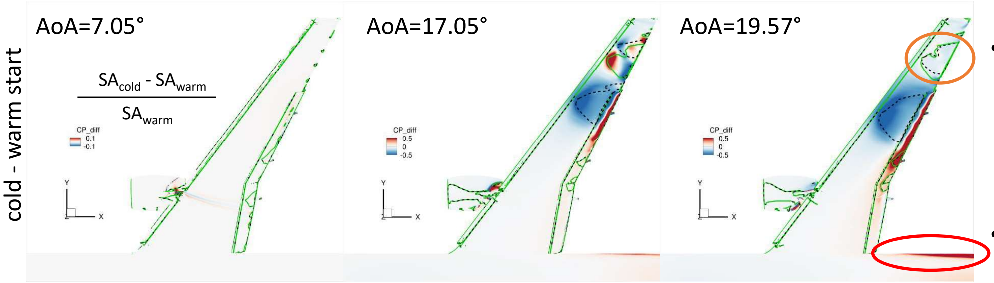

- Out-board region between both approaches similar
- More pronounced difference at fuselage behind the wing

- **Black dashed curves: cold-started**
- **Green solid curves: warm-started**

18

Cold vs Warm Start using SA-noft2

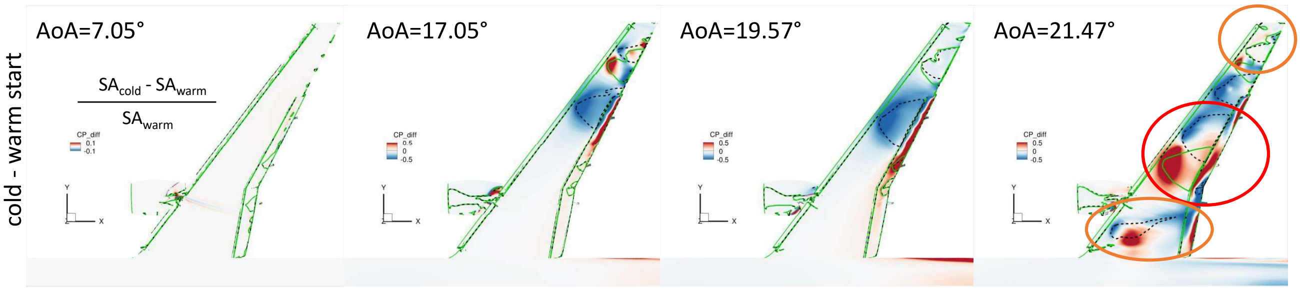

- Mid-span flow separation closer to the bend for warm-started simulation.
- In-board flow separation for cold-started simulation
- Out-board flow separation similar for both

- **Black dashed curves: cold-started**
- **Green solid curves: warm-started**

19

Cold/Warm start conclusions

- Flow separation tends to occur at lower angles of attack for cold-started simulations
- Is sensitivity to initial condition turbulence-model dependent?

Cold vs Warm start for SA-noft2 and with R-QCR corrections

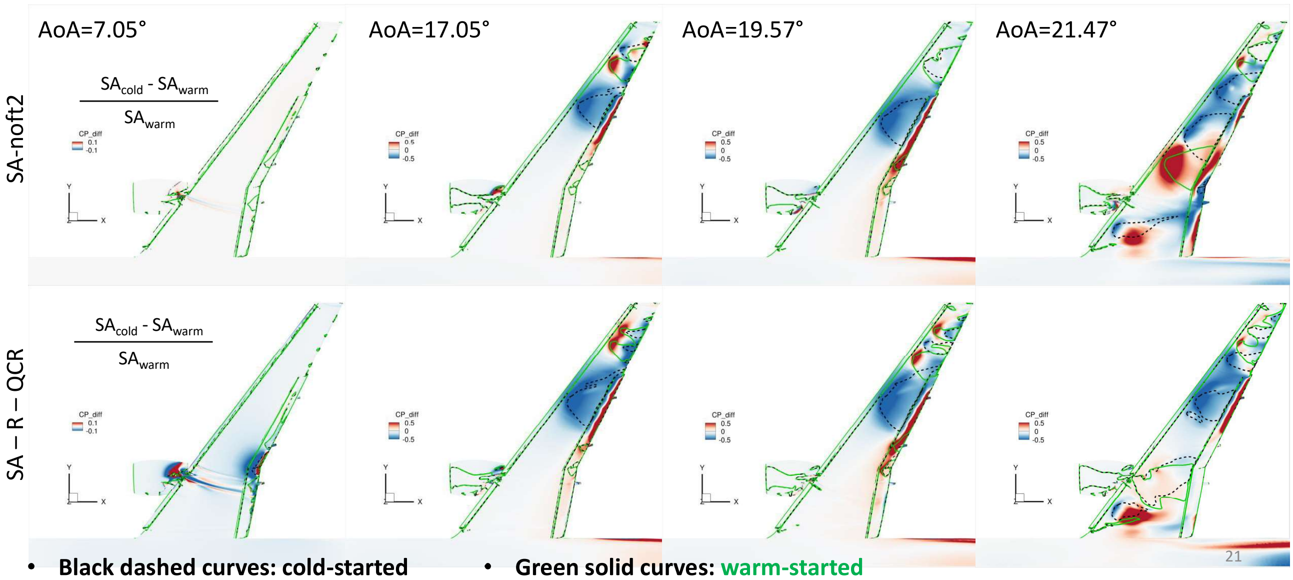

- **Black dashed curves: cold-started**
- **Green solid curves: warm-started**

Cold/Warm start conclusions

- Flow separation tends to occur at lower angles of attack for cold-started simulations
- Is sensitivity to initial condition turbulence-model dependent?
  - This question is hard to answer at the time being. However, there seems to be a trend.
  - Cold-started simulations seem to be less sensitive to turbulence-model effects.
  - R-QCR correction seems to have larger effects on warm-started simulations, as it prevents parts of separated flow at high AoA

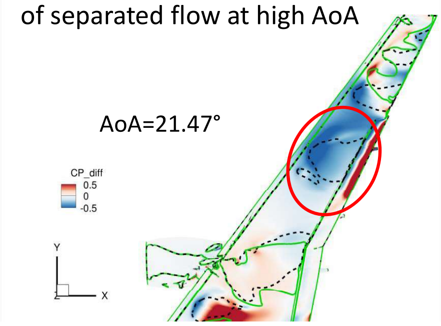

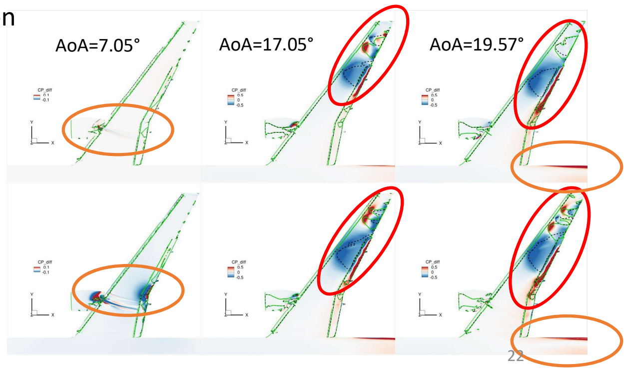

Now, comparing **only warm-started** solutions using

SA-noft2 and **SA-R-QCR**

Comparing warm-started SA-noft2 and SA-R-QCR

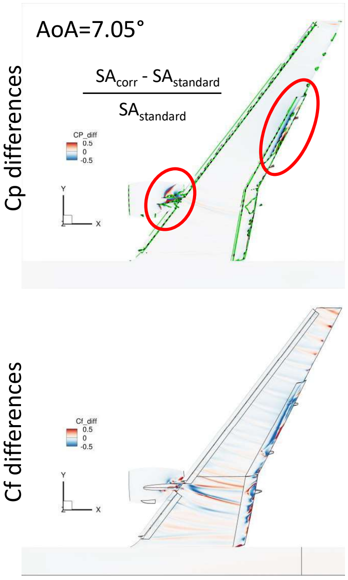

- Plots show relative **differences between Cp contours** of SA with R-QCR correction and SA-noft2 RANS simulations:
  - Blue: Cp of corrected SA solutions < SA-noft2 solution
  - Red: Cp of corrected SA solutions > SA-noft2 solution
- **Green solid curves:** SA-noft2
- **Black dashed curves: SA R-QCR corrected**

- Minor influence of turbulence model on flow over flaps and nacelle

- Plots show relative **differences between Cf contours** of SA with R-QCR correction and SA-noft2 RANS simulations:
  - Blue: Cf of corrected SA solutions < SA-noft2 solution
  - Red: Cf of corrected SA solutions > SA-noft2 solution

24

Comparing warm-started SA-noft2 and SA-R-QCR

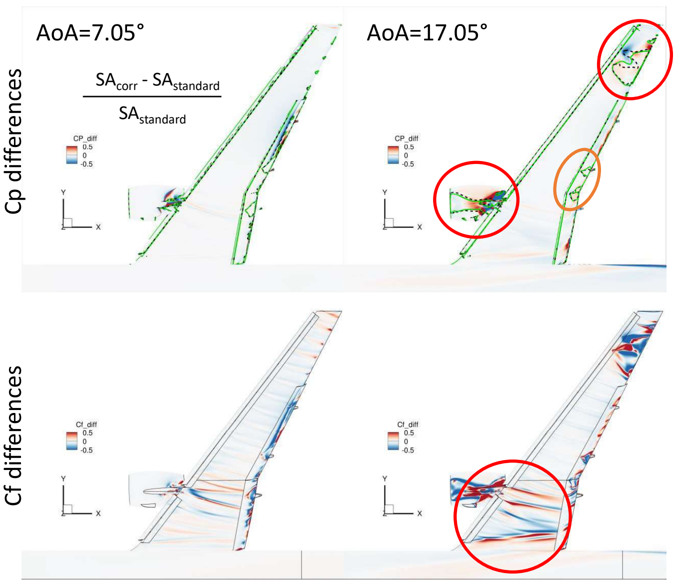

- Differences in Cp mainly near wing-tip and nacelle
- Localized pockets of flow separation for both turbulence models

- Differences in Cf near the wing root become more pronounced with increasing AoA

25

Comparing warm-started SA-noft2 and SA-R-QCR

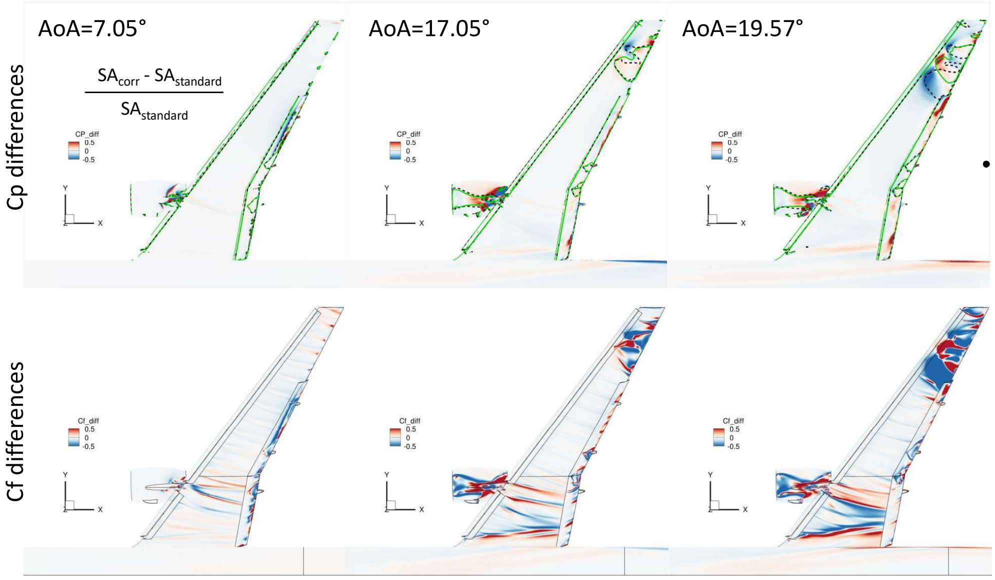

- Trends continue for increasing AoA to 19.57°

26

Comparing warm-started SA-noft2 and SA-R-QCR

- Solutions at 21.47° fundamentally different.
- Main flow separation for SA-R-QCR behind the nacelle.
- Increase pressure recovery over the in-board flaps for SA-R-QCR, despite minor differences in Cf.
- SA-R-QCR: flow separation originating from the slats is more pronounce.

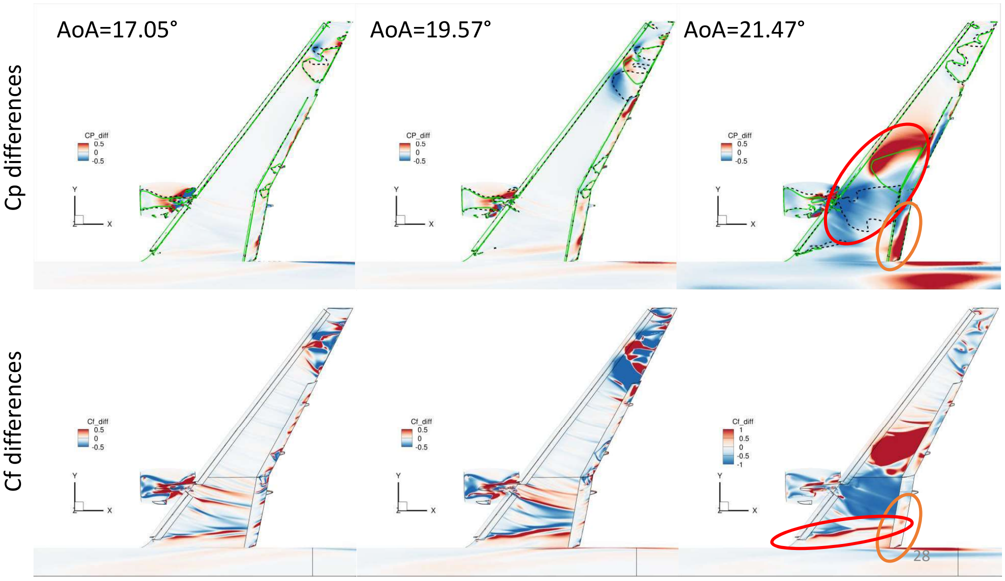

28

Comparing warm-started noFt2 SA and SA-R-QCR

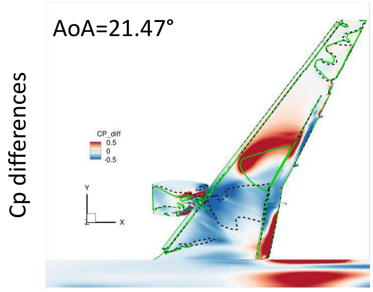

- To confirm observations, here Cf_x plots for each simulation

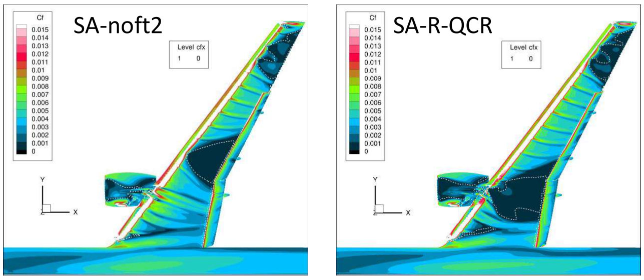

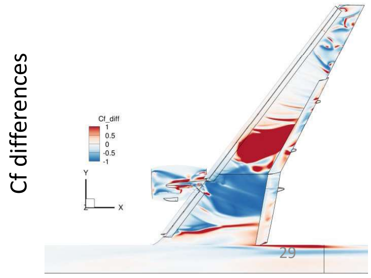

Turbulence model conclusions

- R-QCR correction seems to suppress flow-separation near wing bend, but promotes separation behind the nacelle at high AoA.
- Flow around sharp corners and edges of slats or flaps seem to be sensitive to the choice of turbulence model
- More detailed studies required

Conclusions for CRM-HL

- **No tested RANS turbulence model suitable for accurate $C_{L,max}$ predictions.**
- **Cold started RANS simulations should be avoided!**
- **Experiment-based error** for warm-started simulations at lower angles of attack **within 5%**
- Significant **convergence problems** make purely RANS-based **conclusions** and comparisons **difficult.**
- Presented **RANS** simulations **on their own** seem **not reliable** for complex configurations like CRM-HL, even at moderate angles of attack (~7 degrees)

31

Conclusions for CRM-HL & Outlook

- **No tested RANS turbulence model suitable for accurate $C_{L,max}$ predictions.**
- **Cold started RANS simulations should be avoided!**
- **Experiment-based error** for warm-started simulations at lower angles of attack **within 5%**
- Significant **convergence problems** make purely RANS-based **conclusions** and comparisons **difficult.**
- Presented **RANS** simulations **on their own** seem **not reliable** for complex configurations like CRM-HL, even at moderate angles of attack (~7 degrees)

→ **Combinations or assimilations** of lower fidelity (e.g. RANS), higher-fidelity methods (e.g. WM-LES), and experiments may be required.

→ **Global stability analysis and reduced order models (e.g. ML/AI-based)**

32

ご清聴ありがとうございました

Any questions?

(Personal) open questions

- What do we expect from RANS? What can we expect from RANS?
- Why are we systematically underpredicting lift, but overpredicting drag and pitch? (I.e. Large regions of un-physical flow separation)
- Why do SA models perform better than SST models? (How important is Boussinesq)
- How do SST models perform for warm starts?
- Why do we have convergence problems:
  - Aerodynamic instabilities -> Would RANS "mimic" URANS?
  - Due to flow separation effects
  - Grid
- How can we improve the convergence characteristics? (e.g. selective frequency damping, GMRES)
- Can we use Global Stability Analysis (GSA) to extend the application of RANS (e.g. predicting onset of numerical instabilities + selective frequency damping)?
- Would conclusions change when using different grids or adaptive mesh refinement (AMR)?
- Can URANS simulations improve accuracy (SA and SST)?

Back-up slides

- Convergence

- 7deg:
- 17deg
- 19deg
- 21deg

35

Comments on convergence characteristics

Convergence at off-design conditions with **significantly separated flow** can be **problematic.**

Residuals can depend on numerical schemes and regions with maximum residuals do not necessarily coincide with the those relevant for industrial application. Also, residuals usually only compare two consecutive iterations, which **could understate the total change of results** over longer run times.

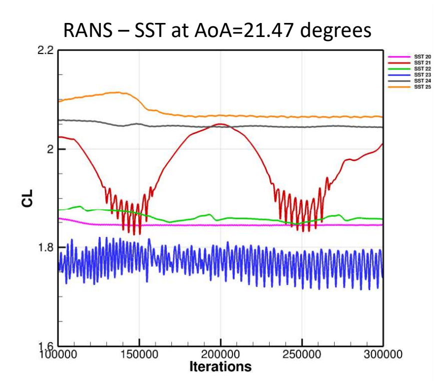

Note that
- All residuals are for all cases of the same order of magnitude
- Pink and grey curves show reasonably steady CL
- Blue and red curves show significant lift fluctuations
- **BUT** pink/blue and grey/red curves have <u>similar residuals</u>

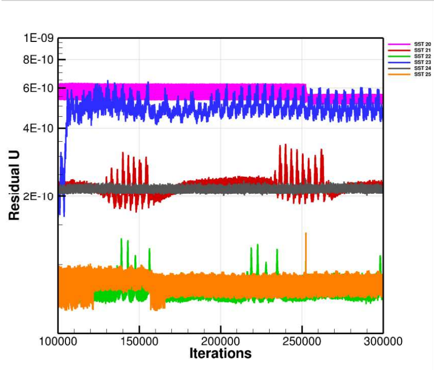

As an **alternative** we propose to assess **fluctuations** of **aerodynamic coefficients**, which are often used for evaluating simulation performances.

Definition of **convergence parameter ConP**:

-> Statistics (root-mean-square and time average) of aerodyn. coefficients computed over 50000 iterations

-> ConvP= log([(CDrms/CDavrg)^2 + (CLrms/CLavrg)^2 + (CMrms/CMavrg)^2]^0.5)

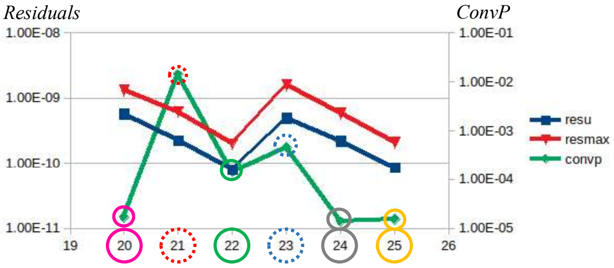

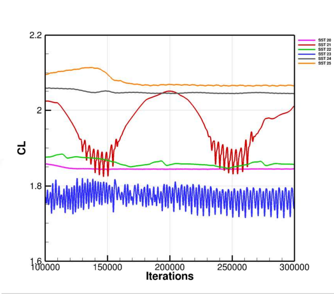

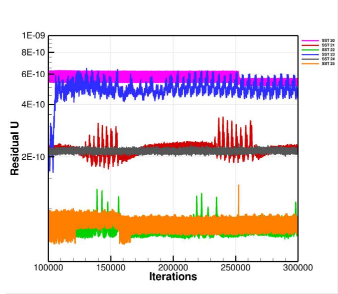

This convergence parameter allows us to
- **separate convergence characteristics** of simulations for the current test case **more clearly**
- **evaluate convergence based on physical quantities**, which are of main interest for practical application

Simulation results with respect to convergence

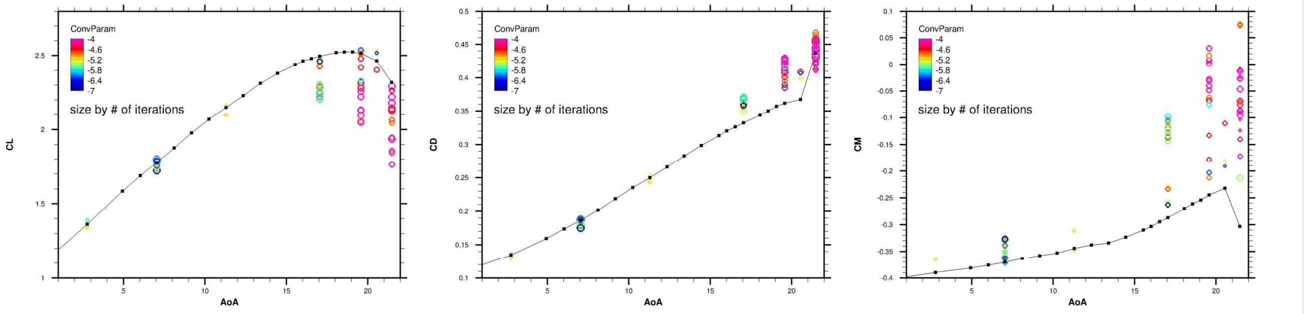

- Using **different turbulence models**, we observe a **significant spread** of **RANS results**, particularly at increased AoA.
- Lift is mostly underpredicted and drag overpredicted.
- **Momentum coefficient** is most **critical** and even at moderate AoA not sufficiently well predicted.
- **SST models** show **no significant improvement** and are much more expensive.
- **Convergence** is **insufficient** near $C_{L,max}$.

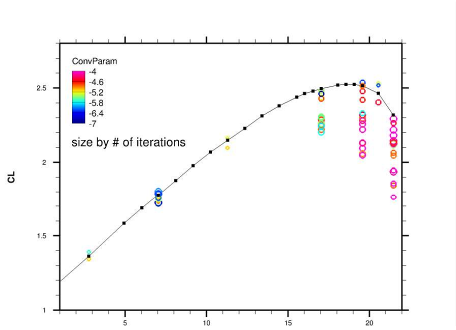

Number of iterations and convergence of Simulations

- **Convergence** is **insufficient** near $C_{L,max}$.
- All simulations were run for at least 200,000 iterations.
- SST models were limited to 300,000 due to computational expenses.

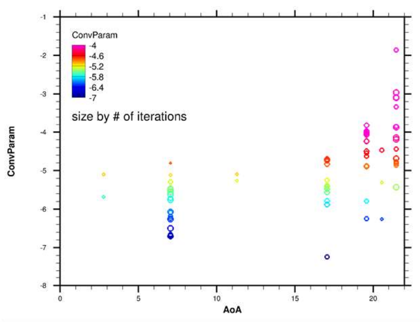

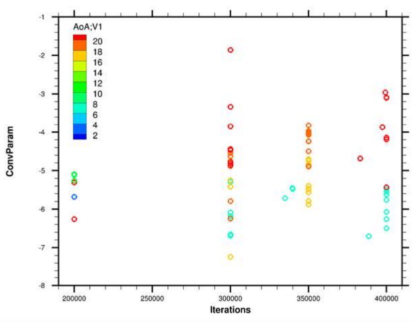

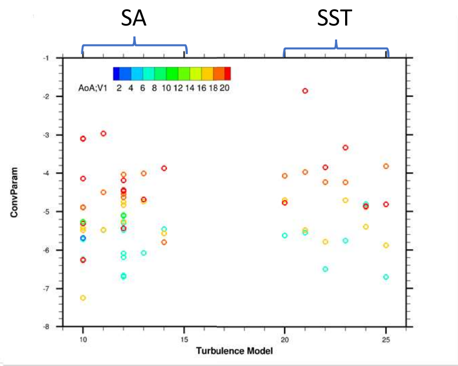

Back-up slides

- Comparison cold vs warm start using different SA models

40

Cold vs Warm Start using SA-noft2

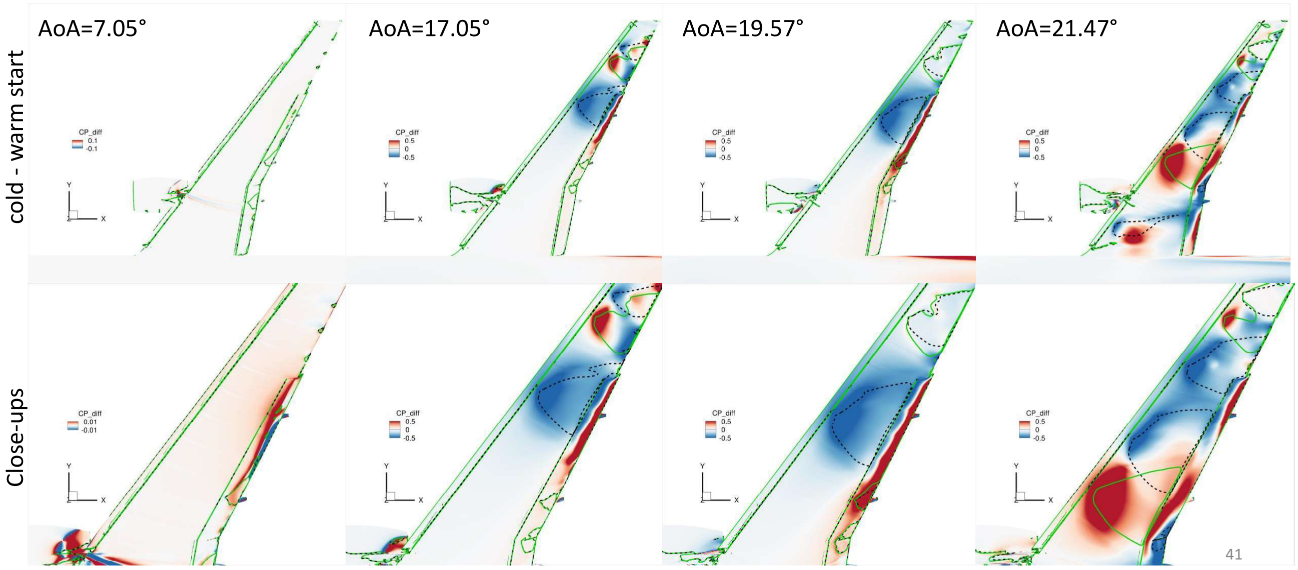

Cold vs Warm Start for SA-noft2 and with rotation and QCR corrections

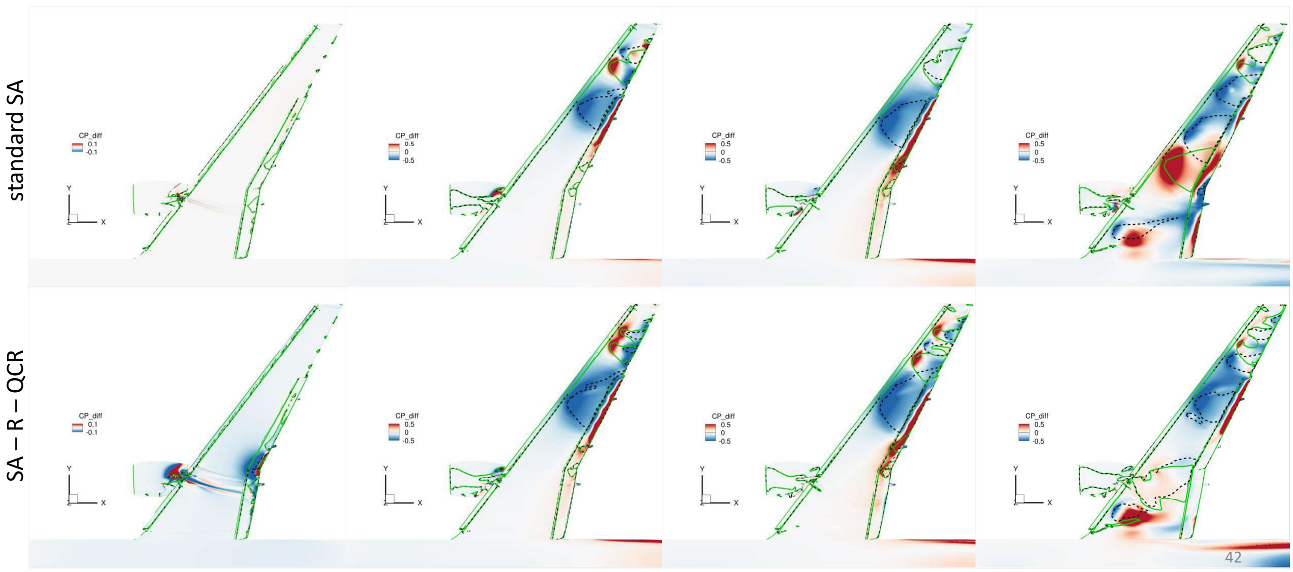

Back-up slides

- Simulation costs

43

Simulation costs

	Standard FaSTAR	Tuned FaSTAR
SA (standard)	96000 coreh/300000 iterations	50000 coreh/300000 iterations
SST	115000 coreh/300000 iterations	65000 coreh/300000 iterations

- SST about 30% more expensive than SA
- Tuned FaSTAR almost twice as fast as standard FaSTAR

44

54th Fluid Dynamics Conference/40th Aerospace Numerical Simulation Symposium
Eighth Aerodynamics Prediction Challenge (APC-8)

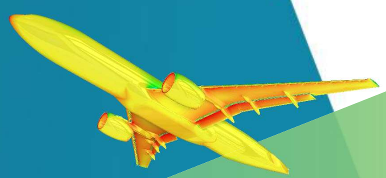

HEXAGON

scFLOWによるCRM-HLの低速高迎角条件における空力特性予測

Numerical Prediction of Aerodynamic Characteristics of CRM-HL at Low Speed and High Angles of Attack by scFLOW

June 29th, 2022

Nakashima Yoshitaka,
Taguchi Seiichi, and Takeda Naoya

Hexagon Manufacturing Intelligence
Design & Engineering Business Unit
CFD Centre of Excellence
／Software Cradle

Background and Objectives

About scFLOW

- **What is scFLOW?**
  - A part of commercial CFD package “Cradle CFD” developed by Hexagon
    - **User-friendly GUI**
    - A comprehensive package
      - **Pre-processor:** Polyhedral mesh generator
      - **Solver:** Unstructured polyhedral mesh thermo-fluid solver
        - **Incompressible to hypersonic flows**
        - Multi-phase flows
        - Granular flows
      - **Post-processor:** Visualization
    - Multiphysics
      - Co-simulation among **MSC Nastran, Marc, Adams, Actran.**

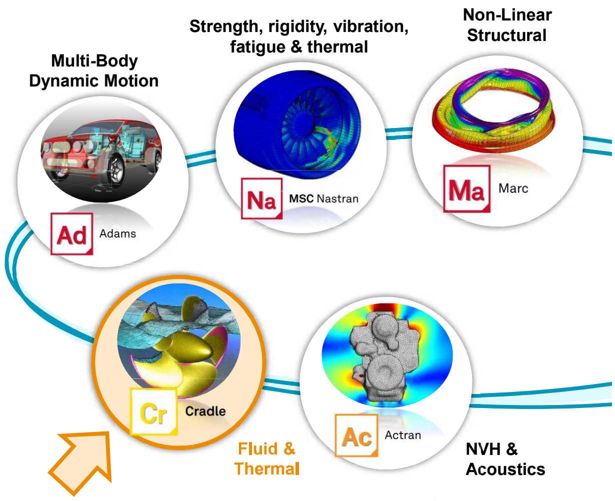

HEXAGON

Background and Objectives

About scFLOW

- **What is scFLOW?**
  - scFLOW has recently been ported to the Fugaku A64FX system and become available on **Fugaku**.


HEXAGON

Press Release

For immediate distribution

23 June 2021

Hexagon adopts the supercomputer Fugaku to revolutionise the use of simulations in product innovation

Partnership with Fujitsu means Cradle CFD customers can complete previously unfeasible simulations faster than ever before

Hexagon has demonstrated how innovation can be accelerated by opening up the possibility of completing complex CFD (computational fluid dynamics) simulations that were previously too time consuming and expensive using the world's fastest

https://www.mscsoftware.com/news/hexagon-adopts-supercomputer-fugaku-revolutionise-use-simulations-product-innovation

https://asia.nikkei.com/Business/Technology/Japan-s-Fugaku-keeps-position-as-world-s-fastest-supercomputer

3 | hexagonmi.com

HEXAGON

Background and Objectives

Validation Works and Objectives

ONERA M6 Wing

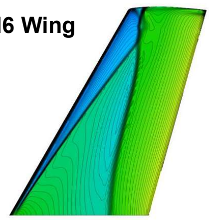

- **Validation of scFLOW on aerospace applications**
  - **AIAA 2020-3029**
    - Hemisphere-cylinder (HC) and ONERA M6 (OM6) wing in NASA's turbulence model resource (TMR).
    - Good agreement with those obtained by NASA's government codes (FUN3D, CFL3D, USM3D).
  - **AIAA 2022-3522**
    - Validate scFLOW on models used at **4th AIAA CFD High Lift Prediction Workshop** (HLPW4).
    - Demonstrate the parallel efficiency on Fugaku.

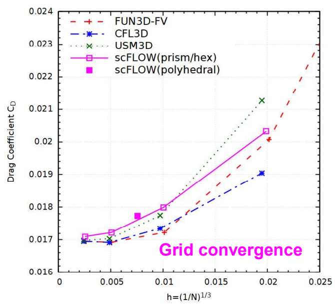

- **Objectives of this work**
  - Further verification study for low speed & high AoA flows of CRM-HL with scFLOW
    - Steady RANS
      - **Iterative convergence characteristics** of aerodynamic coefficient
      - Comparison with **experimental measurement**
      - Research on the **aerodynamic hysteresis** around the stall angle
    - Transient analysis
      - Shows preliminary results

4 | hexagonmi.com

HEXAGON

Numerical Methods

Numerical Mesh

- **Mesh generation by scFLOW**
  - For the **boundary layer elements,** the recommended values of Level-C in Mesh Generation Guidelines on the workshop website were used for the initial thickness and boundary layer growth rate.
  - For this work, Octants are simply refined around the walls, especially at the edges.

Example of Octants specification

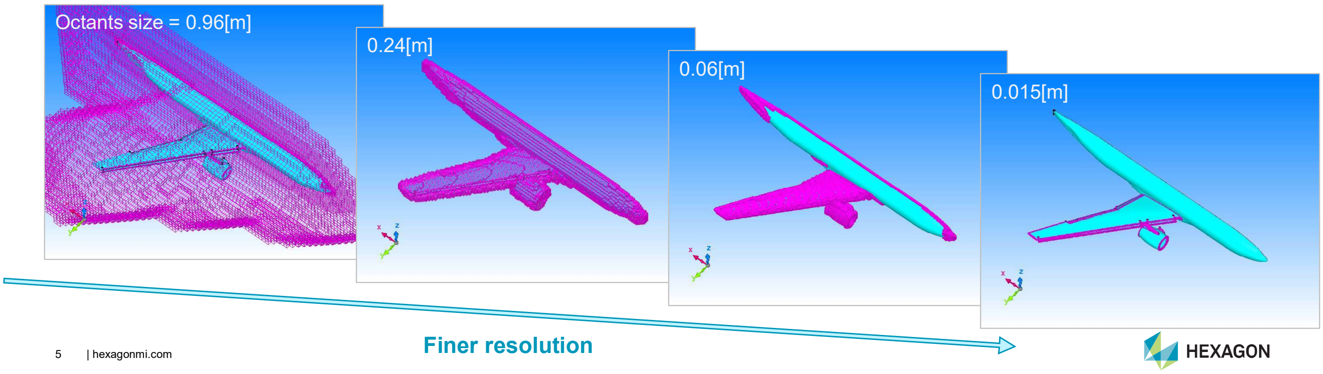

HEXAGON

Numerical Methods

Numerical Mesh

- **Comparison with provided mesh, ANSA103**

Mesh	Elements	Faces
ANSA 103, Level C	276,096,145	764,761,128
Polyhedral Mesh	62,124,074	294,876,783

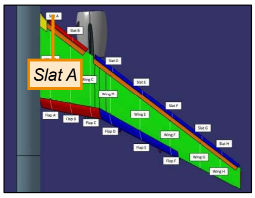

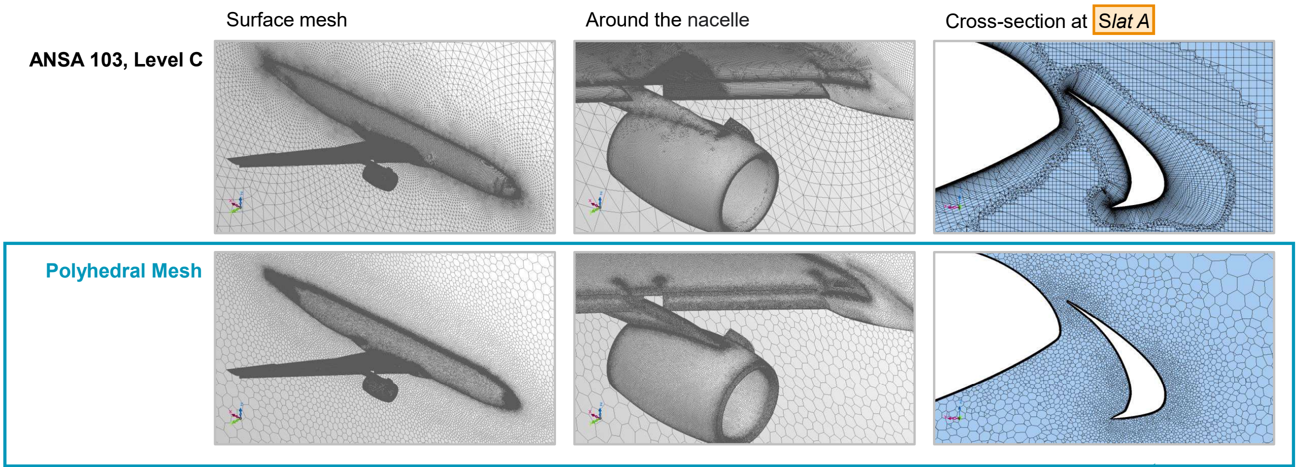

HEXAGON

Numerical Methods

Numerical Procedure

- Discretization method
  - Cell-centered finite volume method, **unstructured polyhedral**, density-based solver
- Inviscid flux
  - **Roe flux**
- Reconstruction
  - **Linearity-preserving U-MUSCL (Nishikawa 2020)**
    - Recovers the accuracy of U-MUSCL even when the mesh is in bad condition
    - κ for the meanflow equations
      - Polyhedral Mesh : κ=0.5
      - ANSA 103 : κ=0.0(more stable but less accurate)
- Viscous flux
  - **Alpha damping scheme (Nishikawa 2010)**
    - Evaluates the gradient at a CV-face by using high-frequency damping term with the parameter alpha in addition to the arithmetic mean of elemental gradients
    - Stable and accurate even for skew mesh (Jalali et al. 2014)

7 | hexagonmi.com

HEXAGON

Numerical Methods

Numerical Procedure

- Calculation method of gradients
  - Polyhedral Mesh : Weighted least squares
  - ANSA 103 : Green-Gauss(more stable but less accurate)
- Non-linear solver in a steady-state analysis
  - Implicit defect correction solver with the residual Jacobian derived exactly from a lower-order discretization with a local pseudo-time step
- Turbulence model
  - **Steady : SA-neg**
  - **Transient : SST-SAS**
- Initial field & calculated AoA
  - **Steady**
    - Uniform Flow : 2.78, 7.05, 11.29, 17.05, 19.57, 20.55, 21.47°
    - AoA Increasing : 17.05 → 19.57 → 20.55 → 21.47°
    - AoA Decreasing : 11.29 ← 17.05 ← 19.57 ← 20.55 ← 21.47°
  - **Transient**
    - Steady results : 7.05, 17.05, 19.57, 21.47°

8 | hexagonmi.com

HEXAGON

Numerical Results

Convergence Histories

- Calculation histories of aerodynamic coefficients, CL, CD, and CM, **Polyhedral Mesh**
  - **Evaluate the averaged flow-field in the last 2,500 cycles**

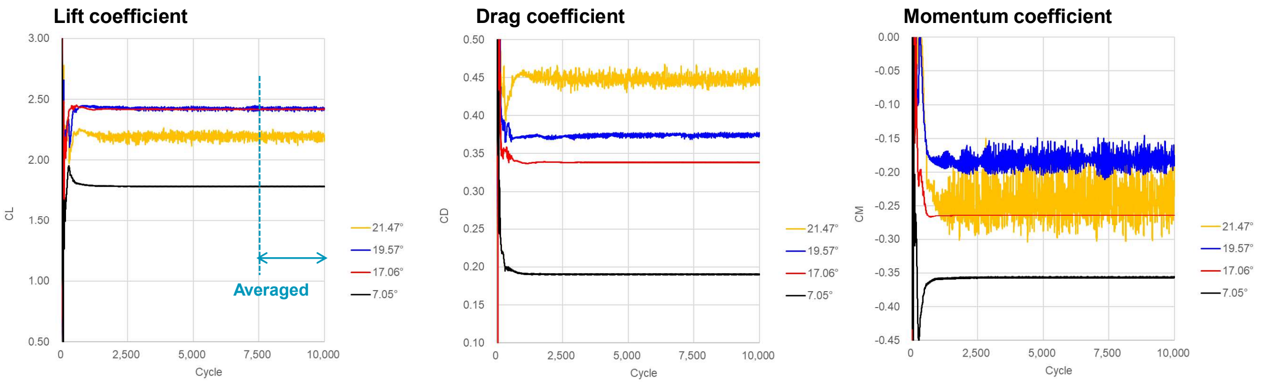

HEXAGON

Numerical Results

AoA Sweep

- Comparison of the aerodynamic coefficients, CL, CD, and CM
  - It has been said that around the stall angle is difficult with the steady RANS, but these results are relatively good.

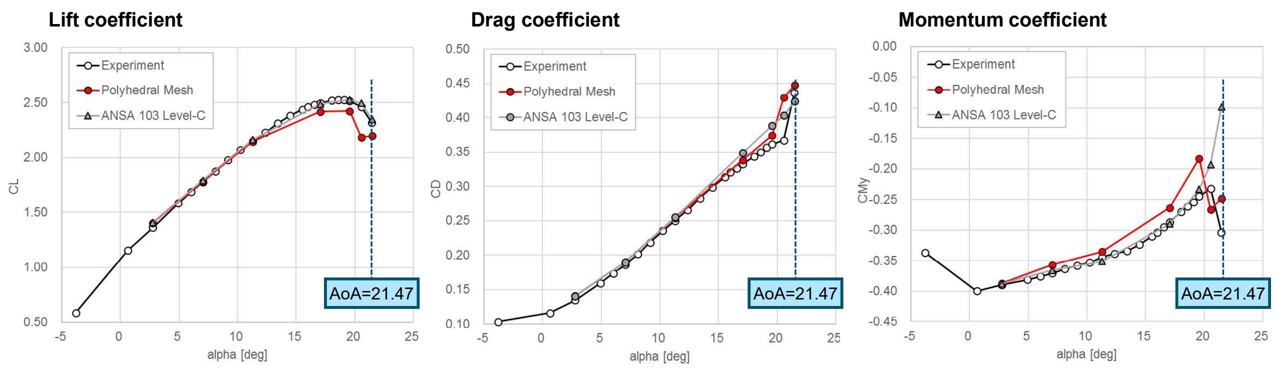

HEXAGON

Numerical Results

AoA Sweep

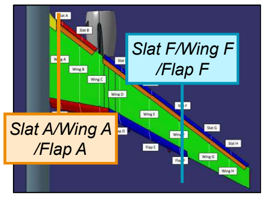

- Comparison of the pressure coefficients, Cp, at AoA=21.47°
  - In terms of the pressure distribution on the wing surface, **Polyhedral Mesh** gives better results.

Slat A/Wing A
/Flap A

Slat F/Wing F
/Flap F

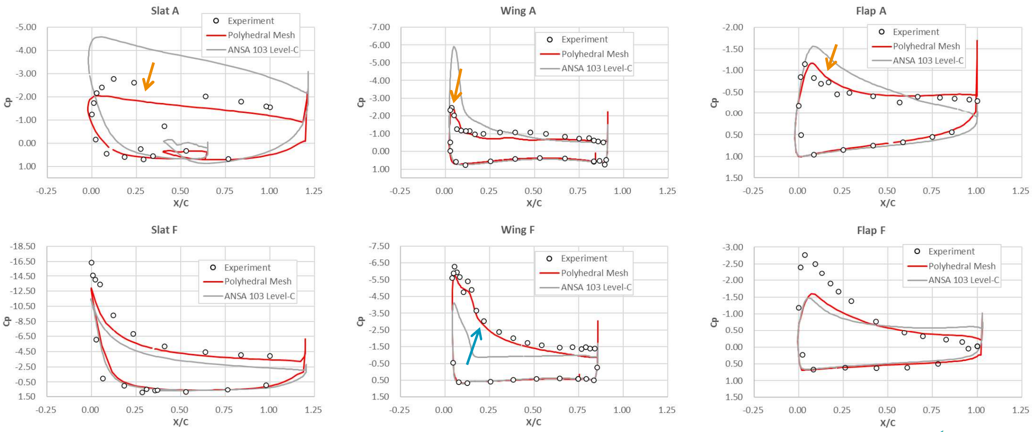

HEXAGON

Numerical Results

AoA Sweep

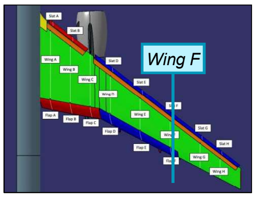

- Comparison of the oil flow visualization at AoA=21.47°
  - Polyhedral Mesh predicts well the flow separation around the wing root and attached flow around the section *Wing F*.

Experimental oil flow visualization | **Polyhedral Mesh** | **ANSA 103, Level-C**

Around wing root

Around *Wing F*

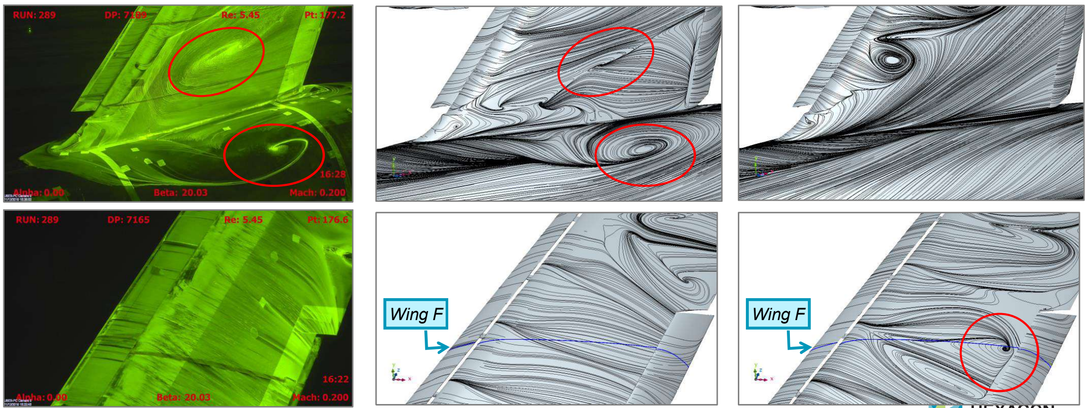

HEXAGON

Numerical Results

Aerodynamic Hysteresis

- Comparison of the aerodynamic coefficients, CL, CD, and CM, among 3 sets of initial conditions: a uniform flow (Uniform Flow), the result at a lower AoA (AoA Increasing), and the result at a higher AoA (AoA Decreasing)

Lift coefficient

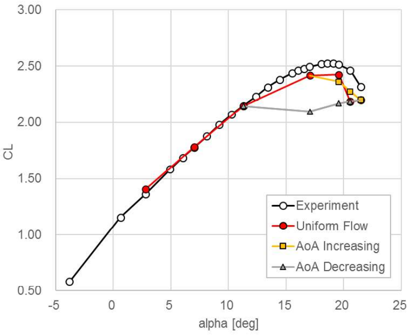

Drag coefficient

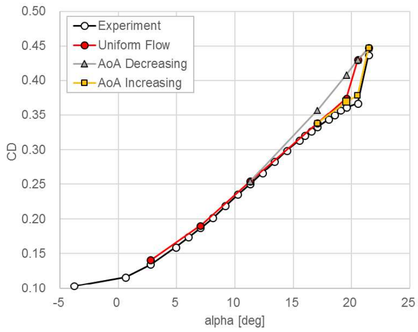

Momentum coefficient

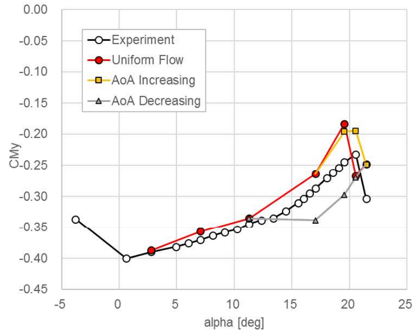

HEXAGON

Numerical Results

Aerodynamic Hysteresis

- Comparison of the aerodynamic coefficients, CL, CD, and CM, among 3 sets of initial conditions: a uniform flow (Uniform Flow), the result at a lower AoA (AoA Increasing), and the result at a higher AoA (AoA Decreasing)

Lift coefficient

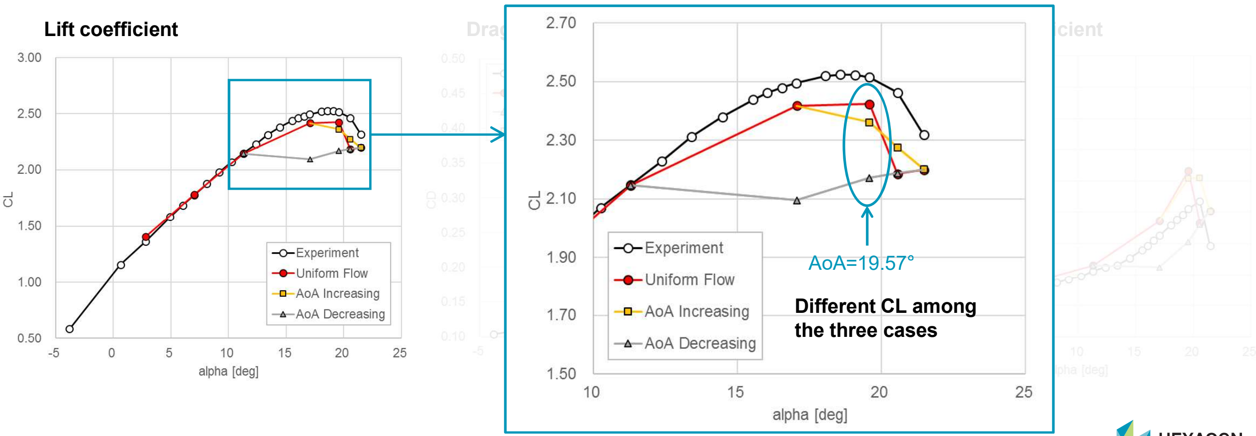

HEXAGON

Numerical Results

Aerodynamic Hysteresis

- Comparison of oil flow and iso-surfaces of the vorticity, AoA=19.57°
  - **Separation behind the nacelle or at the wing root** occurs depend on the initial field

Uniform Flow **AoA Increasing** **AoA Decreasing**

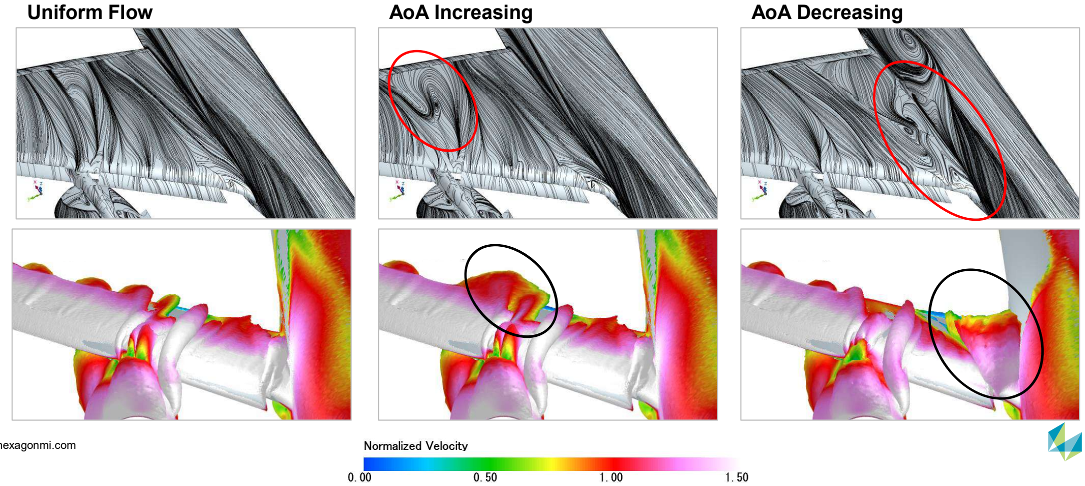

HEXAGON

Numerical Results

Transient Analysis

- Comparison of the aerodynamic coefficients, CL, CD, and CM
  - Preliminary calculation of transient analysis **can not improve** the steady RANS results.

Lift coefficient

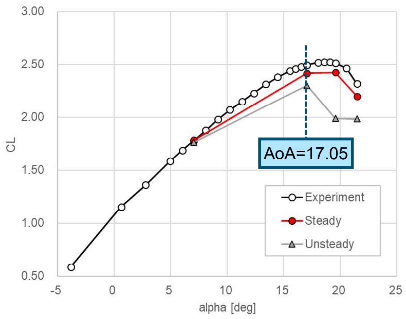

Drag coefficient

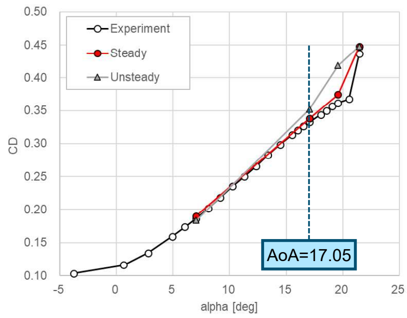

Momentum coefficient

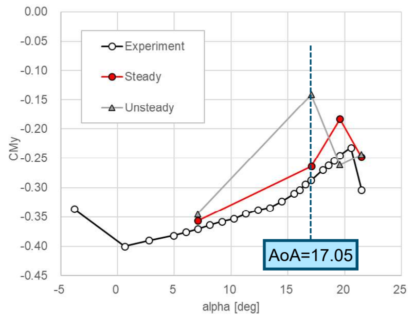

HEXAGON

Numerical Results

Transient Analysis

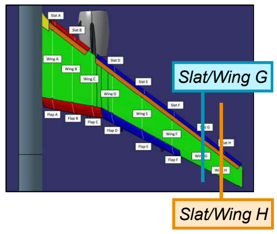

- Comparison of the pressure coefficients, Cp, and wall shear stress at AoA=17.05°

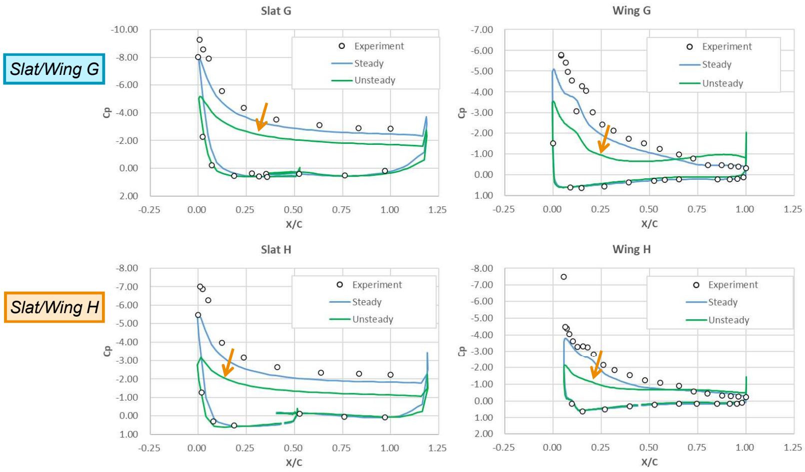

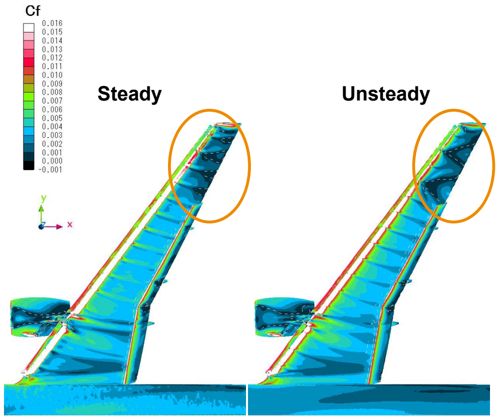

HEXAGON

Conclusions & Future Work

Conclusions & Future work

- **Conclusions**
  - Verification study of CRM-HL with a polyhedral finite-volume turbulent-flow solver, scFLOW was performed.
    - **Steady results** were successfully obtained.
    - The coefficients CL, CD, and CM are relatively good agreement with those of experiment. Especially, prediction at a higher AoA after the stall is difficult. However, Polyhedral Mesh got better results in terms of surface pressure by **capturing the separation accurately**.
    - **Aerodynamic hysteresis** is observed: especially for AoA=19.55°, steady-state results are different among the three cases of angle-increase, decrease, and uniform flow start.
    - Preliminary calculation of transient analysis could not improve the steady RANS results.
- **Future work**
  - Study the **transient analysis** and **adaptive mesh refinement approach** to capture the separation phenomena more accurately and improve the resulting aerodynamic coefficient prediction.

HEXAGON

June 29, 2022
Eighth Aerodynamics Prediction Challenge (APC-8)
1C10

Aerodynamics prediction of CRM-HL using RANS by TAS code

TASによるCRM-HLのRANS定常空力解析

○Furuya Ryutaro (Ryoyu Systems Co., Ltd.)
Murayama Mitsuhiro (JAXA)
Ito Yasushi (JAXA)
Tanaka Kentaro (Ryoyu Systems Co., Ltd.)

Cases calculated 2

- **Test Cases**
  - Case1: $C_{L,max}$ study (warm & cold starts)
  - Case3: Flap deflection study
  - Case4: Turbulence model study in 2D simulation (SA-noft2-R(C_{rot}=1) & SA)

	Case 1	Case 3	Case 4
Geometry	3D CRM-HL		2D CRM-HL
Flap deflection (inboard/outboard)	40°/37°	43°/40°	–
AoA	(2.78°) 7.05° (11.29°) 17.05° 19.57° 21.47°	7.05° 17.05°	16.00°
Grid	240-JAXA-unstructured*1	2.2-Pointwise-Unstr-PrismTet-V2_43/40*1	Family 1*2
Grid Level	C-level*3	D-level*3	L1～7*4

*1 Grid downloaded from HLPW-4 website
*2 Grid provided by NASA TMR
*3 A-level (coarsest) to D-level (finest)
*4 L1 (coarsest) to L7 (finest)

Computational condition & Numerical methods

- **Computational conditions**
  - Case1, 3
    - Mach = 0.2, Re = 5.49 x 10^6 (C_{ref} = 275.8 in), T_{ref} = 289.4K
  - Case4
    - Mach = 0.2, Re = 5.00 x 10^6 (C_{ref} = 1), T_{ref} = 272.1K
- **Numerical methods**

Code	TAS
Governing Equations	RANS (Reynolds Averaged Navier-Stokes) Eq.
Discretization	Cell-vertex finite volume method
Convection term	HLLEW (Harten-Lax-vanLeer-Einfeldt-Wada)
Reconstruction method	2^{nd} order Unstructured MUSCL
Time integration	LU-SGS implicit
Turbulence model	SA-noft2-R (C_{rot}=1) (fully turbulent) SA (fully turbulent) for Case 4

- **Computational Resources**
  - JAXA Supercomputer System generation 3 (JSS3) was used for these computations.

Surface grids (Cases 1 & 3)

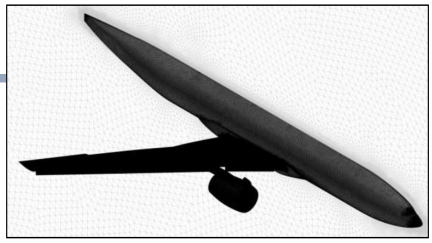

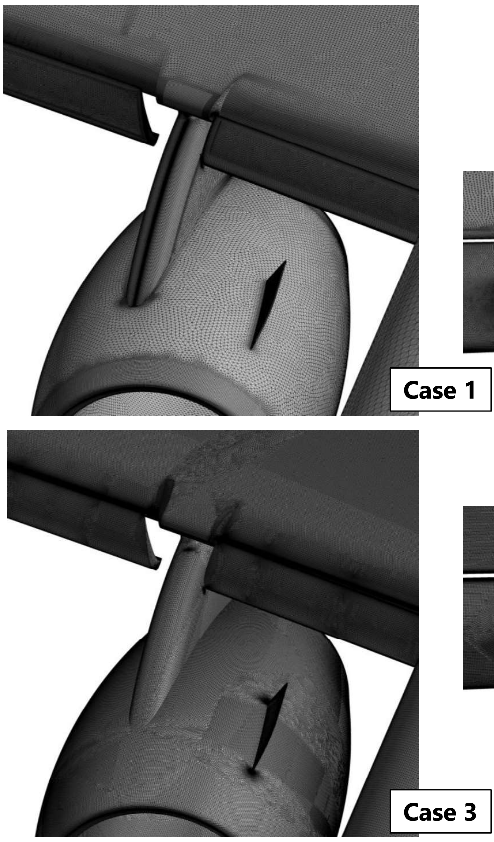

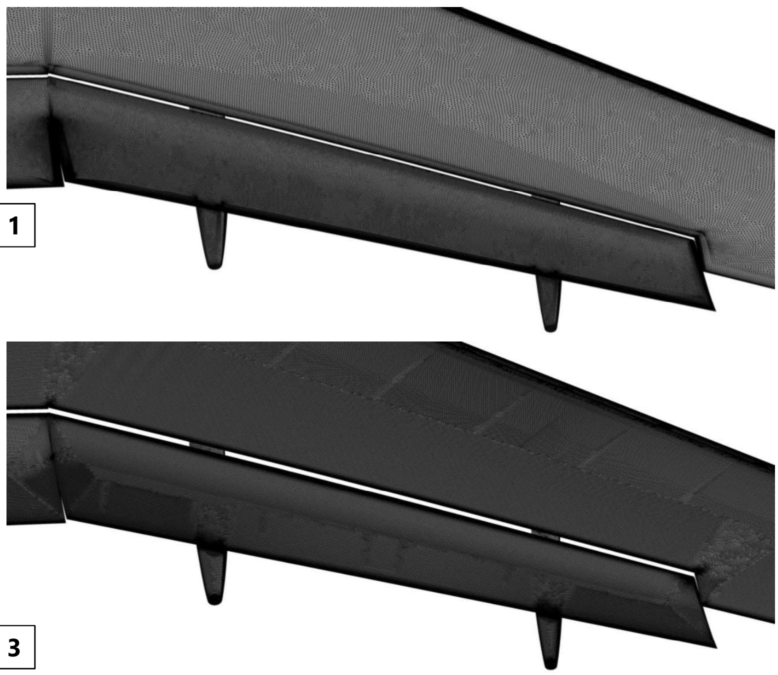

Sectional views of grids (Cases 1, 3 & 4) 5

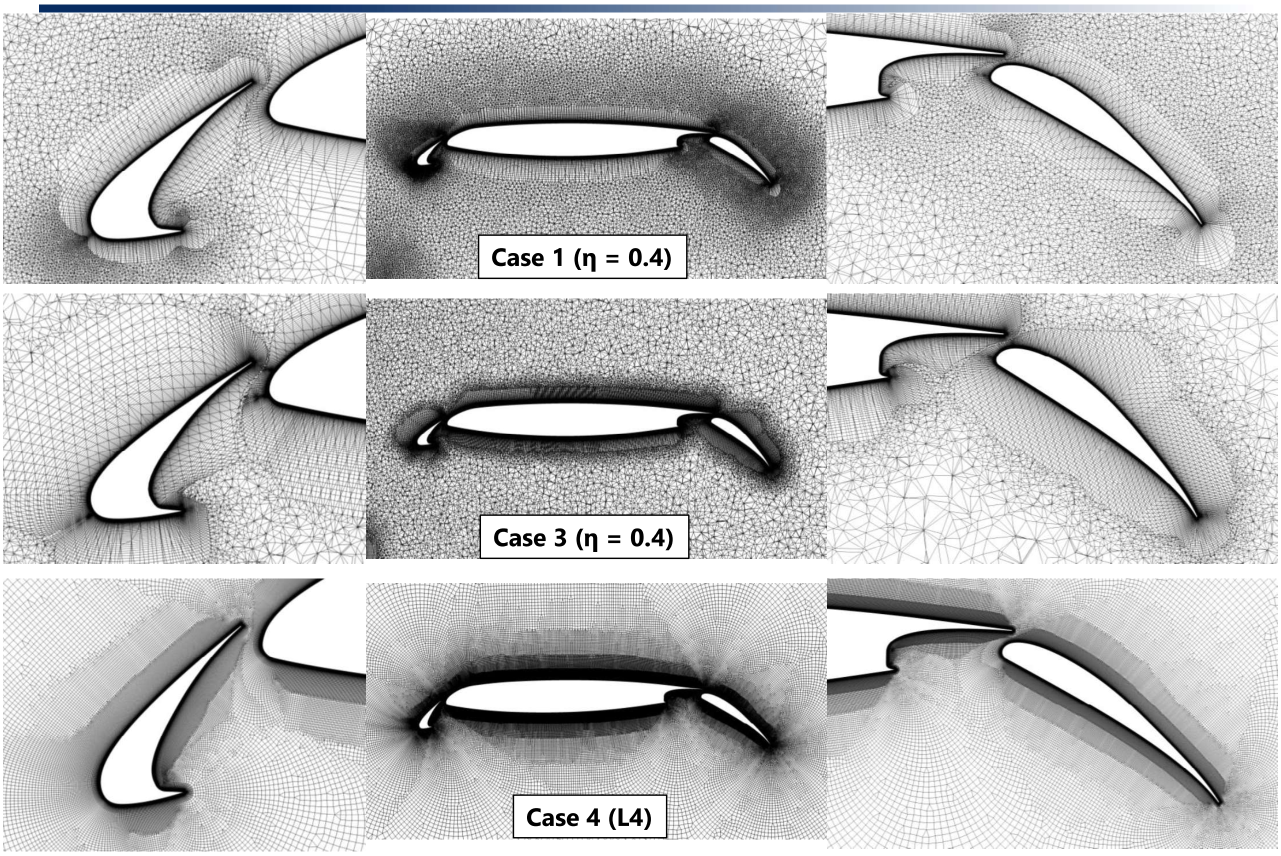

Aerodynamic coefficients (Case 1) 6

- **CFD results with warm and cold starts are compared with experiment.**
- **Compared with experiment, CFD tends to predict lower C_L, and higher C_D and C_M at high angles of attack.**
- **CFD with warm and cold starts provides different results at high angles of attack. CFD with warm starts predicts**
  - Slightly higher C_L, lower C_D and higher C_M before the stall occurs.
  - Significantly higher C_M after the stall occurs.
- **CFD with warm starts seems to provide better results before the stall occurs. Flow fields are compared in the following slides.**

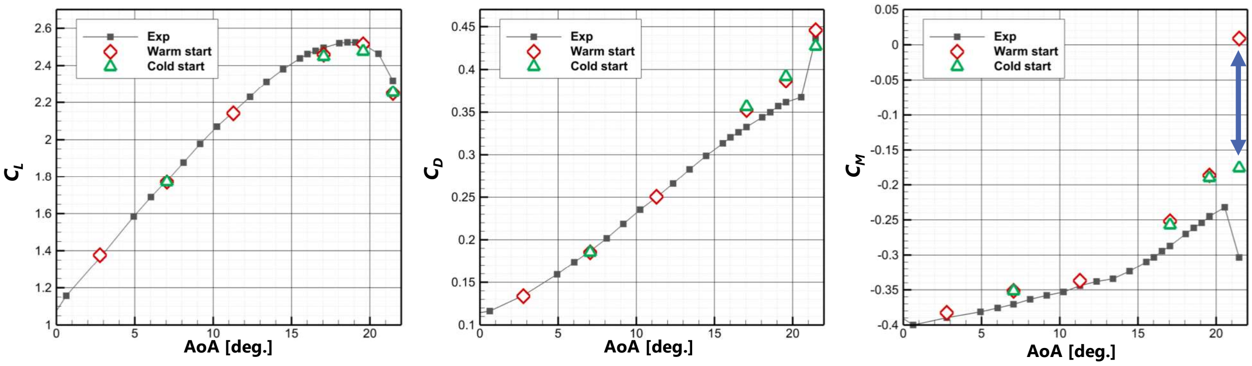

Surface Cf contours (Warm vs Cold starts)

7

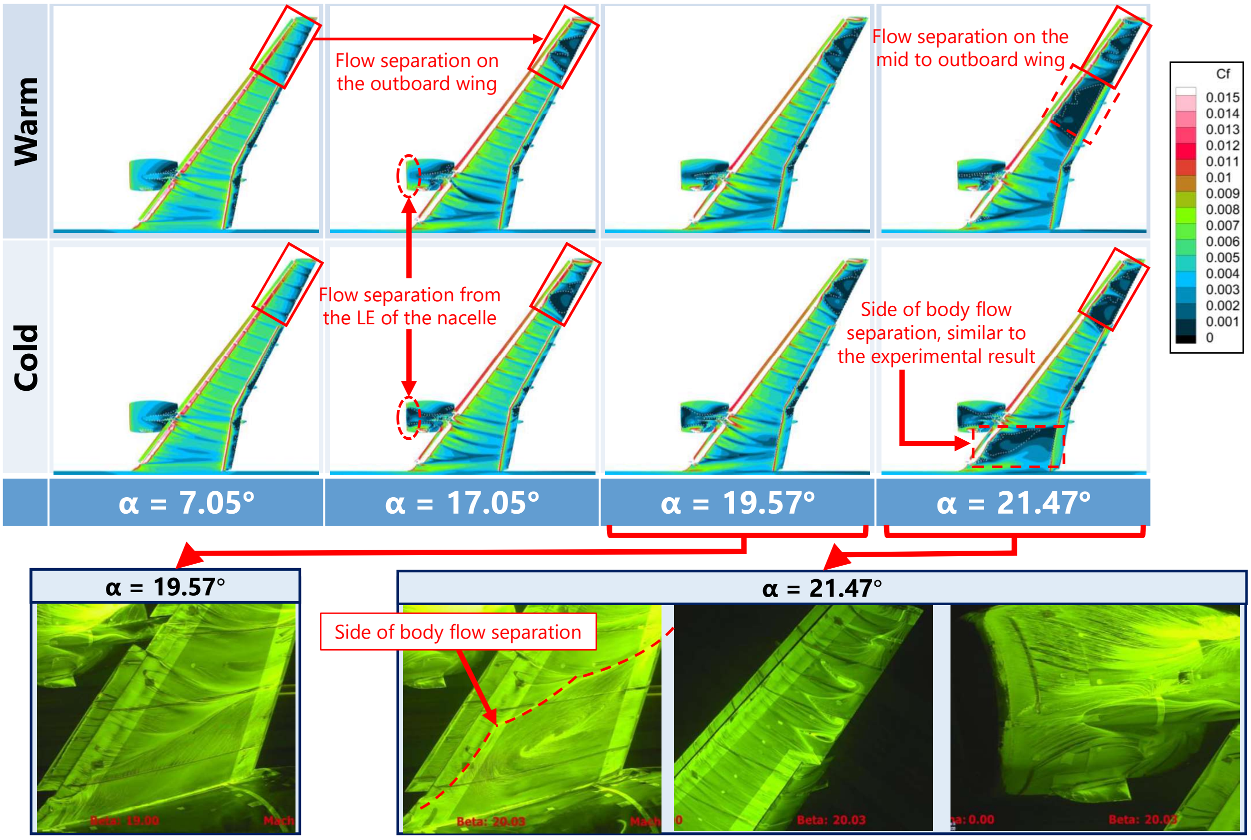

Spanwise sectional C_l & C_m distributions at α=21.47°

8

- **Compared CFD results with cold start, warm start result predicts**
  - Lower C_l at the mid to outboard wing and higher C_l at the inboard wing.
  - Higher C_m due to the larger separation on the mid to outboard wing and smaller separation on the inboard wing and outboard flap.

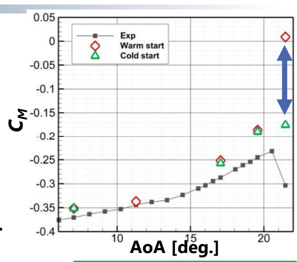

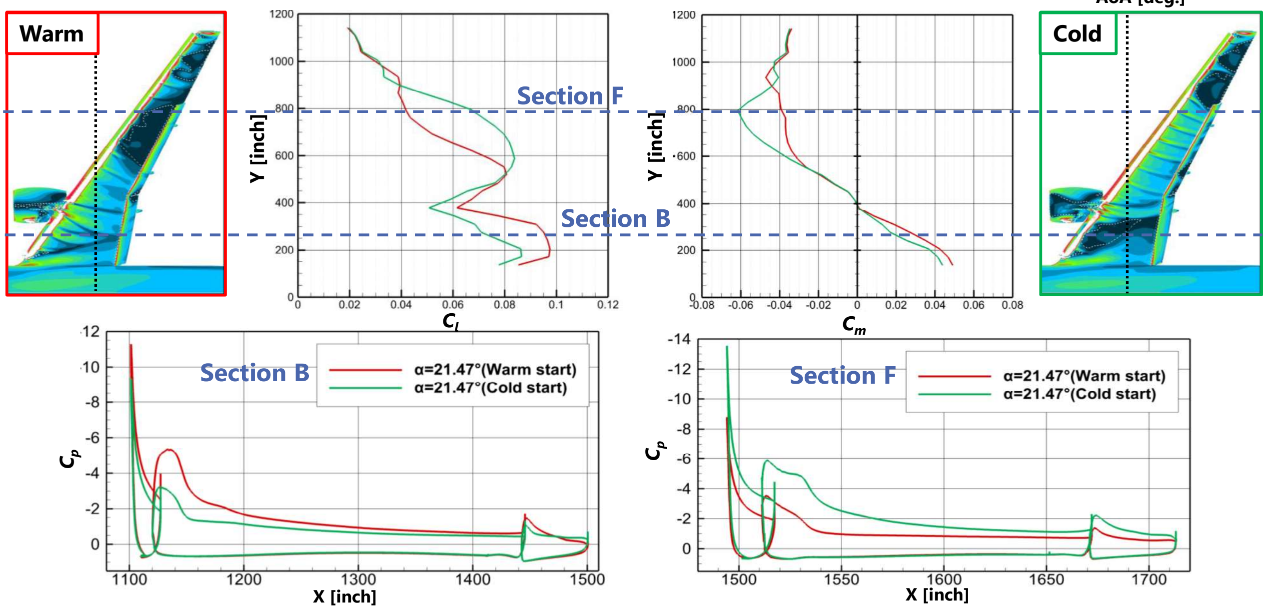

Aerodynamic coefficients (Case 3)

9

- **CFD results only with Warm starts for the flap 40°/37° & 43°/40° configs are compared with experiment.**
- **For the flap 43°/40° config, compared with experiment, CFD predicts**
  - Lower C_L & higher C_M at α = 7.05 & 17.05°.
  - Comparable C_D at α = 7.05° & higher C_D at α = 17.05°
- **Compared with CFD result of the flap 40°/37° config, that of the flap 43°/40° config provides**
  - Lower C_L and C_D at α = 7.05°, while higher C_L and C_D at α = 17.05°.
  - Higher C_M at α = 7.05°, but comparable C_M at α = 17.05°.

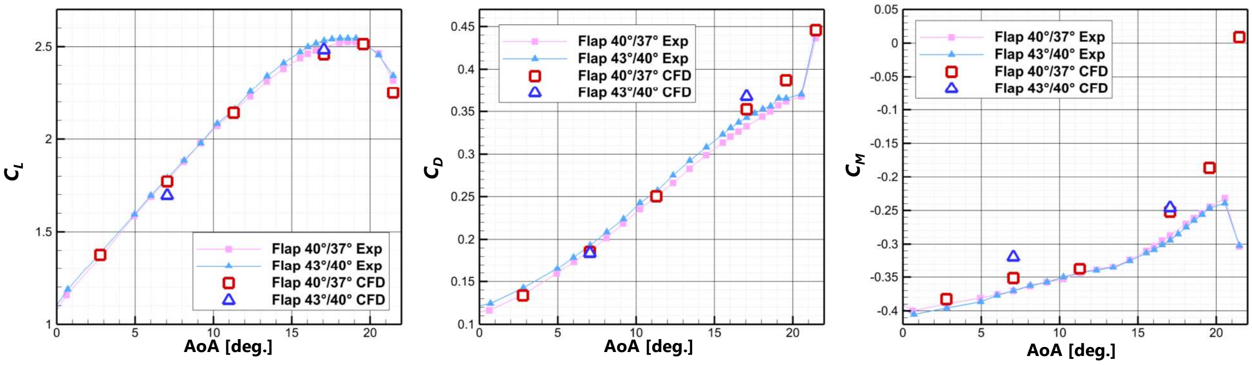

Aerodynamic coefficients (Case 3)

10

- Compared with experiment, TAS code predicts lower ΔC_L of the 43°/40° config at α = 7.05°. This trend is similar to results of other CFD codes participating in HLPW-4.
- Aerodynamic coefficients predicted by TAS code at α = 17.05° are closer to the experimental result than those at α = 7.05°.

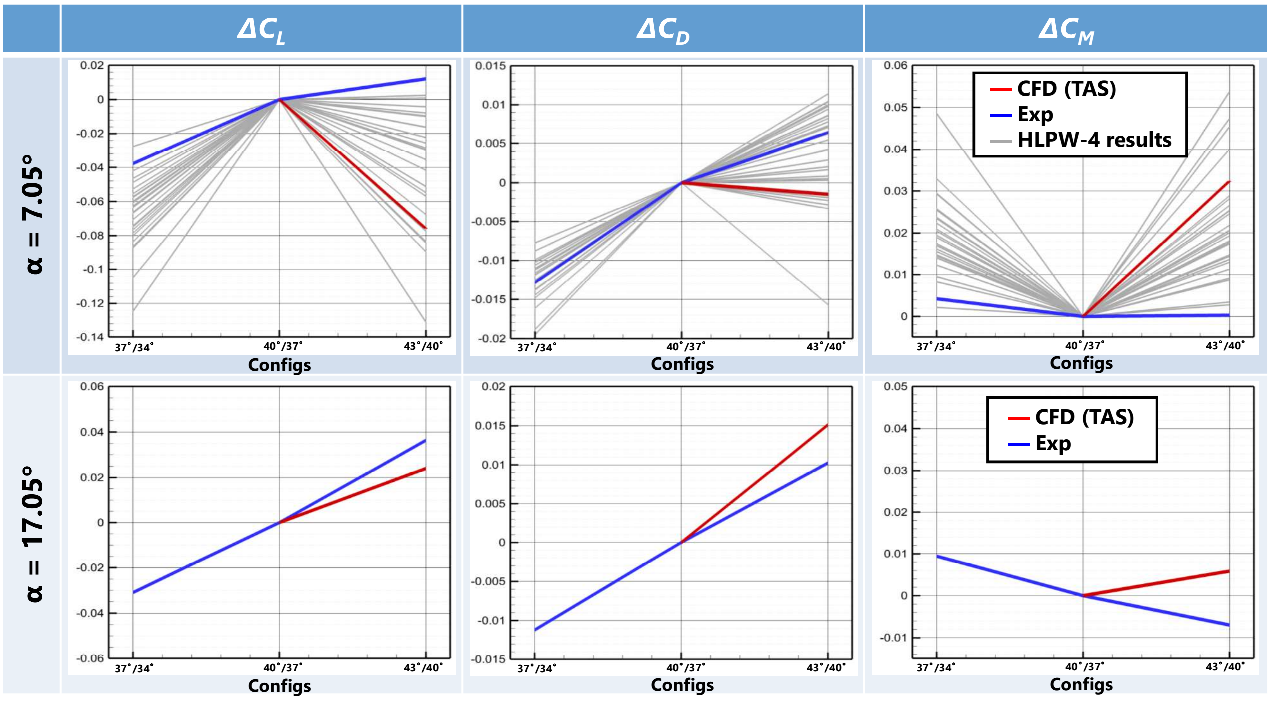

Surface Cf contours (flap 40°/37° vs 43°/40° configs) 11

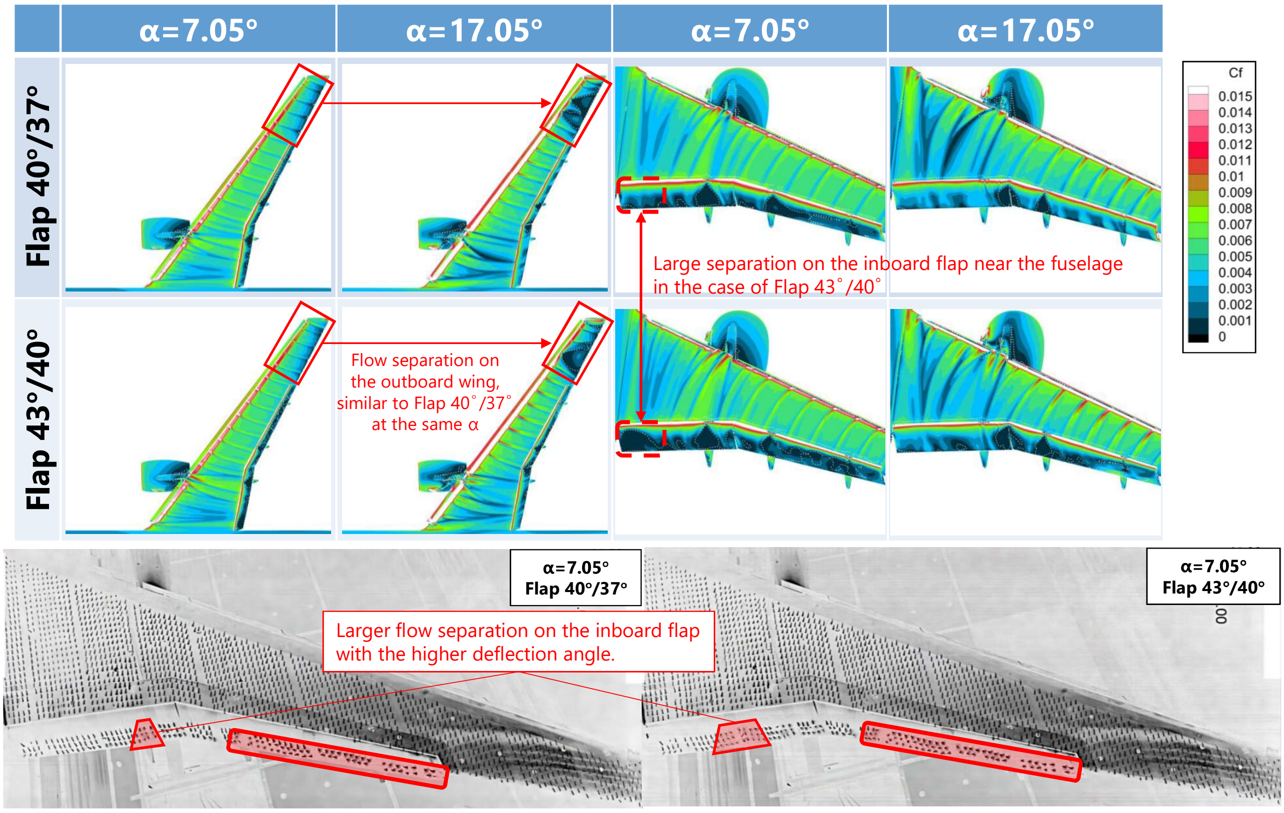

Aerodynamic coefficients (Case 4) 12

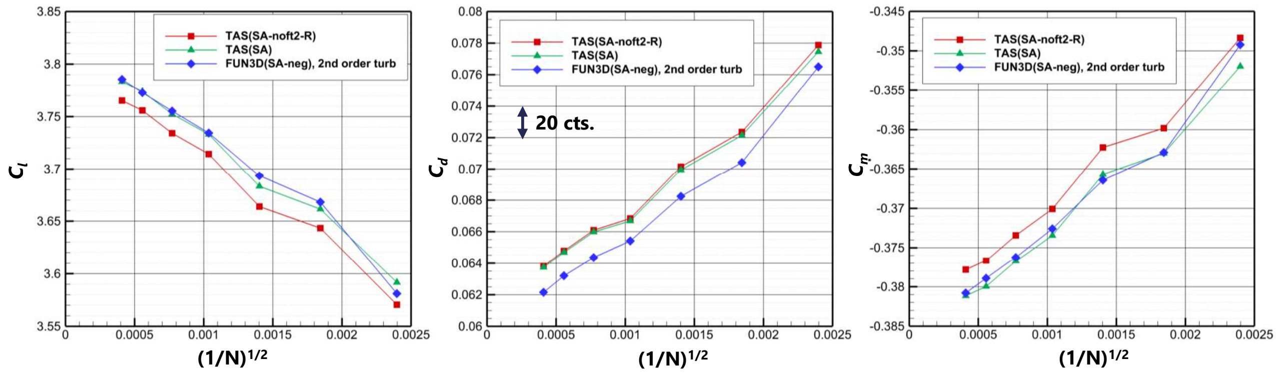

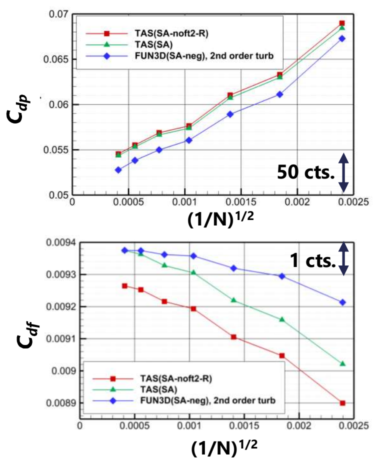

- **Compared to FUN3D, TAS with SA predicts**
  - Similar C_l & C_m at all grid levels
  - 10~17 cts. larger C_d & C_{dp} at all grid levels
  - C_{df} converged at the finest grid

- **Compared to TAS with SA, TAS with SA-noft2-R predicts**
  - 0.018~0.021 lower C_l & 0.0032~0.0036 higher C_m in all grid levels
  - Similar C_d & C_{dp} at all grid levels
  - About 1 cts. lower C_{df} at all grid levels

Summary

13

- **$C_{L,max}$ study**
  - CFD results were obtained with warm and cold starts.
  - Compared with experiment, CFD results with both warm and cold starts predicted lower C_L, and higher C_D and C_M.
  - Compared with CFD with cold starts, CFD with warm starts provided results closer to the experiment before the stall occurred.
- **Flap deflection study**
  - For the flap 43°/40° config, compared with experiment, CFD predicts
    - Lower C_L & higher C_M at α = 7.05 & 17.05°.
    - Comparable C_D at α = 7.05° & higher C_D at α = 17.05°
  - Compared with experiment, TAS code predicted lower ΔC_L of the 43°/40° config at α = 7.05°. This trend was similar to results of other CFD codes participating in HLPW-4.
- **Turbulence model study in 2D simulation**
  - SA in TAS code were verified by comparison with FUN3D results.
  - Compared to SA in TAS code, SA-noft2-R(C_{rot}=1) shows
    - Lower C_l, C_{df} and higher C_m
    - Similar C_d and C_{dp}

22KT017850

APC-8 （講演番号:1C11）

CflowによるCRM-HLの検証解析

Prediction of Low-speed Flows for the CRM-HL Configuration using Cflow

山内優果、安田 英将、澤木 悠太、上野 陽亮
Yamauchi Yuka, Yasuda Hidemasa, Sawaki Yuta, Ueno Yosuke
Kawasaki Heavy Industries, Ltd.
Aerodynamics Engineering Section

カワる、サキへ。
Changing forward

2022年6月29日（水）
第54回流力講演会/第40回ANSS@盛岡

Kawasaki Powering your potential

Outline

- Objective
- Focus of APC-8
  1. Grid dependency study
  2. Effect of turbulence model
     - SA-neg vs SA-noft2-R-QCR
     - SA-noft2-R-QCR vs SA-noft2-R (effect of QCR)
     - SA-noft2-R-QCR crot 1.0 vs 2.0 (sensitivity analysis of crot)
- Summary

Objective

■ Participation case

	Case 1	Case 2	Case 3	Case 4
Submitted	〇	×	△	〇

■ Focus on the results of **Case1** in this presentation

● Case1

	SA-neg	SA-noft2-R-QCR	SA-noft2-R
Cflow Grid	〇	〇	〇
JAXA Grid	〇	×	×
Pointwise Grid	〇	×	×

Focus 1: SA-neg column (Cflow Grid, JAXA Grid, Pointwise Grid). Focus 2: Cflow Grid row (SA-neg, SA-noft2-R-QCR, SA-noft2-R).

➢ **Focus 1 : Grid dependency study**
- CflowGrid vs. JaxaGrid vs. PointwiseGrid

Grid feature study and code to code comparisons

➢ **Focus 2 : Effect of turbulence model**
- SA-neg vs. SA-R-QCR vs. SA-R

Which turbulence model approaches the WTT results?

Numerical Method

CFD tool	Cflow (KHI in-house)
Governing Equations	**RANS** (Reynolds Averaged Navier-Stokes equations)
Spatial Discretization	Cell-centered finite volume method with 2nd-order accurate reconstruction based on MUSCL
Inviscid Flux	**SLAU** (Simple Low-dissipation AUSM scheme)
Viscous Flux	2nd-order accurate central difference
Turbulence Modeling	**SA-neg** (Negative Spalart-Allmaras One-Equation Model) **SA-noft2-R/R-QCR** (for investigation of turbulence model effect)
Time Integration	**MFGS** implicit method with **local** time stepping

References for *Cflow* details

1. Ueno, Y. and Ochi, A., "***Airframe Noise Prediction Using Navier-Stokes Code with Cartesian and Boundary-fitted Layer Meshes,***" 25th AIAA/CEAS Aeroacoustics Conference, (AIAA 2019-2553).
2. Atsushi Hashimoto, Takashi Aoyama, Yuichi Matsuo, Makoto Ueno, Kazuyuki Nakakita, Shigeru Hamamoto, Keisuke Sawada, Kisa Matsushima, Taro Imamura, Akio Ochi, and Minoru Yoshimoto, "***Summary of First Aerodynamics Prediction Challenge (APC-I),***" 54th AIAA Aerospace Sciences Meeting, AIAA SciTech, (AIAA 2016-1780).
3. Yasushi Ito, Mitsuhiro Murayama, Atsushi Hashimoto, Takashi Ishida, Kazuomi Yamamoto, Takashi Aoyama, Kentaro Tanaka, Kenji Hayashi, Keiji Ueshima, Taku Nagata, Yosuke Ueno and Akio Ochi, "***TAS Code, FaSTAR and Cflow Results for the Sixth Drag Prediction Workshop,***" *Journal of Aircraft*, Vol. 55, No. 4, pp. 1433-1457, 2018.
4. Yasushi Ito, Mitsuhiro Murayama, Yuzuru Yokokawa, Kazuomi Yamamoto, Kentaro Tanaka, Tohru Hirai, Hidemasa Yasuda, Atsushi Tajima and Akio Ochi, "***JAXA's and KHI's Contribution to the Third High Lift Prediction Workshop,***" Journal of Aircraft, Vol. 56, No. 3, pp.1080-1098, 2019.

Grid comparison

*These conform to the mesh generation guidelines(fuselage cell size, chord/spanwise spacing, y+ etc.) of HLPW4 and are equivalent to LevelC.

	CflowGrid	JaxaGrid	PointwiseGrid
Total number of cells	384M	209M	142M
Cell size @x≈44m	55mm	39mm	24mm
xz plane	wing surface @y=16m	wing surface @y=16m	wing surface @y=16m

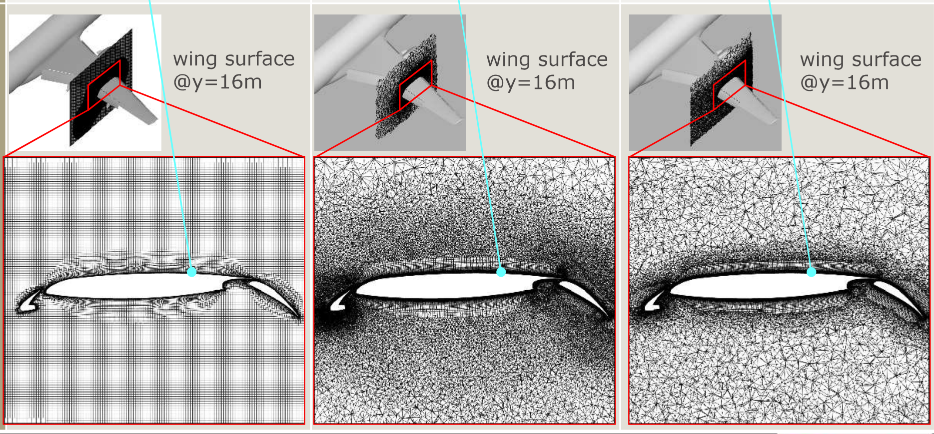

Grid dependency study

	SA-neg	SA-R-QCR	SA-R
CflowGrid	○	○	○
JaxaGrid	○		
PointwiseGrid	○		

In this presentation, CL is averaged and flow visualization is instantaneous.

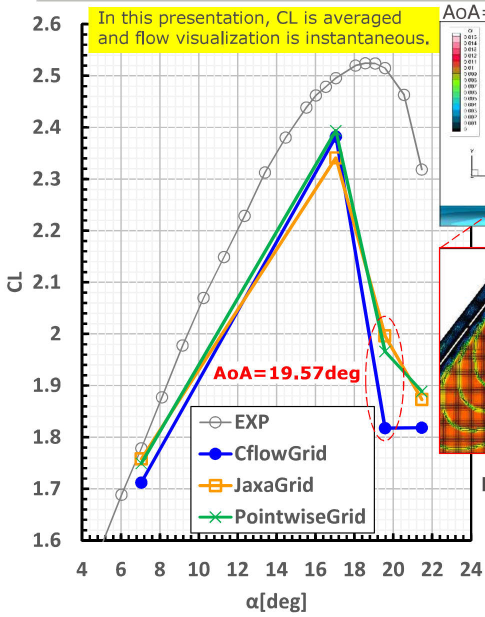

AoA=19.57deg

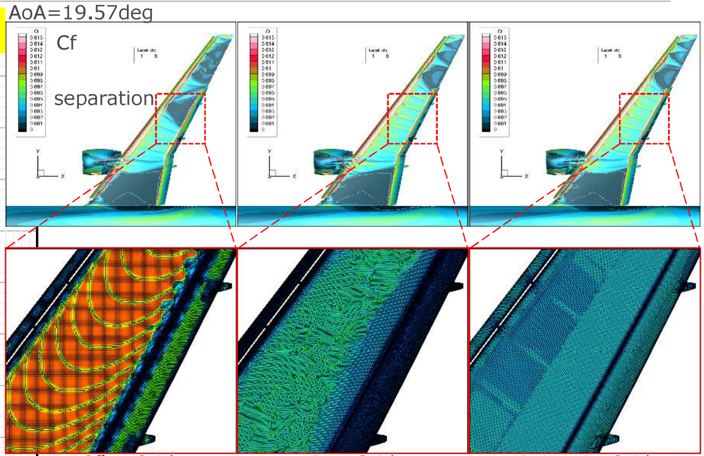

CflowGrid JaxaGrid PointwiseGrid

Largest cell size

cell volume of first cell off the wall : 0 – 0.0035[m³]

- CflowGrid has the largest grid spacing on the wing.

There is a possibility that it is necessary to pay attention to the surface grid spacing of the wing even if the grid is the same Level C.

Effect of turbulence model

Motivation for changing turbulence model

	SA-neg	SA-R-QCR	SA-R
CflowGrid	○	○	○
JaxaGrid	○		
PointwiseGrid	○		

AoA=17.98deg (equivalent to AoA=19.57deg for CFD)

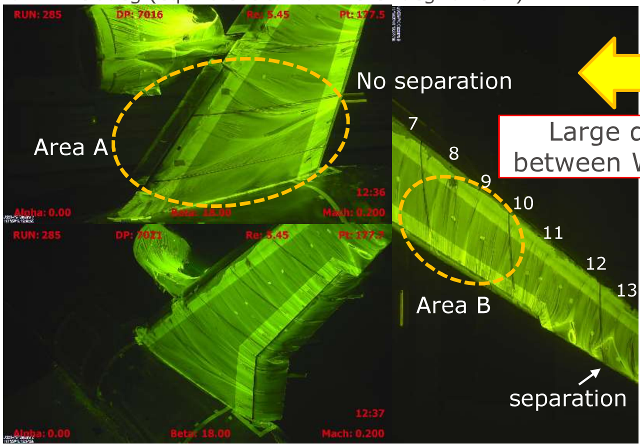

Large differences between WTT and CFD

AoA=19.57deg

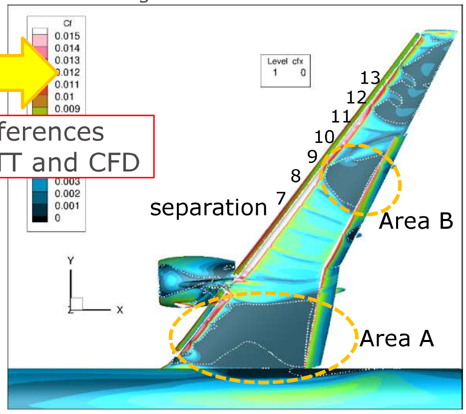

In the case of SA-neg, large separation occurs at AoA=19.57deg in 3 grids.

- Change Turbulence Model to Reduce Separation in CFD
  - to suppress separation on area A → add QCR
  - to suppress separation on area B → add R (Rotation Correction)

Turbulence model is changed to SA-R-QCR to assess wing outboard/root effects.

Next slide

Kawasaki Powering your potential

Effect of turbulence model

SA-neg vs. SA-R-QCR

	SA-neg	SA-R-QCR	SA-R
CflowGrid	○	○	○
JaxaGrid	○		
PointwiseGrid	○		

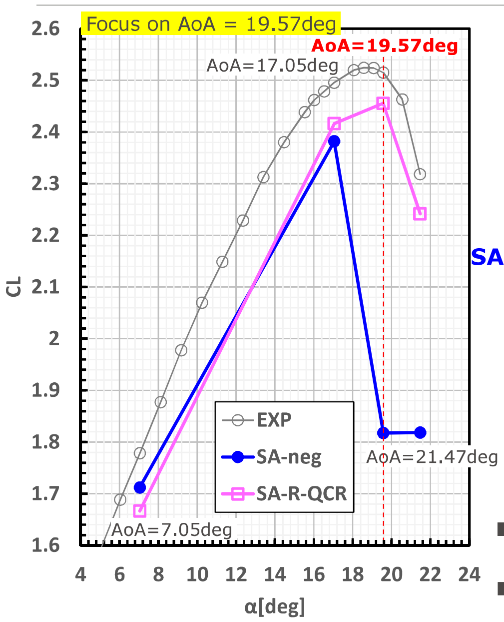

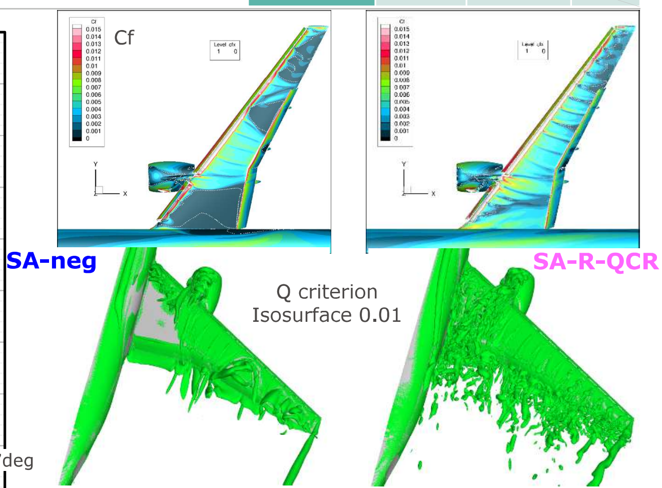

- By changing the turbulence model from SA-neg to SA-R-QCR CL approaches the WTT results.
- Differences appeared in both the corner flow and the vortex generated from the outboard wing.

Application of both R and QCR supress root and outboard separation.

Kawasaki Powering your potential

Effect of turbulence model SA-R-QCR vs. SA-R (1/2)

	SA-neg	SA-R-QCR	SA-R
CflowGrid	○	○	○
JaxaGrid	○		
PointwiseGrid	○		

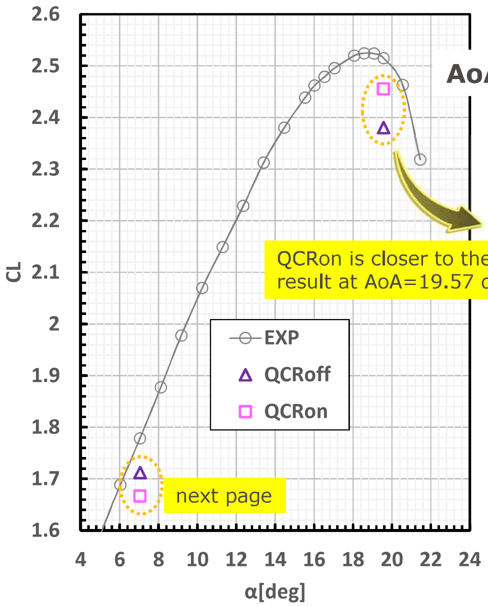

AoA=19.57deg

p.9 and 10 shows effect of QCR at AoA=19.57 and 7.05deg.

dCp(□ - △)

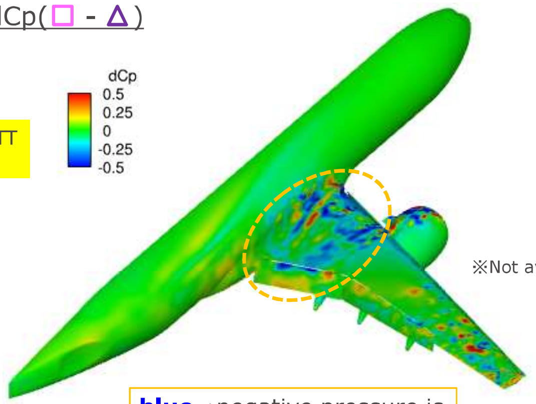

※Not avaraged

blue→negative pressure is **large@QCRon**

- QCRon approaches WTT at a high AoA.
- There is a difference between QCRon and QCRoff on the wing root side ; the negative pressure of QCRon is larger on the wing root side.

Effect of turbulence model SA-R-QCR vs. SA-R (2/2)

	SA-neg	SA-R-QCR	SA-R
CflowGrid	○	○	○
JaxaGrid	○		
PointwiseGrid	○		

AoA=7.05deg

The total CL of QCRoff is larger at AoA=7.05deg, differing from at AoA=19.57deg, and is close to the WTT result. (see p.9)

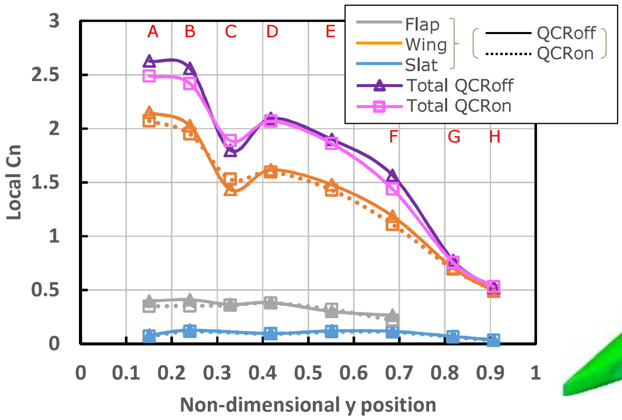

red→negative pressure is **large@QCRoff**

dCp(□ - △)

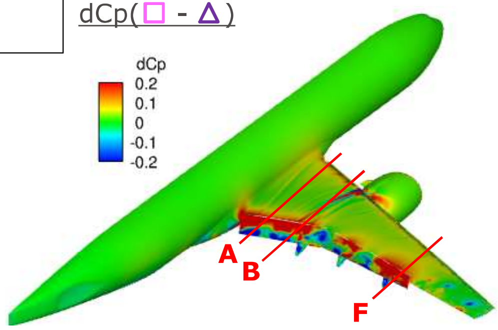

- QCRoff has a larger Cn than QCRon in the A and B sections on the wing root side and in the F section of the outboard wing.
- The Cp distribution in the flap is different between QCRon and QCRoff.
- It is necessary to see not only the integral value but also the flow field.

The turbulence model approaching the WTT result at high and low AoAs are not identical.

Effect of turbulence model Sensitivity of Crot (SA-R-QCR)

	SA-neg	SA-R-QCR	SA-R
CflowGrid	○	○	○
JaxaGrid	○		
PointwiseGrid	○		

Based on this study, it is considered that QCR is effective in predicting high AoA. (see p.9)
=>We change the Crot of the Rotation Correction in the turbulence model SA-R-QCR to analyze its sensitivity.

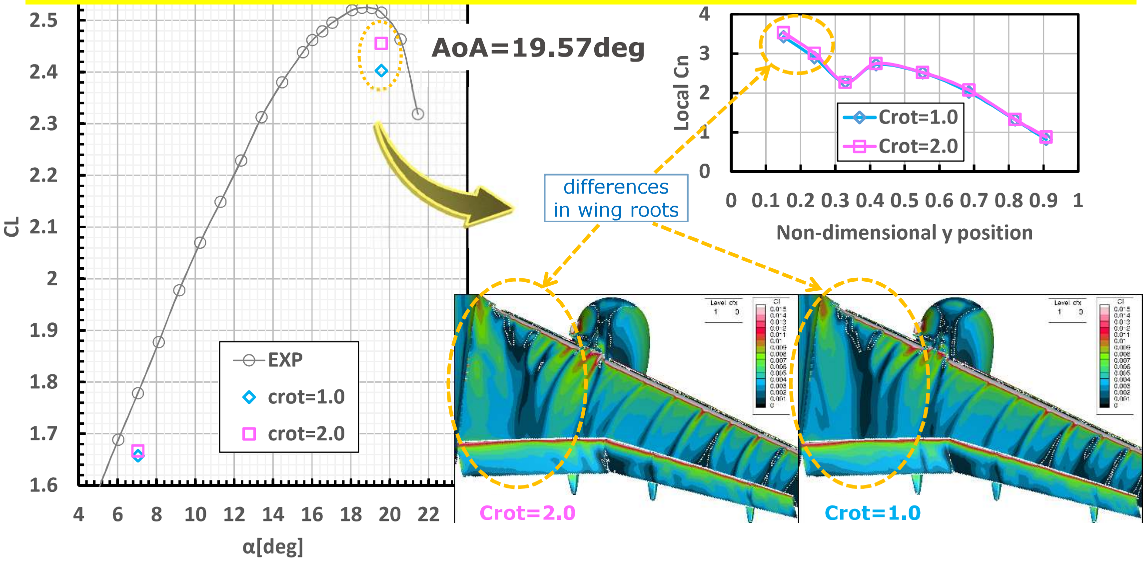

- The sensitivity analysis of Crot without changing the condition of QCRon shows a difference on the wing root side.

In this study, Crot = 2.0 is better.

Kawasaki Powering your potential

Summary

- The grid dependency on the 3 grids and the effects of the turbulence model on the CRM-HL configuration were investigated.
- Lessons Learned
  - Grid dependency study
    - There is a possibility that it is necessary to pay attention to the surface grid spacing of the wing even if the grid is the same Level C.
  - Effect of turbulence model
    - At AoA=19.57deg, the **SA-R-QCR (Crot=2.0)** had the closest value to the WTT.
    - The turbulence model approaching the WTT result at high and low AoAs are not identical.
    - When SA-R/SA-R-QCR is applied, the effect of turbulence model is commonly observed sensitively on the wing root side.
    - In this study, Crot=2.0 of R (Rotation Correction) is closer to the WTT result than Crot=1.0.

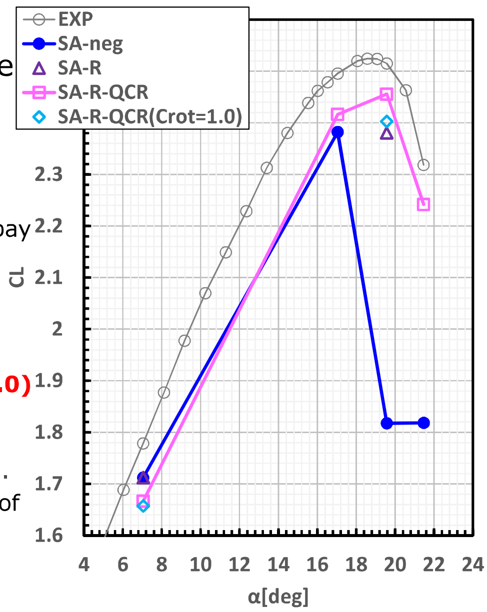

Kawasaki Powering your potential


世界の人々の豊かな生活と地球環境の未来に貢献する
“Global Kawasaki”
Kawasaki
Powering your potential

Eighth Aerodynamics Prediction Challenge (APC-8)
2022/06/29

1C12

Aerodynamic Prediction of CRM-HL Using Hierarchical Cartesian Grid and Immersed Boundary Method

〇Funada Masaya, Imamura Taro
(The University of Tokyo)
Sugaya Keisuke
(JAXA)

Agenda

- Background
- Objective
- Numerical methods
- Case4 : 2D CRM-HL
- Case1 : 3D CRM-HL
- Conclusions

Background 1

- UTCart (The University of Tokyo Cartesian grid based automatic flow solver)
  - Unstructured hierarchical Cartesian grid
  - Automatic and robust grid generation
  - The Immersed Boundary Method with a wall function*1

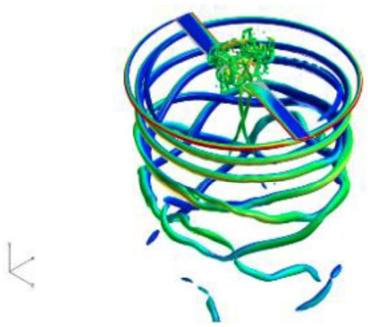

菅谷, and 今村, 流力ANSS2021

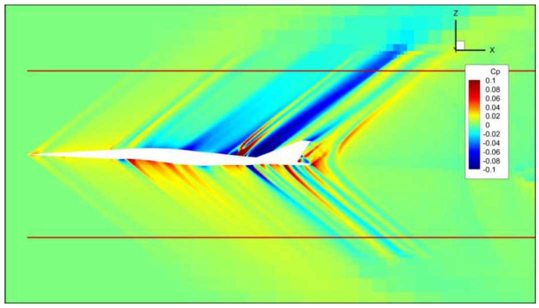

1) Tamaki, Harada, and Imamura, AIAA J., Vol 55, 2017

Background 2

- Until now, the upper limit of the number of grids in UTCart has been about 200 million
  - Some variables exceed the integer4 limit
  - Visualization software do not support integer8
- Extend the upper limit of number of grids
  - The type of some variables has been changed to integer8
  - Visualization data is output separately

  →Flow simulations with about 400 million grids can now be performed

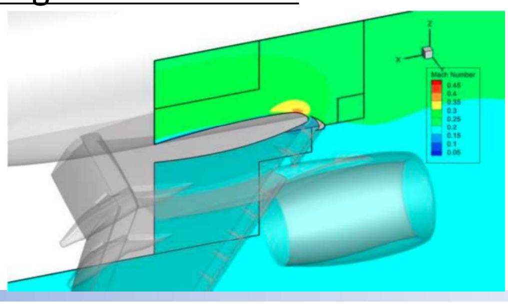

Objective

- **To evaluate the prediction accuracy of Immersed Boundary Method with a wall function for low-speed simulations of high-lift device configuration**
  - The effects of grid width are investigated
  - Steady computations
    - Case4 : 2D CRM-HL
    - Case1 : 3D CRM-HL
      - Up to 400 million grids

Immersed Boundary Method

- Flow variables are extrapolated from Image Point (IP)
- Wall function is used to determine the wall shear stress
- Assuming that tangential velocity is linear between the wall and IP

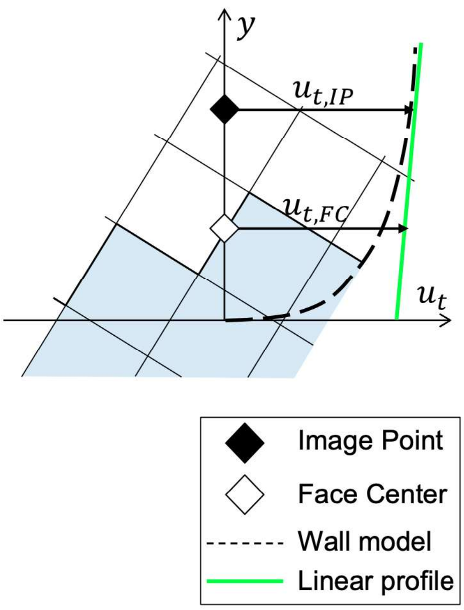

Numerical methods

Governing Equation	RANS
Turbulence Model	SA-noft2
Inviscid Flux	SLAU+3rd-order MUSCL
Viscous Flux	2nd-order central difference
Time Integration	MFGS (Local Time Stepping)
Wall Boundary Condition	IB+SA wall model
Distance between IP and wall	$3\Delta x$
Initial Condition	Free stream

東京大学 THE UNIVERSITY OF TOKYO

7

Case4
2D CRM-HL

東京大学 THE UNIVERSITY OF TOKYO

Computational grid

- CFL number is 20 in all grids

	#1	#2	#3	#4	#5	#6	#7
Minimum grid width	1.590×10^{-4}	9.538×10^{-5}	4.768×10^{-5}	2.980×10^{-5}	1.703×10^{-5}	8.515×10^{-6}	4.585×10^{-6}
Grid number	177,164	291,797	577,771	921,351	1,606,333	3,207,629	5,950,335

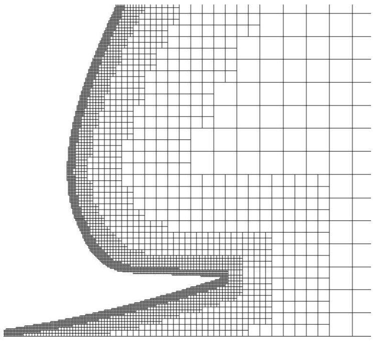

Grid #1

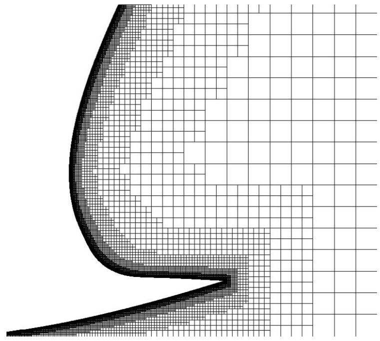

Grid #7

Aerodynamic coefficients

- A fair agreement between UTCart and FUN3D*1 at finest grid
- In the third finest grid, UTCart results differ from FUN3D results
  - IP is in the buffer layer (y_{IP}^{+} : 10~30)
- If IP is not in the buffer layer, the prediction accuracy is reasonable

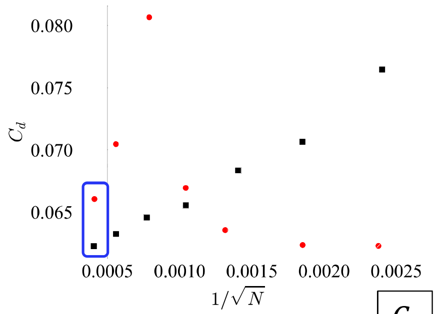

C_d

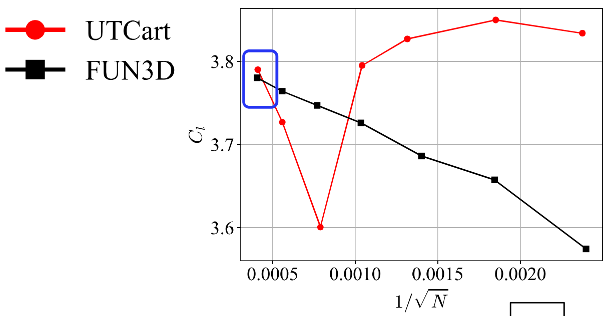

C_l

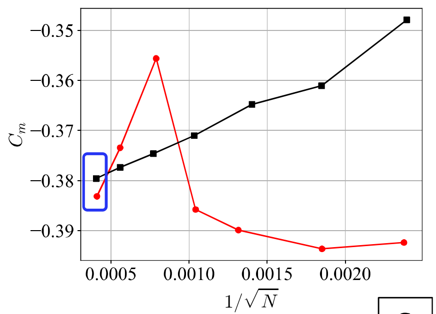

C_m

1) https://turbmodels.larc.nasa.gov/

Surface pressure coefficient

- A fair agreement with FUN3D results, except for #5-grid

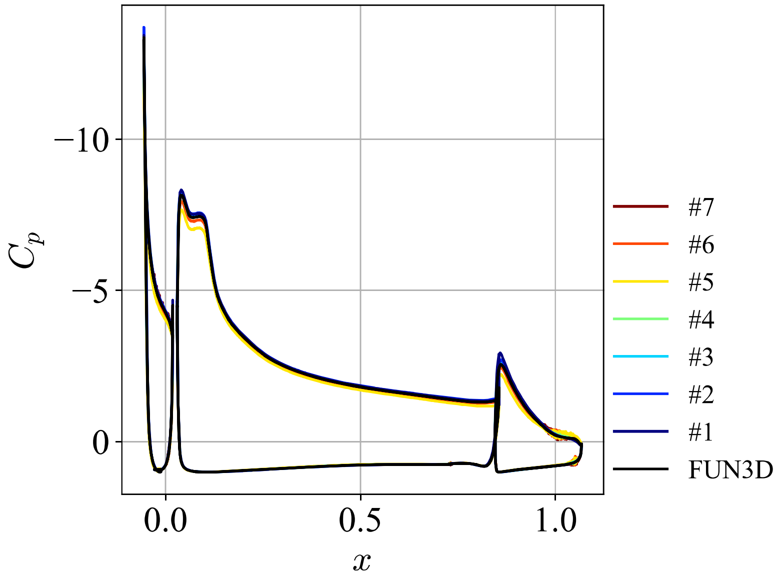

Case1
3D CRM-HL

Computational grid

- Unstructured hierarchical Cartesian grid
- Three grids are used
- IP is in the log layer

	100M-grid	200M-grid	400M-grid
Number of Grids	103,640,578	194,862,769	409,626,109
Reference Grid width (Δx_{ref})	$9.537 \times 10^{-4} C_{MAC}$	$6.936 \times 10^{-4} C_{MAC}$	$4.768 \times 10^{-4} C_{MAC}$
CFL number	2	20	20

	wing	fuselage	fairing	flap	slat	nacelle	pylon
Minimum grid width	Δx_{ref}	$4\Delta x_{ref}$	$0.5\Delta x_{ref}$	Δx_{ref}	Δx_{ref}	$4\Delta x_{ref}$	$2\Delta x_{ref}$

Computational grid

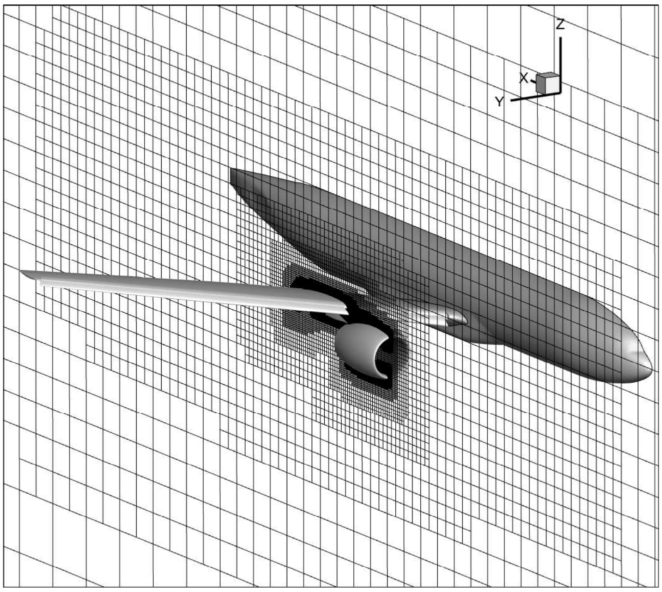

200M-grid

Time history

- Almost converged solutions

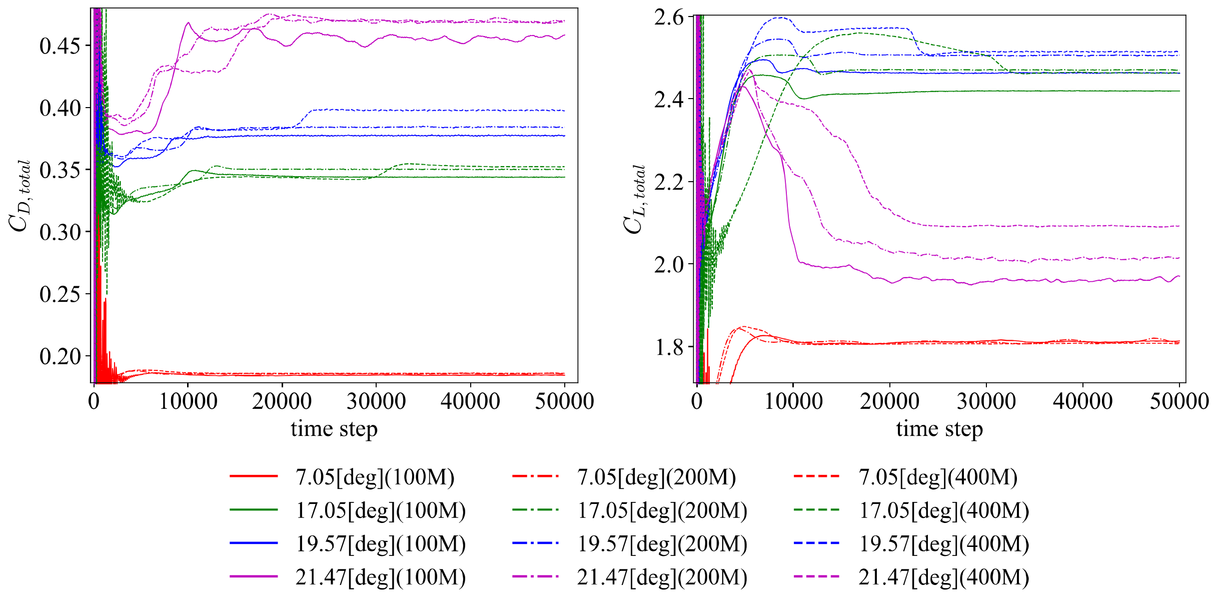

東京大学 THE UNIVERSITY OF TOKYO

Aerodynamic coefficients

- A fair agreement between UTCart and exp. at low AoA
- Smaller C_L, larger C_D, and larger C_M of UTCart than those of exp. at high AoA
- No grid convergence in C_D and C_M at high AoA

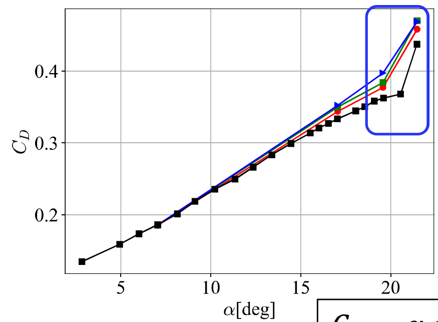

$C_D - \alpha$ curve

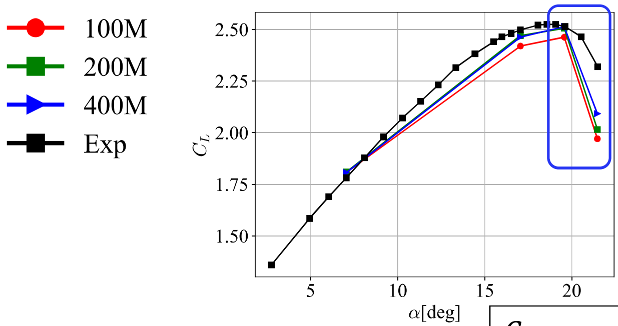

$C_L - \alpha$ curve

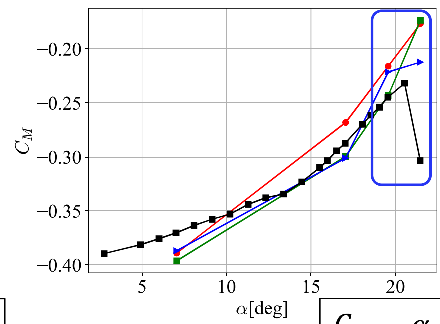

$C_M - \alpha$ curve

東京大学 THE UNIVERSITY OF TOKYO

1) https://hiliftpw.larc.nasa.gov

Skin friction at $C_{L,max}$ (19.57[deg])

- Larger outboard separation compared to exp.
  - Smaller C_L, larger C_D, and larger C_M
  - Also reported in RANS simulations in HLPW*1
- The position of the separation area depends on the grid width

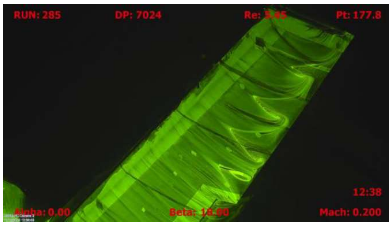

oil-flow photograph*1

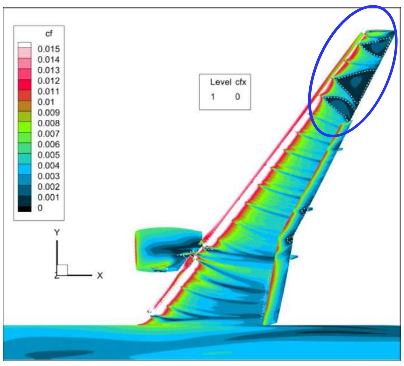

100M-grid

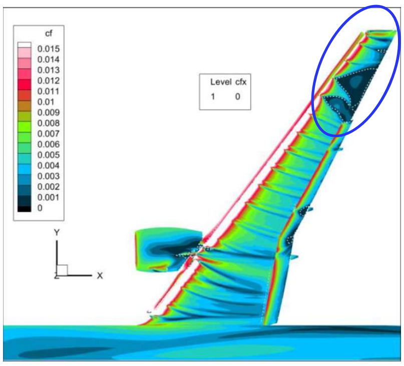

200M-grid

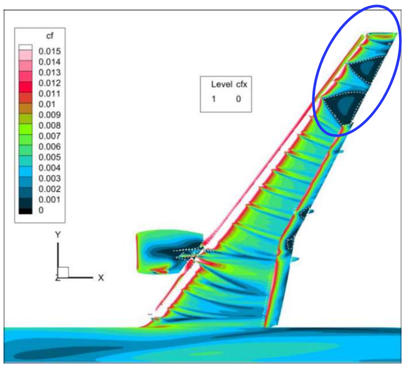

400M-grid

東京大学 THE UNIVERSITY OF TOKYO

1) https://hiliftpw.larc.nasa.gov

Conclusion

- **Steady flow simulations around CRM-HL were conducted with UTCart (IB+SA wall model)**
  - Case4 : 2D CRM-HL
    - A fair agreement between UTCart and FUN3D at finest grid
    - If IP is in the log layer, the prediction accuracy is reasonable
  - Case1 : 3D CRM-HL
    - A fair agreement to exp. at low AoA
    - Larger outboard separation compared to exp. at high AoA
    - The calculation results were dependent on grid width
    - Grid convergence was not observed in C_D and C_M at high AoA

→ <u>IB+SA wall model can analyze high-lift device configurations with reasonable accuracy</u>

東京大学 THE UNIVERSITY OF TOKYO

The 54th Fluid Dynamics Conference/ The 40th Aerospace Numerical Simulation Symposium
29th June 2022

APC-8の集計結果

Summary of Eighth Aerodynamics Prediction Challenge (APC-8)

橋本 敦 (JAXA)
Hashimoto Atsushi(JAXA)

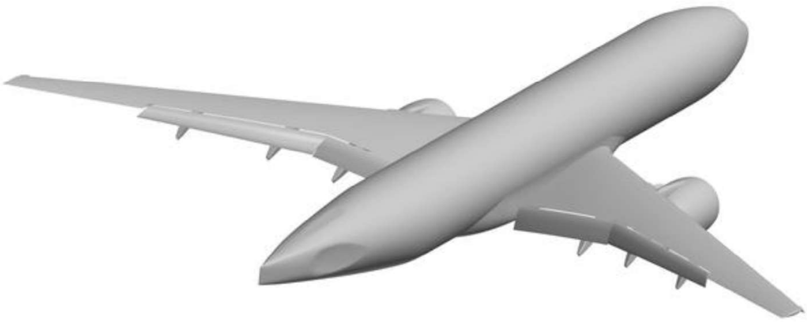

Statistics of submitted data

- Organizations and number of submitted data(total 21 data)
  - National research institutes：JAXA(9)
  - Aerospace industry: KHI(8)
  - Vender: Hexagon(1)
  - University: Univ. of Tokyo(3)
- Grid
  - HLPW4 grid generated by MEGG3D: 7
  - HLPW4 gird generated by Pointwise: 2
  - HLPW4 grid generated by ANSA: 2
  - Custom grid: 7
  - TMR提供格子(FAMILY1): 3
- Code
  - Unstructured solver(19)
  - Unstructured Cartesian solver(3)
- Turbulence model
  - SA(21)
- Initial condition
  - Cold start(17)：Calculation from the uniform flow solution
  - Warm start(4)：Calculation from the low angle of attack solution

Participants of Case 1

ID	Name	Organization	Code	Grid (generated by)	Description of the grid	Turbulence Model	Initial Condition
A1	Zauner Markus	JAXA	FaSTAR (Unstructured solver)	HLPW4(MEGG3D)		SA-noft2	Cold start
A2						SA-noft2-R-QCR2000	
A3						SA-noft2	Warm start
A4						SA-noft2-R-QCR2000	
B1	山内優果	KHI	Cflow (Unstructured solver)	HLPW4(MEGG3D)		SA-neg	Uniform flow
B2				HLPW4(Pointwise)	Pointwise grid(1.3.C)		
B3				HLPW4(ANSA)	ANSA(101.C)		
B4				Custom	Orthogonal octree + Body-Fitted layer grid	SA-neg	
B5						SA-R-QCR	
C1	古谷龍太郎	JAXA	TAS (Unstructured solver)	HLPW4(MEGG3D)		SA-noft2-R(Crot=1)	Uniform flow
C2							Low angle of attack
D1	中島吉隆	Hexagon	scFLOW (Unstructured solver)	Custom	Polyhedral mesh generated by scFLOW	SA-neg	Uniform flow
E1	船田雅也	Univ. of Tokyo	UTCart (Unstructured Cartesian solver)	Custom	Hierarchical orthogonal grid(100M)	SA-noft2 +Wall function	Uniform flow
E2					Hierarchical orthogonal grid(200M)		
E3					Hierarchical orthogonal grid(400M)		

3

Participants of Cases 3 and 4

Case 3

ID	Name	Organization	Code	Grid (generated by)	Description of the grid	Turbulence Model	Initial Condition
B6	山内優果	KHI	Cflow (Unstructured solver)	HLPW4(ANSA)	ANSA(101_43/40.C)	SA-neg	Uniform flow
B7				Custom	Orthogonal octree + Body-Fitted layer grid		
C3	古谷龍太郎	JAXA	TAS (Unstructured solver)	HLPW4(Pointwise)	Pointwise-Smoothed grid(2.2-Pointwise-Unstr-PrismTet-V2_43/40)	SA-noft2-R(Crot=1)	Low angle of attack

Case 4

ID	Name	Organization	Code	Grid	Description of the grid	Turbulence Model	Initial Condition
B8	山内優果	KHI	Cflow (Unstructured solver)	TMR提供格子 (FAMILY1)		SA-neg	Uniform flow
C4	古谷龍太郎	JAXA	TAS (Unstructured solver)	TMR提供格子 (FAMILY1)		SA-noft2-R(Crot=1)	Uniform flow
C5						SA	

4

Case 1 : Steady computation

- Conditions
  - 3D CRM-HL flap angle : 40°/37°(inboard/outboard)
  - M = 0.2, Re = 5.49 x 10^6 (C_{ref} = 275.8inches), T_{ref} = 521°R
  - AoA = 7.05, 17.05, 19.57, 21.47deg

5

CL-Alpha, Case 1

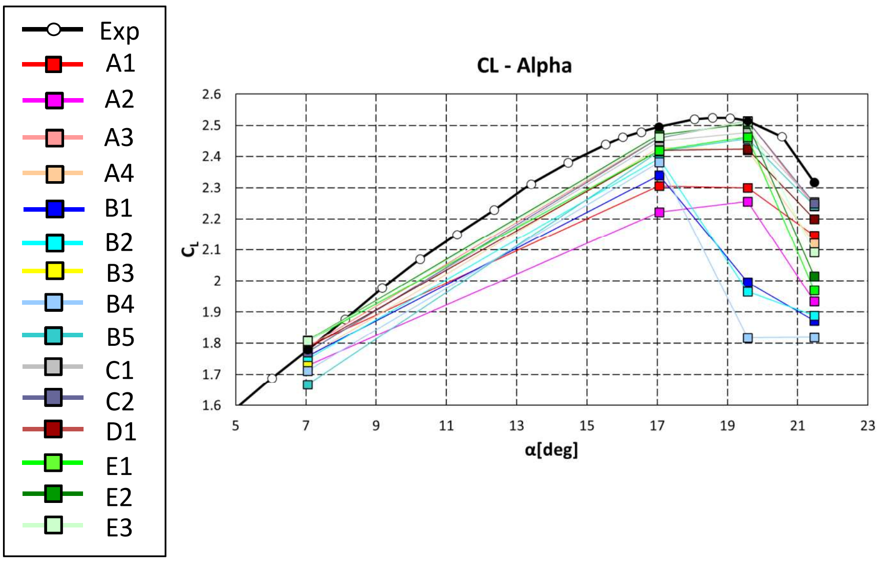

HLPW4
All Best-Practice Results
(03_GMGW3_HLPW4_RANS.pdf, p.17)

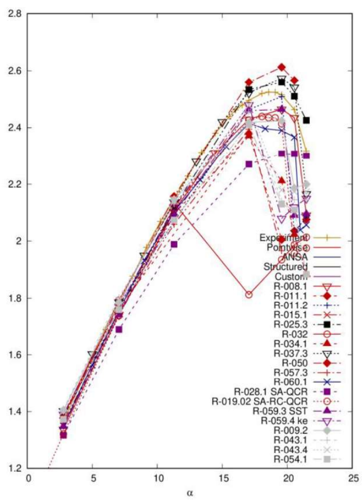

6

CD-Alpha, Case 1

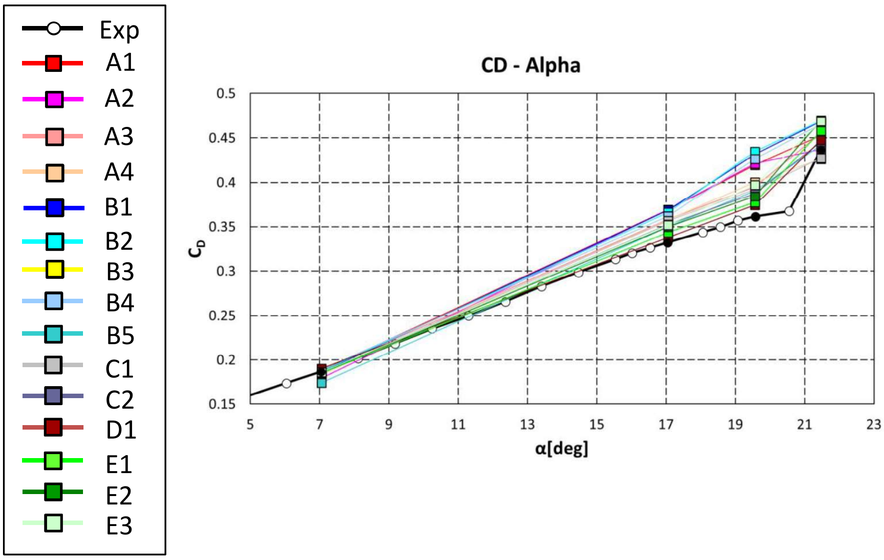

HLPW4
All Best-Practice Results
(03_GMGW3_HLPW4_RANS.pdf, p.17)

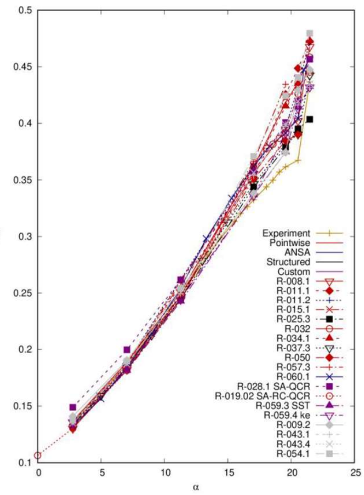

7

Cm-Alpha, Case 1

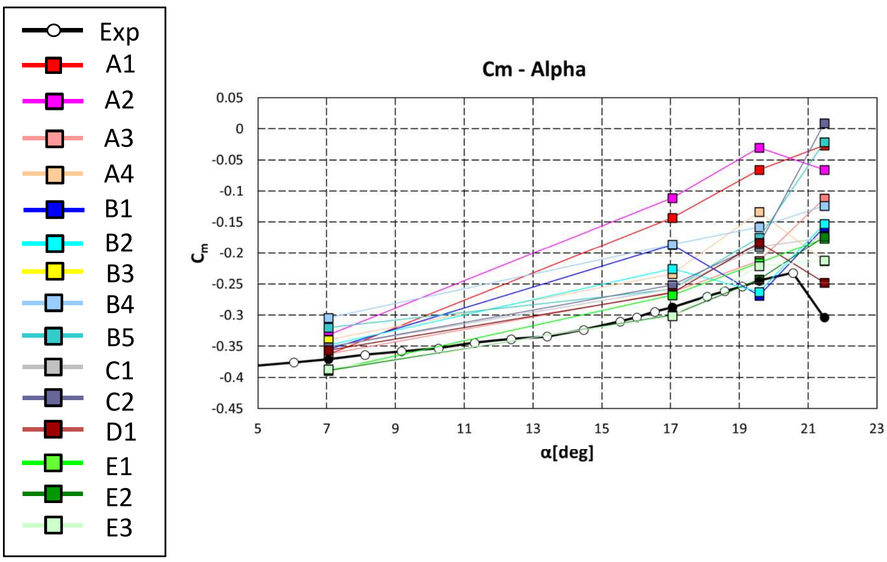

HLPW4
All Best-Practice Results
(03_GMGW3_HLPW4_RANS.pdf, p.17)

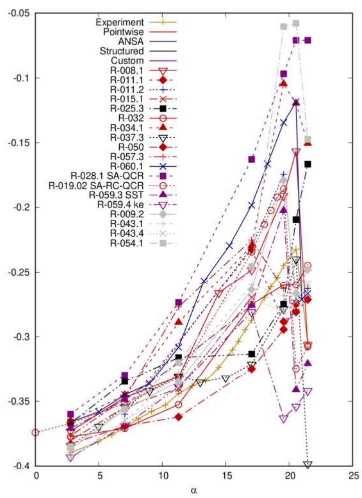

8

Surface Cf Contours（Case 1, 7.05deg, Viewpoint 1）

ID-Grid(generated by)

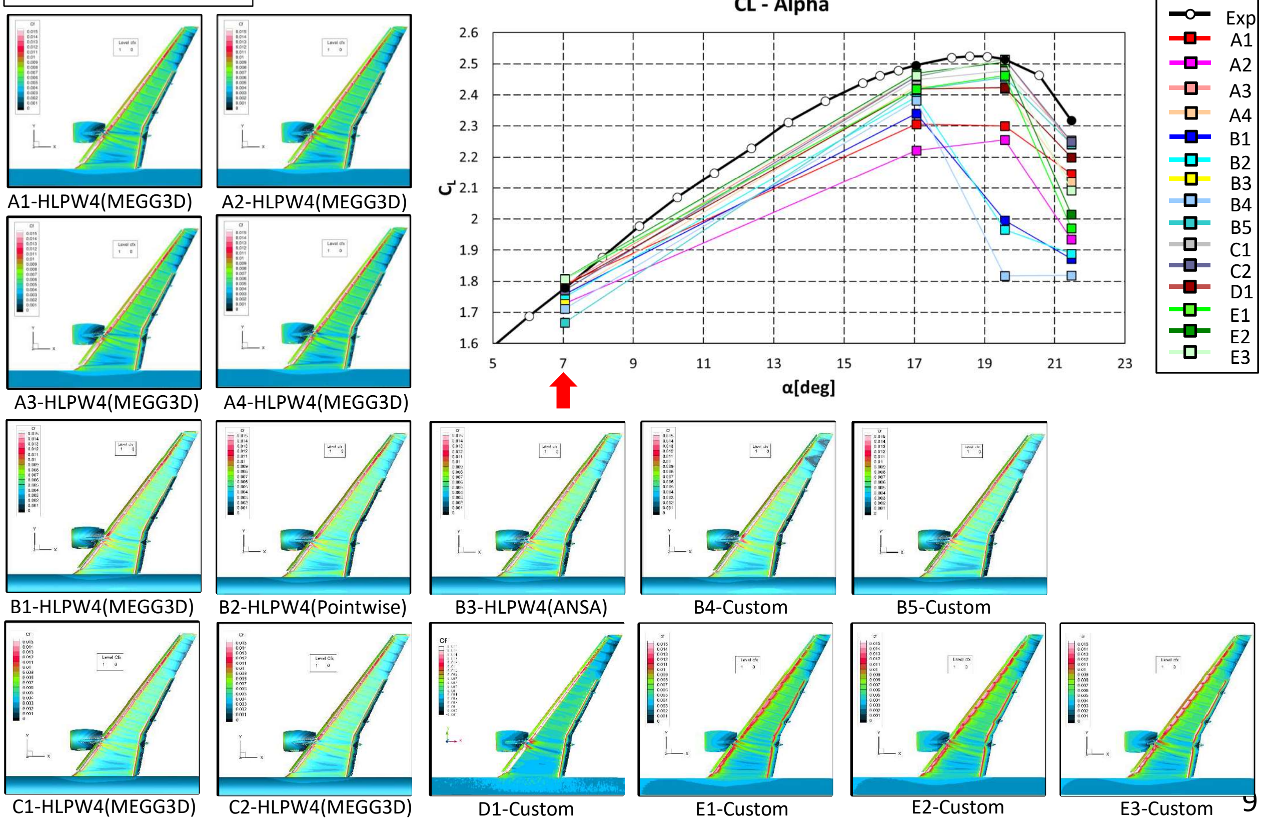

9

Surface Cf Contours（Case 1, 17.05deg, Viewpoint 1）

ID-Grid(generated by)

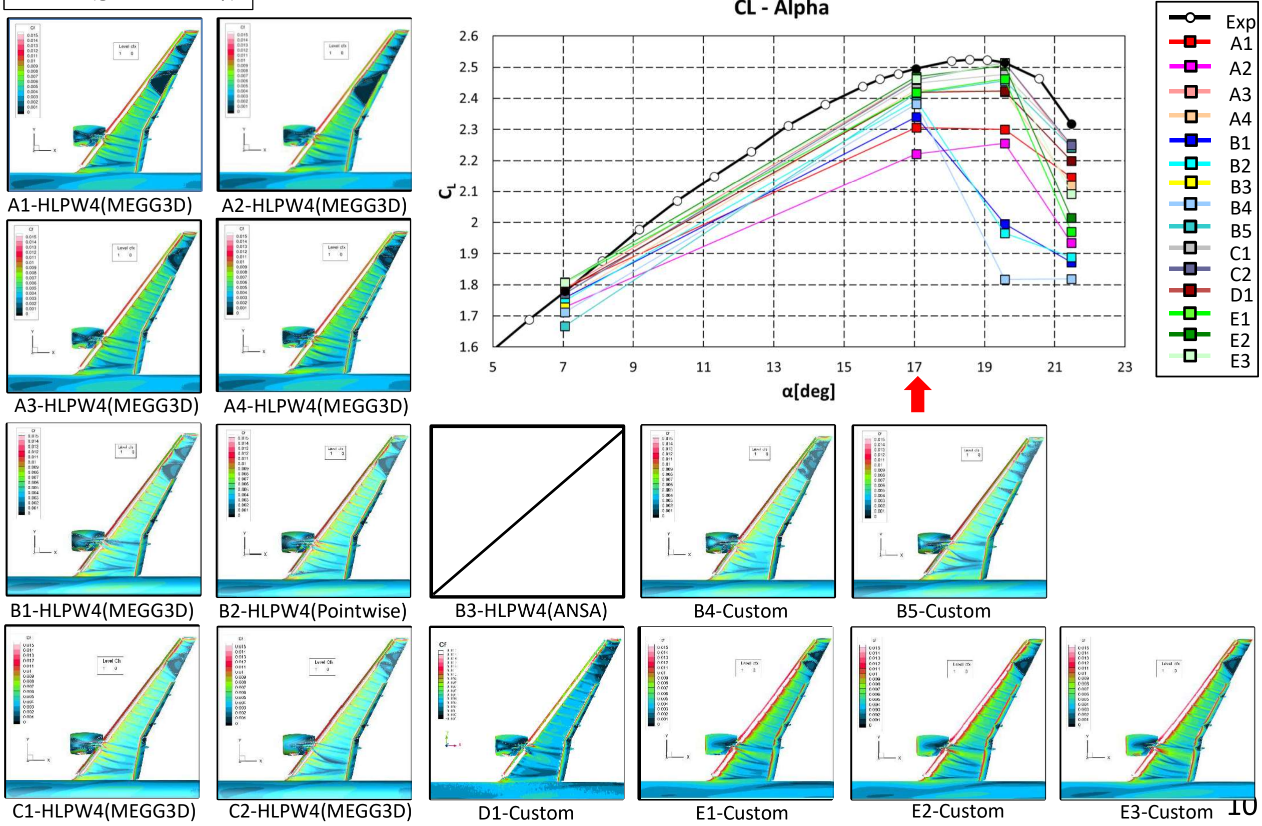

10

Surface Cf Contours（Case 1, 19.57deg, Viewpoint 1）

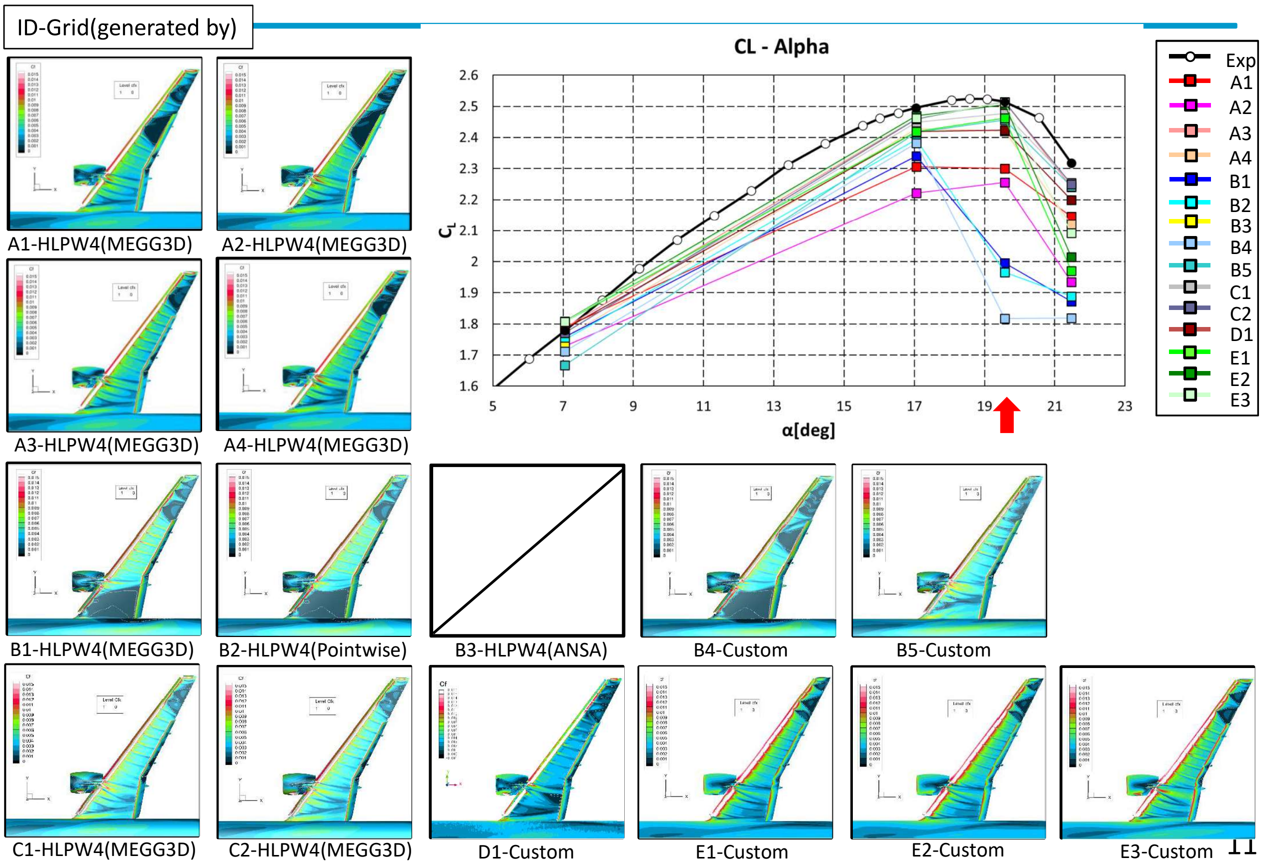

Surface Cf Contours（Case 1, 21.47deg, Viewpoint 1）

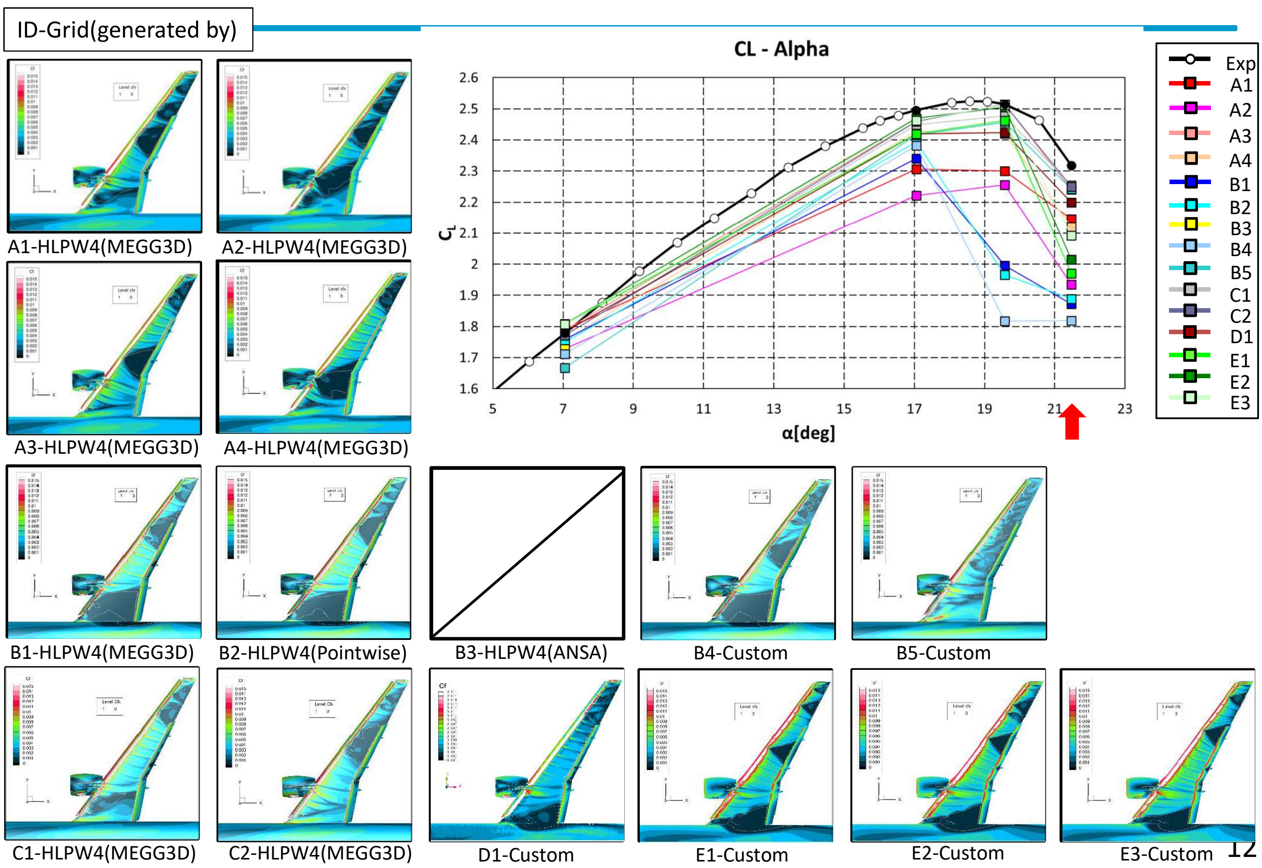

Surface Cf Contours（Case 1, 7.05deg, Viewpoint 2）

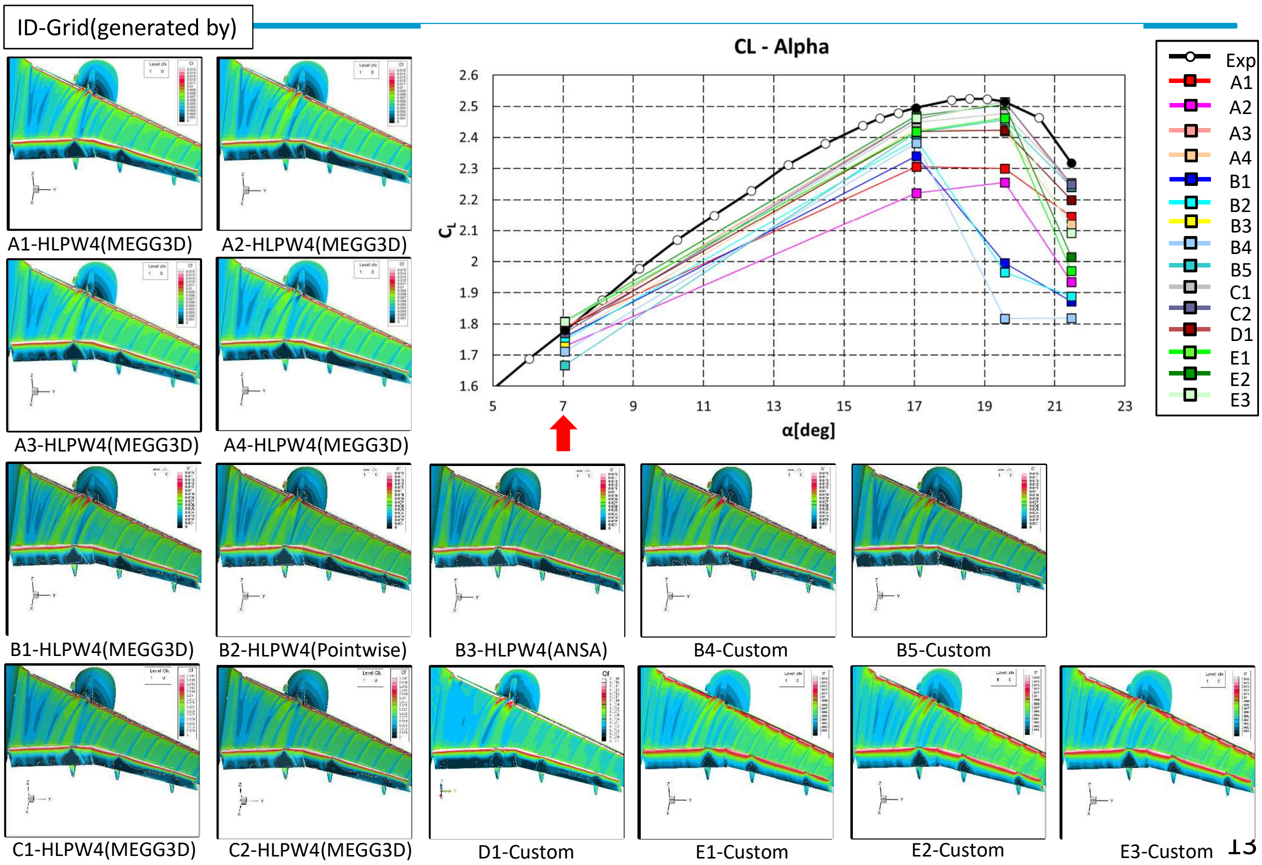

Surface Cf Contours（Case 1, 17.05deg, Viewpoint 2）

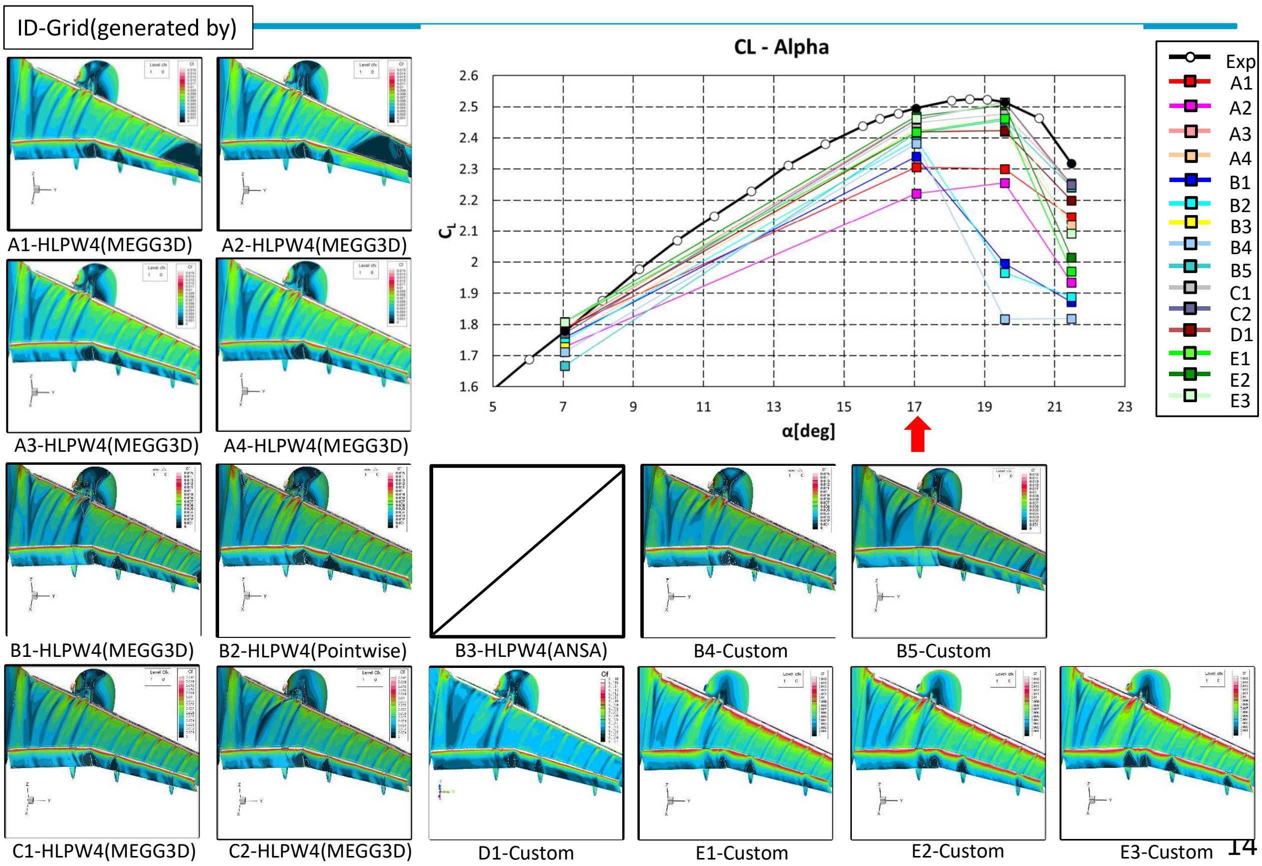

Surface Cf Contours（Case 1, 19.57deg, Viewpoint 2）

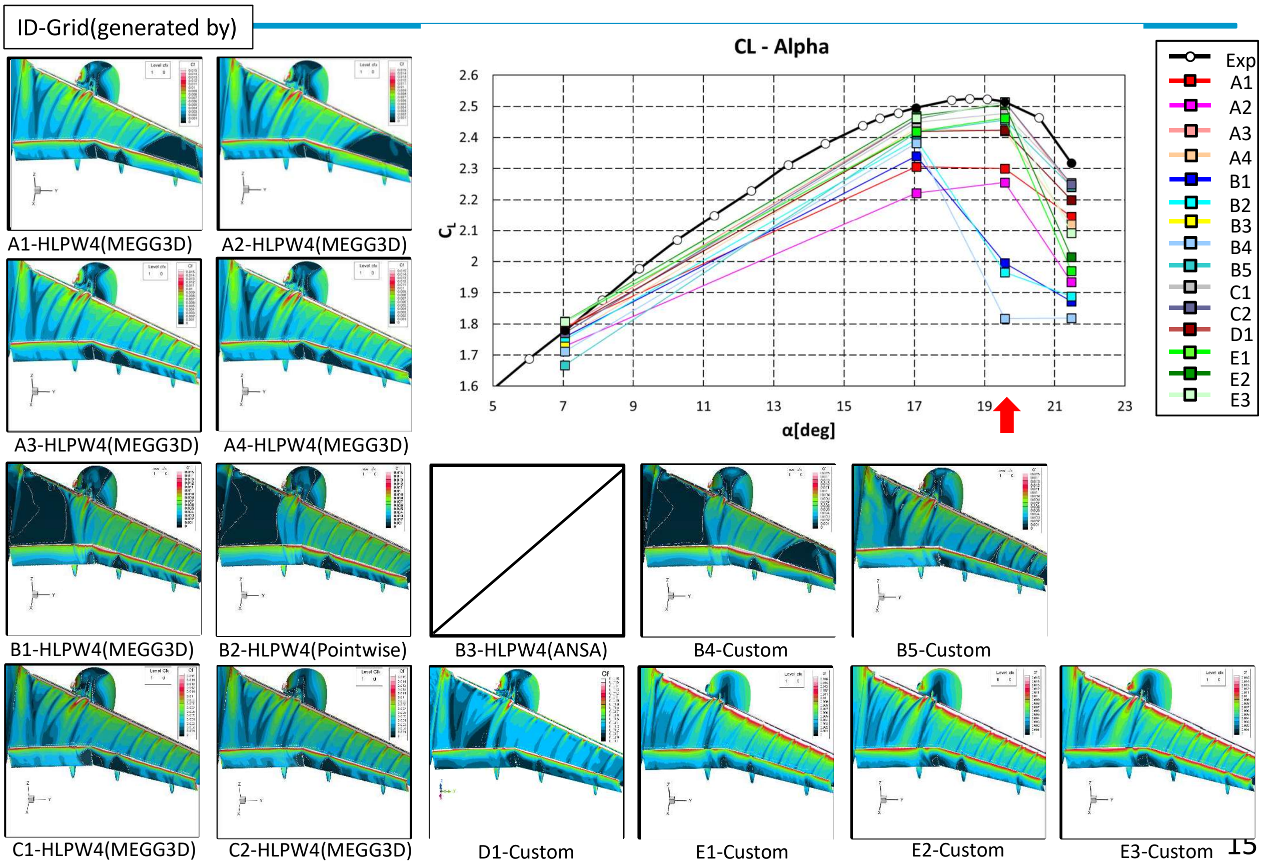

Surface Cf Contours（Case 1, 21.47deg, Viewpoint 2）

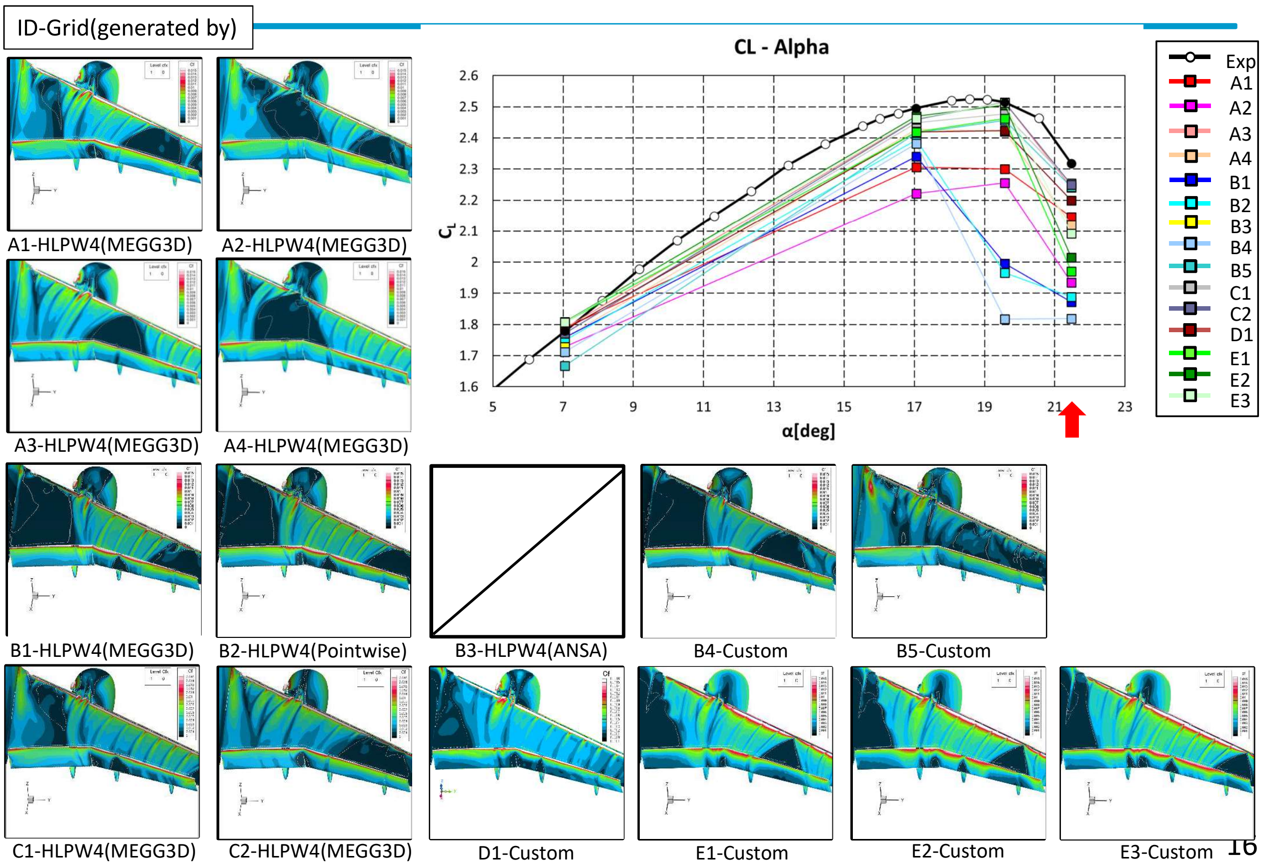

Surface Cf Contours（Case 1, 7.05deg, Viewpoint 2）

ID-Grid(generated by)

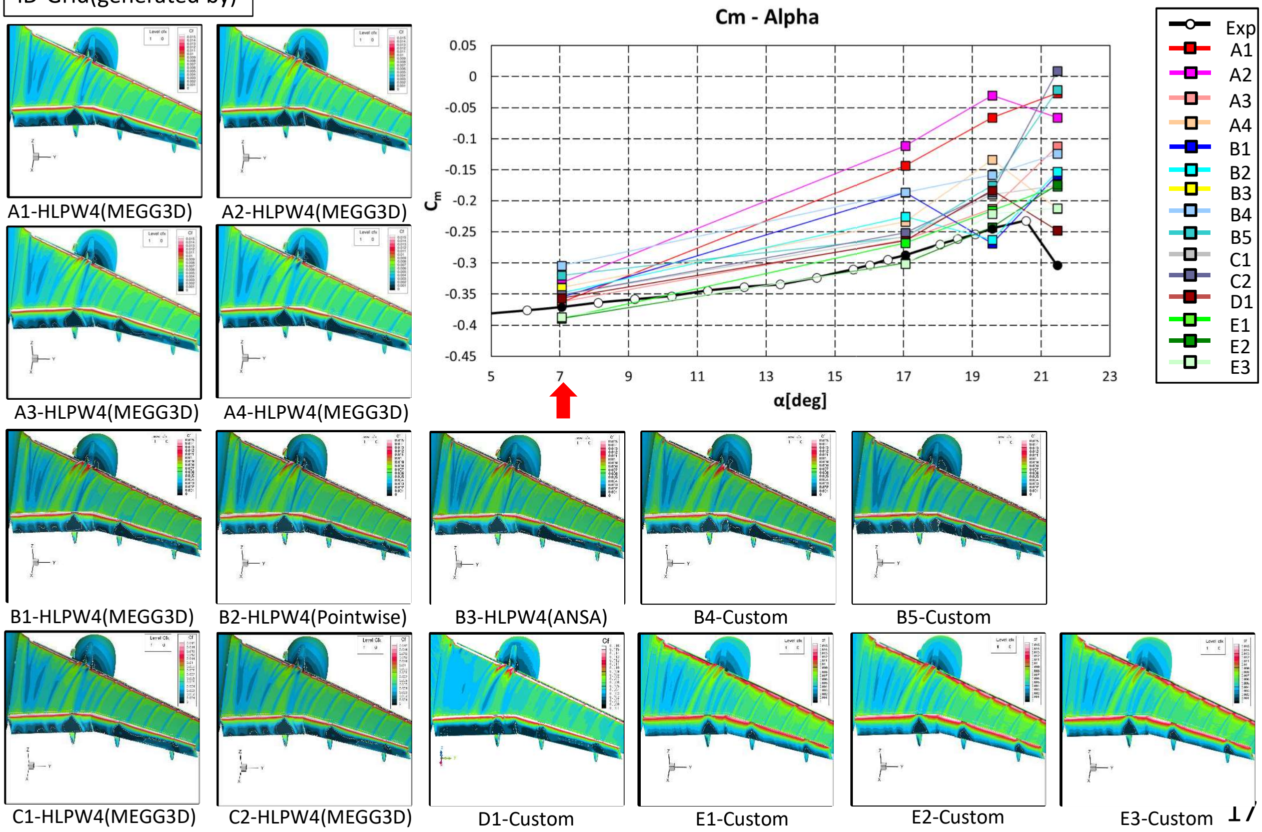

17

Surface Cf Contours（Case 1, 17.05deg, Viewpoint 2）

ID-Grid(generated by)

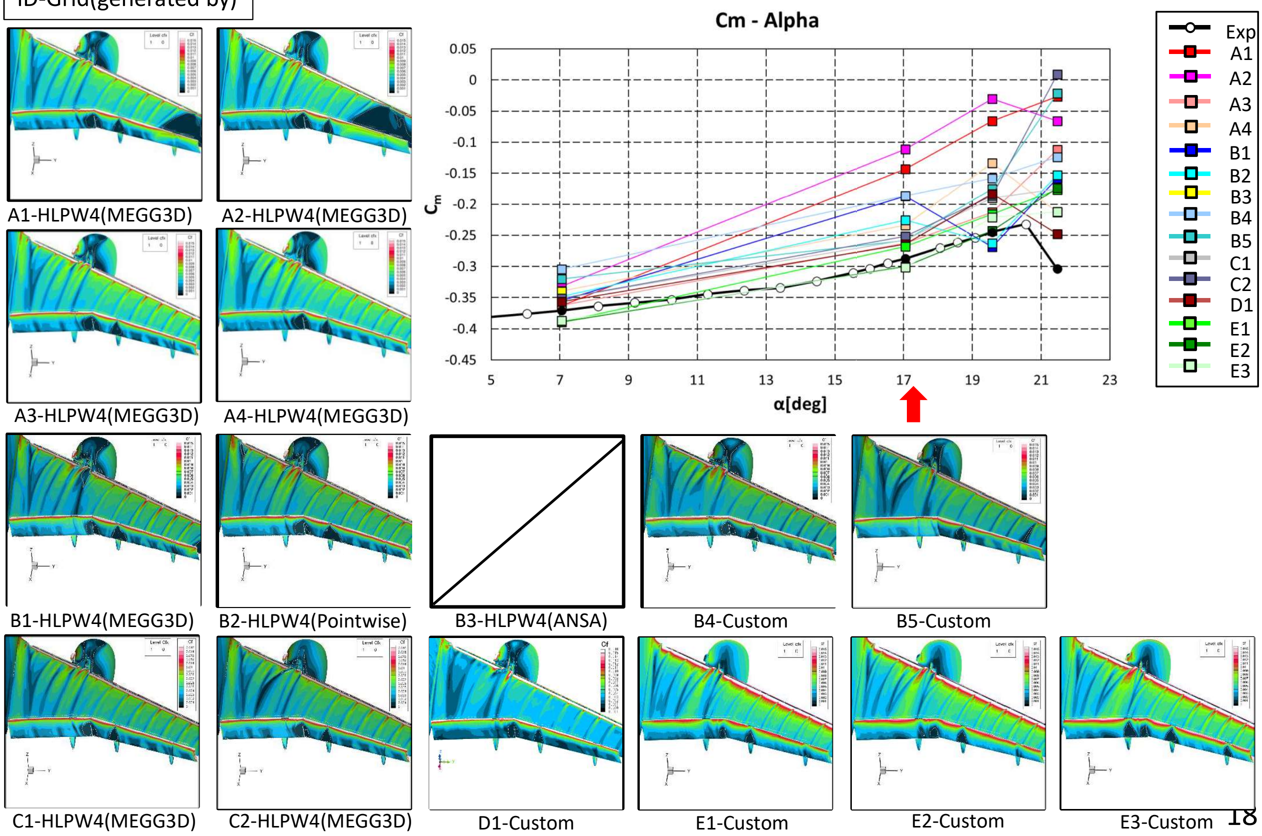

18

Surface Cf Contours（Case 1, 19.57deg, Viewpoint 2）

ID-Grid(generated by)

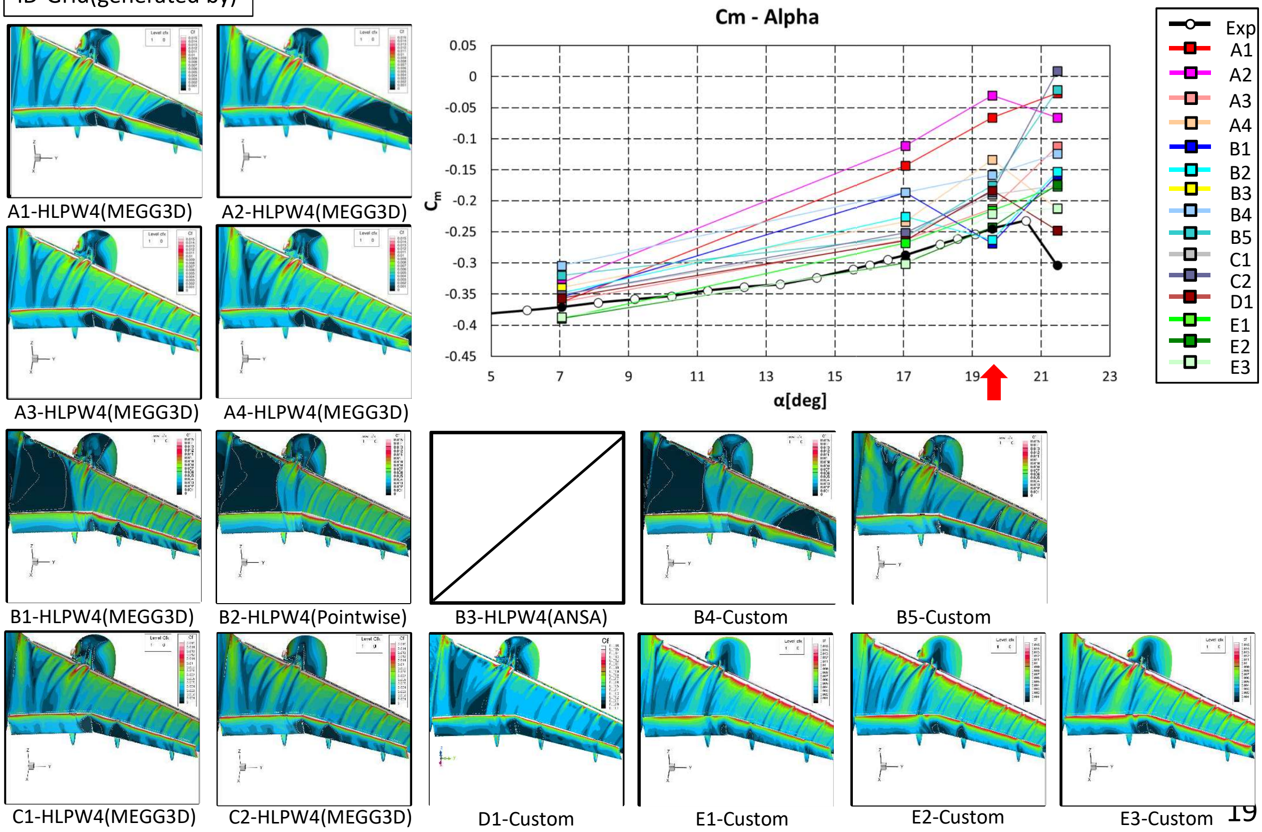

19

Surface Cf Contours（Case 1, 21.47deg, Viewpoint 2）

ID-Grid(generated by)

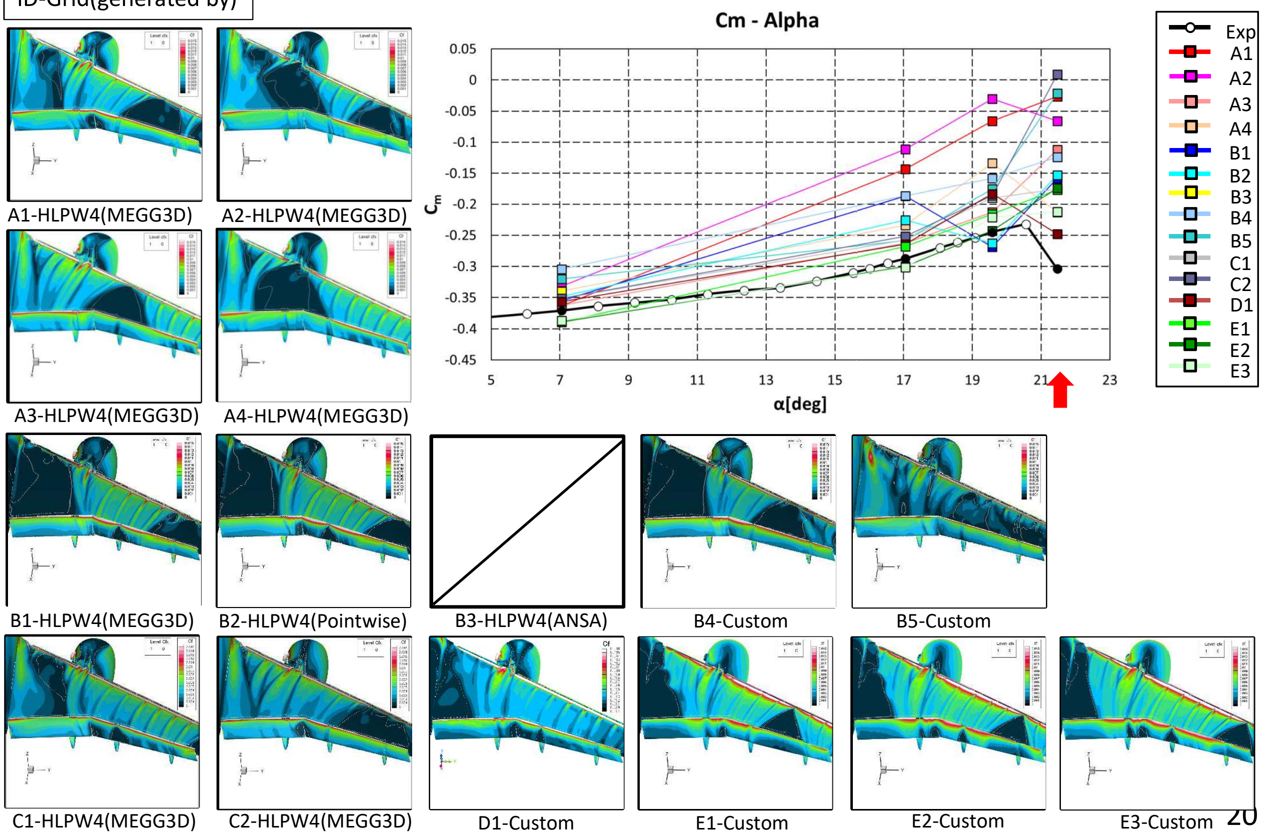

20

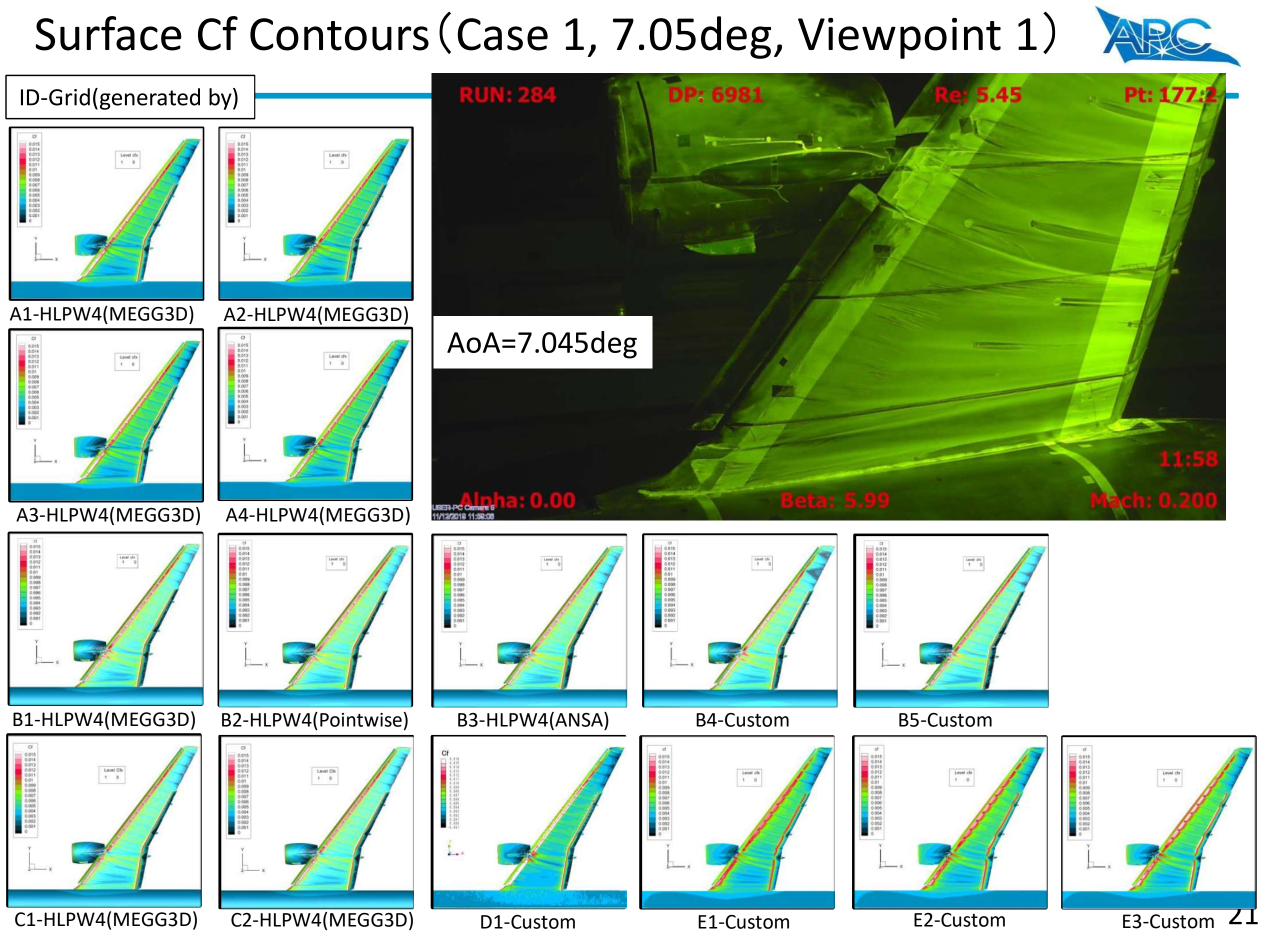
Surface Cf Contours（Case 1, 7.05deg, Viewpoint 1）
APC
ID-Grid(generated by)
RUN: 284
DP: 6981
Re: 5.45
Pt: 177.2
AoA=7.045deg
11:58
Alpha: 0.00
Beta: 5.99
Mach: 0.200
A1-HLPW4(MEGG3D)
A2-HLPW4(MEGG3D)
A3-HLPW4(MEGG3D)
A4-HLPW4(MEGG3D)
B1-HLPW4(MEGG3D)
B2-HLPW4(Pointwise)
B3-HLPW4(ANSA)
B4-Custom
B5-Custom
C1-HLPW4(MEGG3D)
C2-HLPW4(MEGG3D)
D1-Custom
E1-Custom
E2-Custom
E3-Custom
21

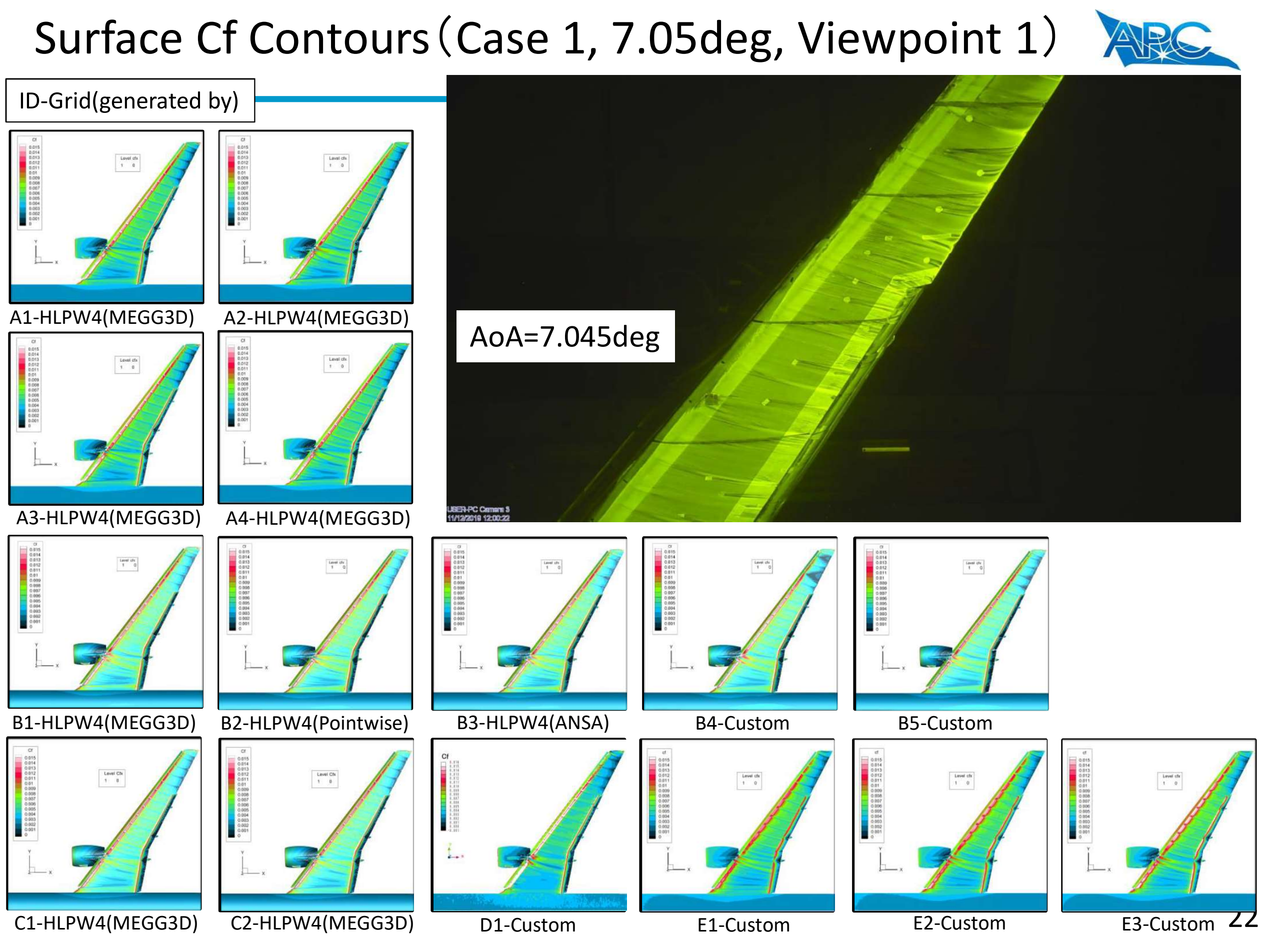
Surface Cf Contours（Case 1, 7.05deg, Viewpoint 1）
APC
ID-Grid(generated by)
AoA=7.045deg
A1-HLPW4(MEGG3D)
A2-HLPW4(MEGG3D)
A3-HLPW4(MEGG3D)
A4-HLPW4(MEGG3D)
B1-HLPW4(MEGG3D)
B2-HLPW4(Pointwise)
B3-HLPW4(ANSA)
B4-Custom
B5-Custom
C1-HLPW4(MEGG3D)
C2-HLPW4(MEGG3D)
D1-Custom
E1-Custom
E2-Custom
E3-Custom
22

Surface Cf Contours（Case 1, 7.05deg, Viewpoint 2）

ID-Grid(generated by)

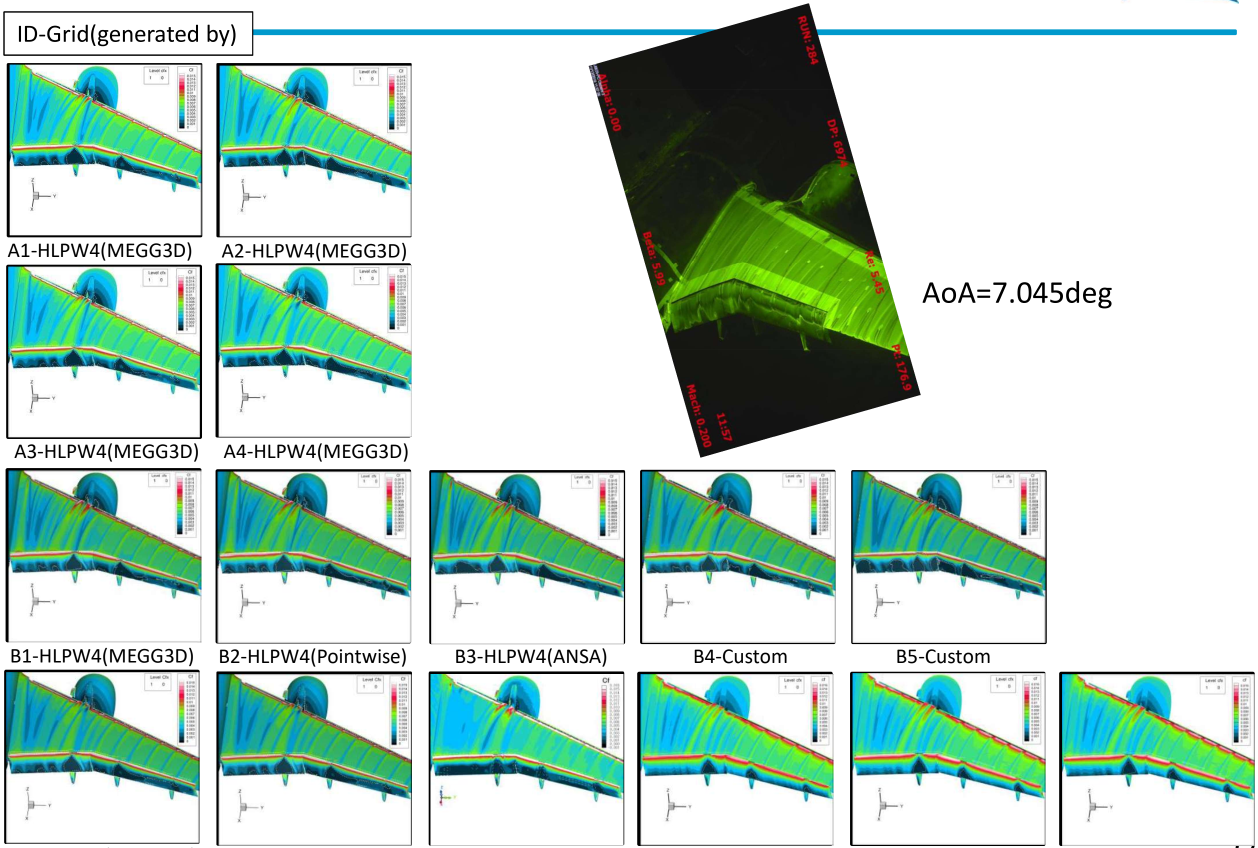

A1-HLPW4(MEGG3D) A2-HLPW4(MEGG3D) A3-HLPW4(MEGG3D) A4-HLPW4(MEGG3D)
B1-HLPW4(MEGG3D) B2-HLPW4(Pointwise) B3-HLPW4(ANSA) B4-Custom B5-Custom
C1-HLPW4(MEGG3D) C2-HLPW4(MEGG3D) D1-Custom E1-Custom E2-Custom E3-Custom

23

Surface Cf Contours（Case 1, 19.57deg, Viewpoint 1）

ID-Grid(generated by)

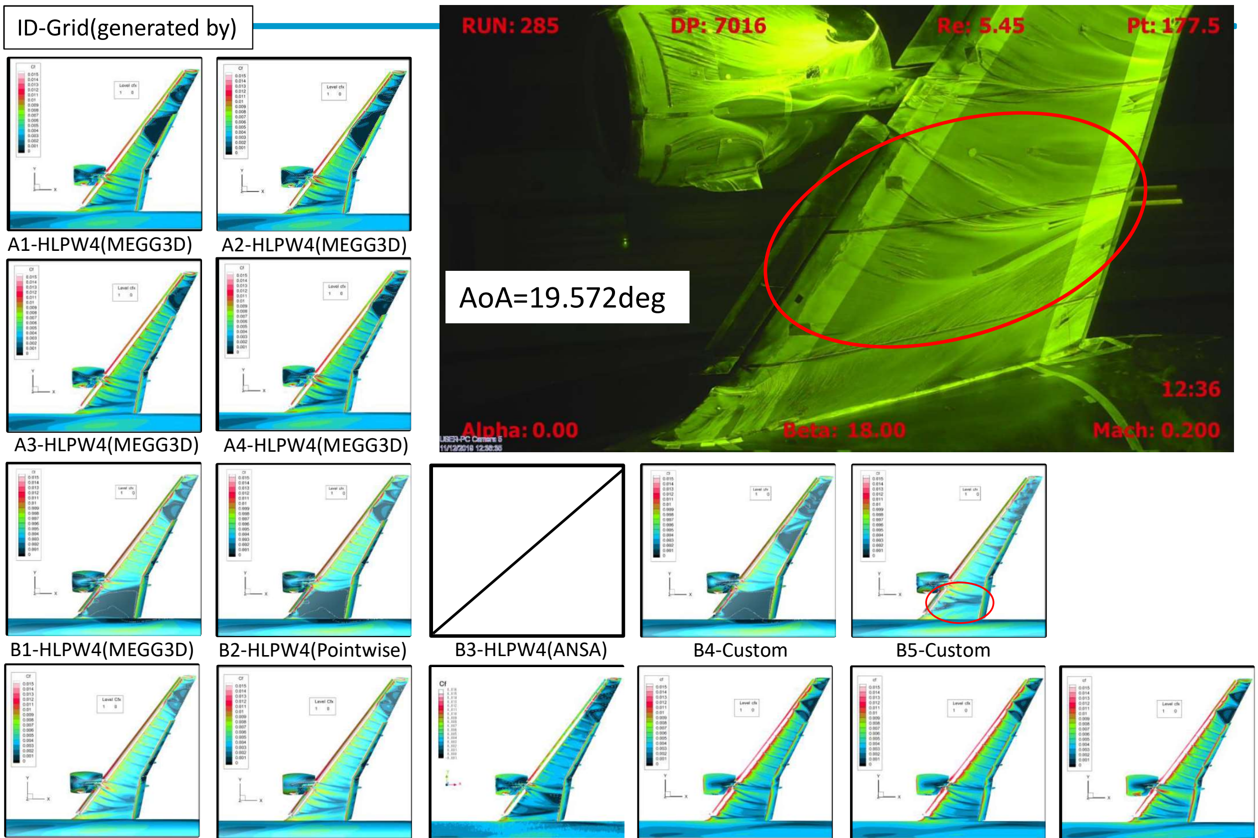

A1-HLPW4(MEGG3D) A2-HLPW4(MEGG3D) A3-HLPW4(MEGG3D) A4-HLPW4(MEGG3D)
B1-HLPW4(MEGG3D) B2-HLPW4(Pointwise) B3-HLPW4(ANSA) B4-Custom B5-Custom
C1-HLPW4(MEGG3D) C2-HLPW4(MEGG3D) D1-Custom E1-Custom E2-Custom E3-Custom

24

Surface Cf Contours (Case 1, 19.57deg, Viewpoint 1)

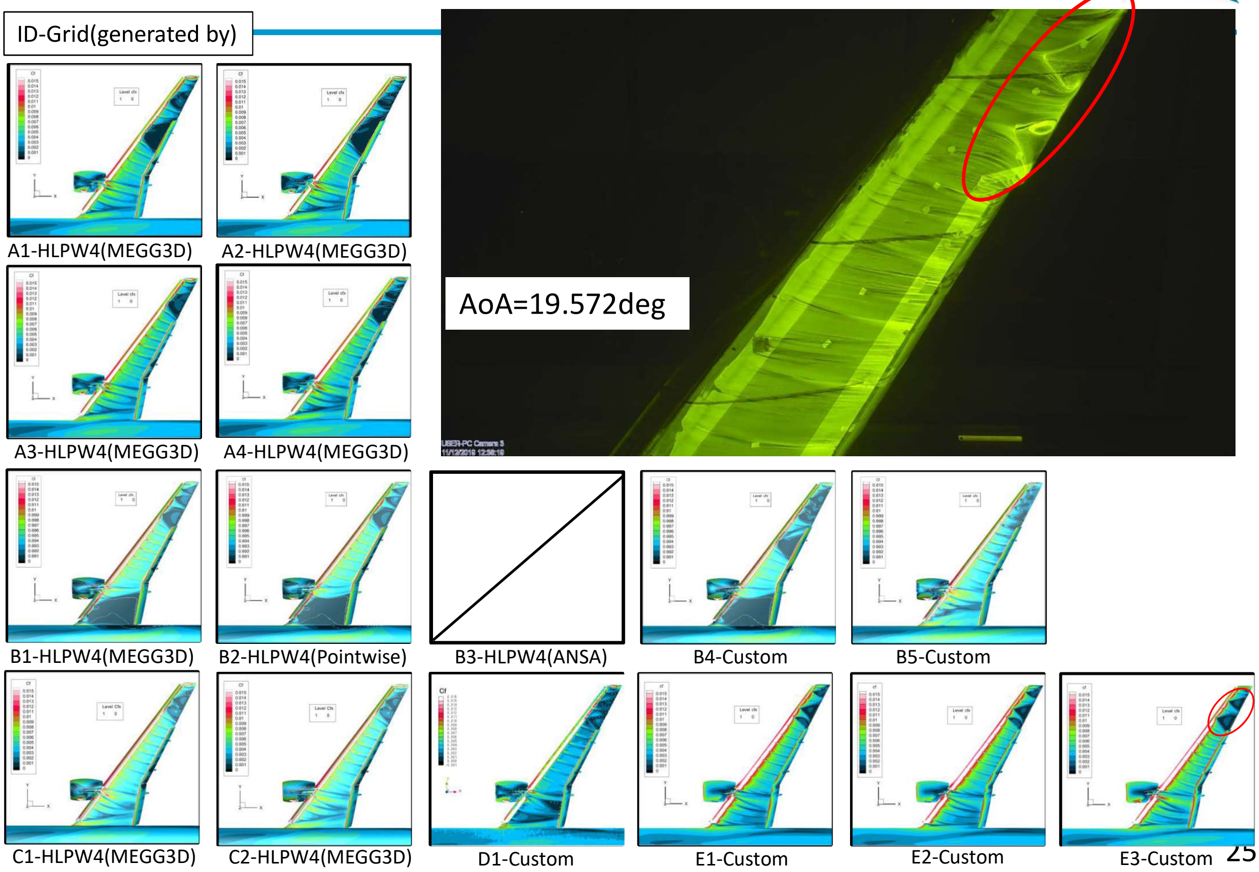

25

Surface Cf Contours (Case 1, 19.57deg, Viewpoint 2)

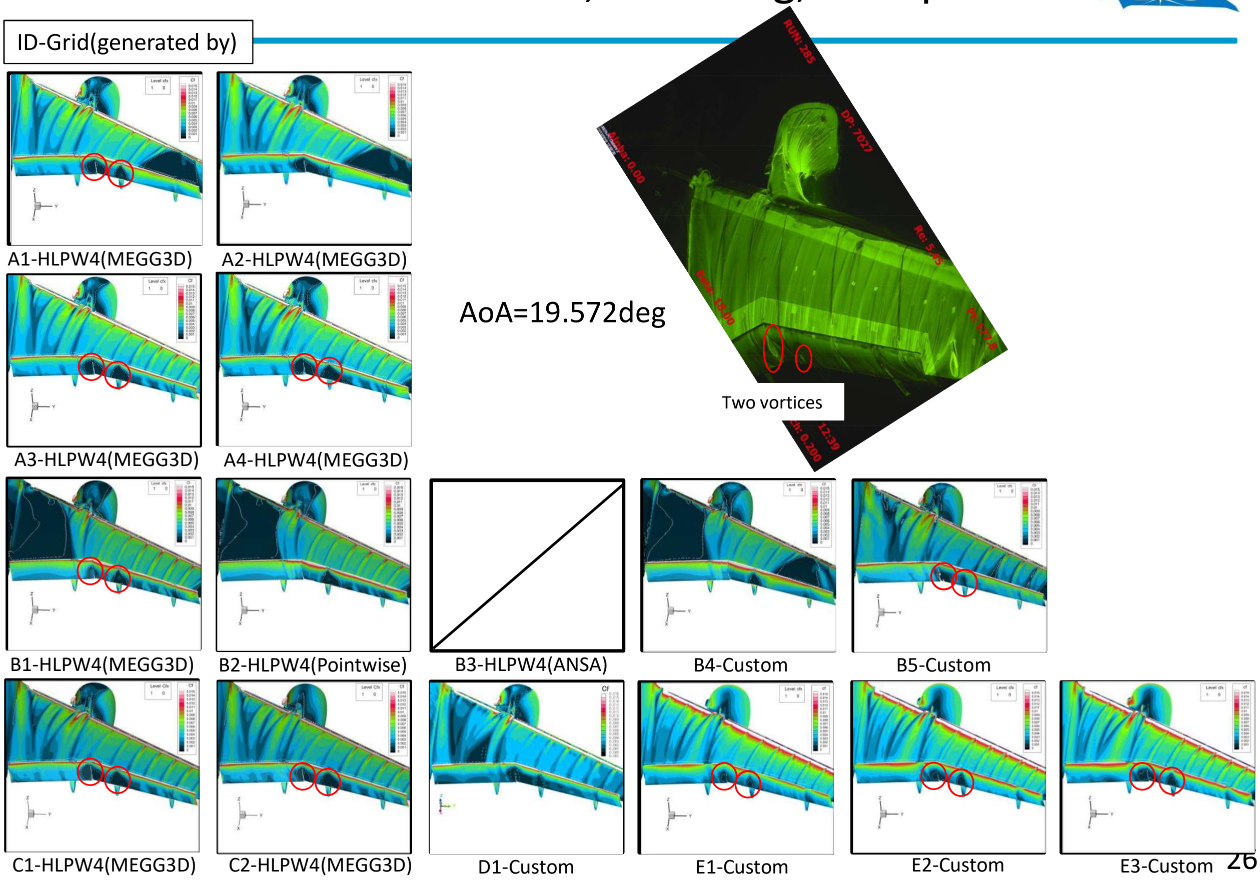

26

Surface Cf Contours（Case 1, 21.47deg, Viewpoint 1）

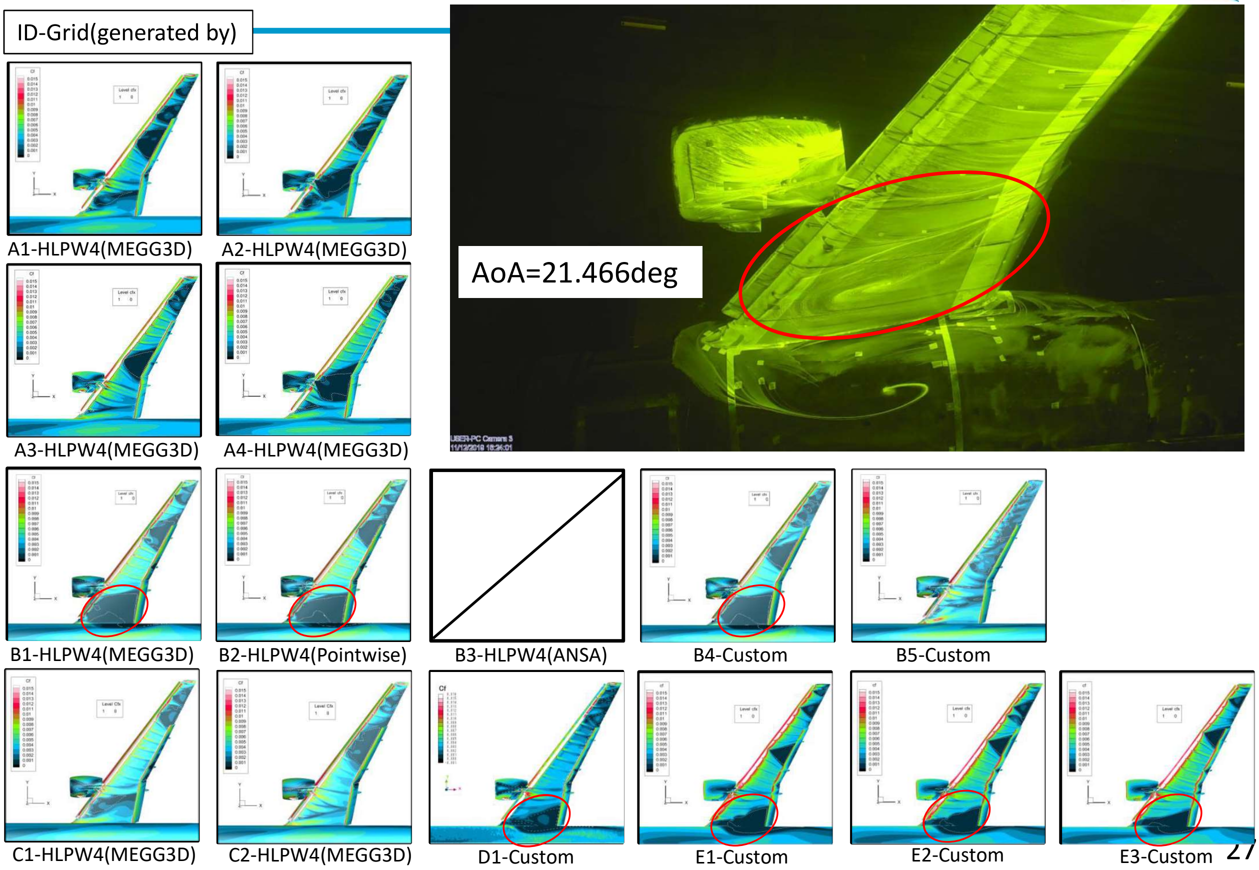

27

Surface Cf Contours（Case 1, 21.47deg, Viewpoint 1）

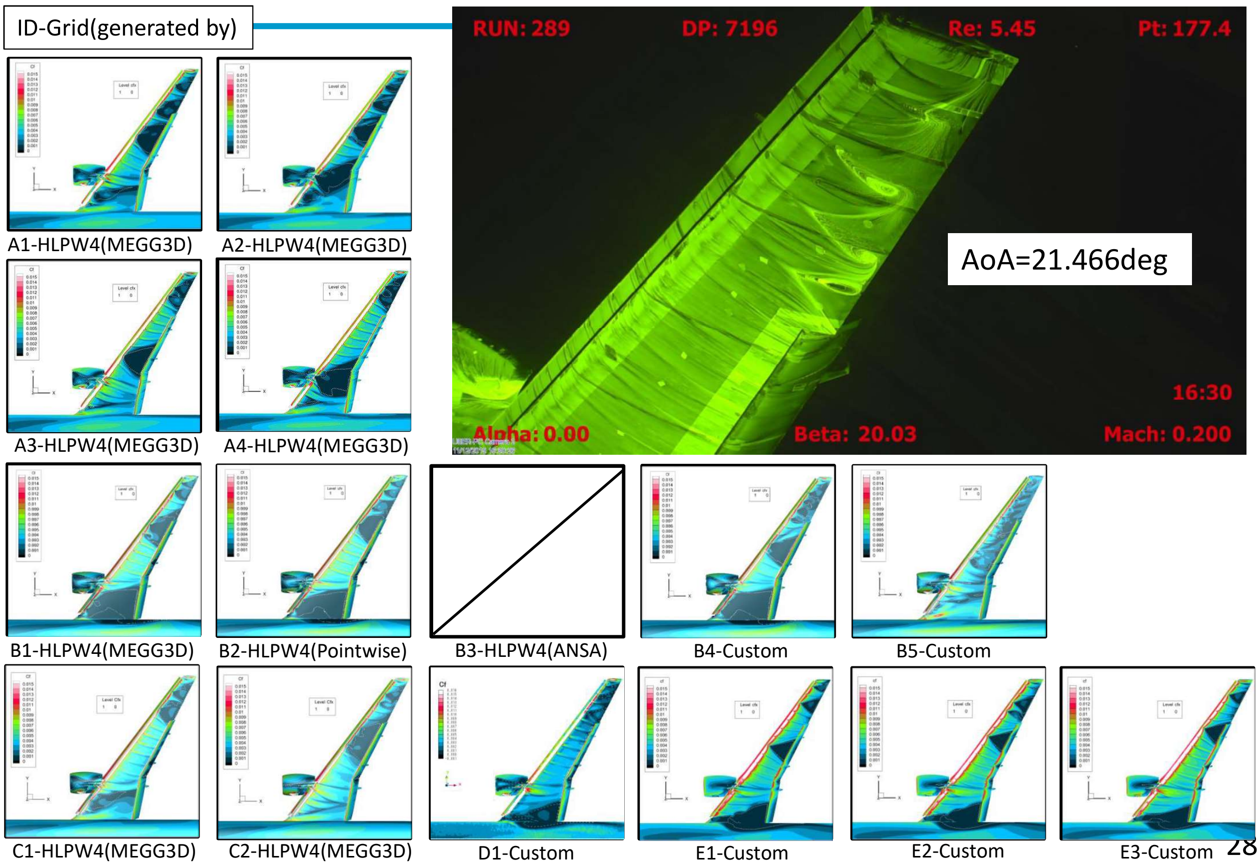

28

Surface Cf Contours（Case 1, 21.47deg, Viewpoint 2）

ID-Grid(generated by)

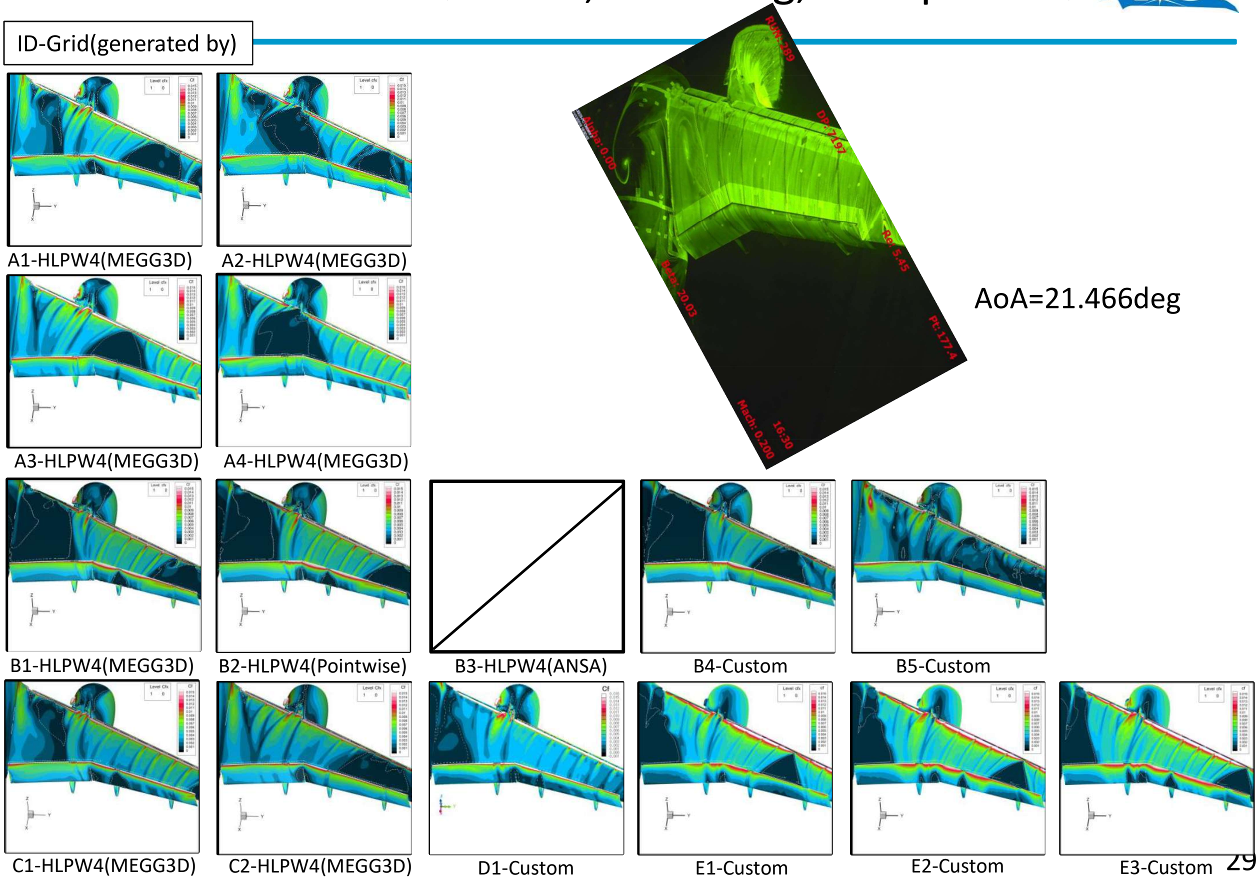

29

Surface Cp distribution （Case 1, 7.05deg）

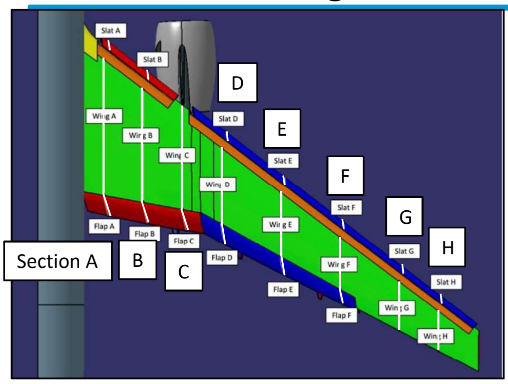

https://hiliftpw.larc.nasa.gov/Workshop4/DataForm.html

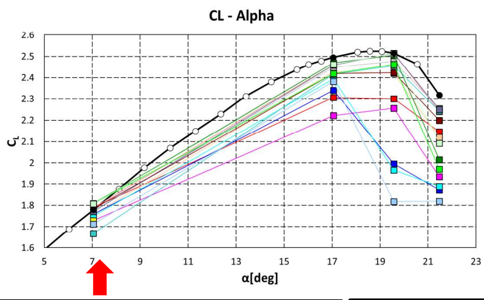

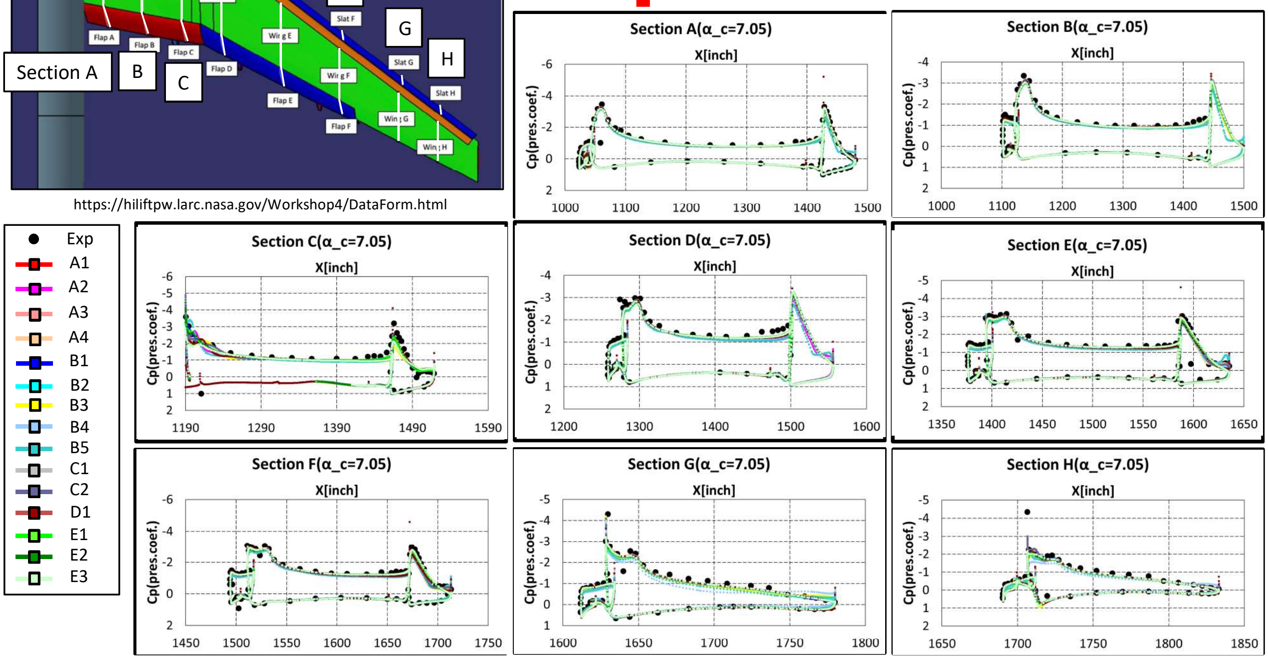

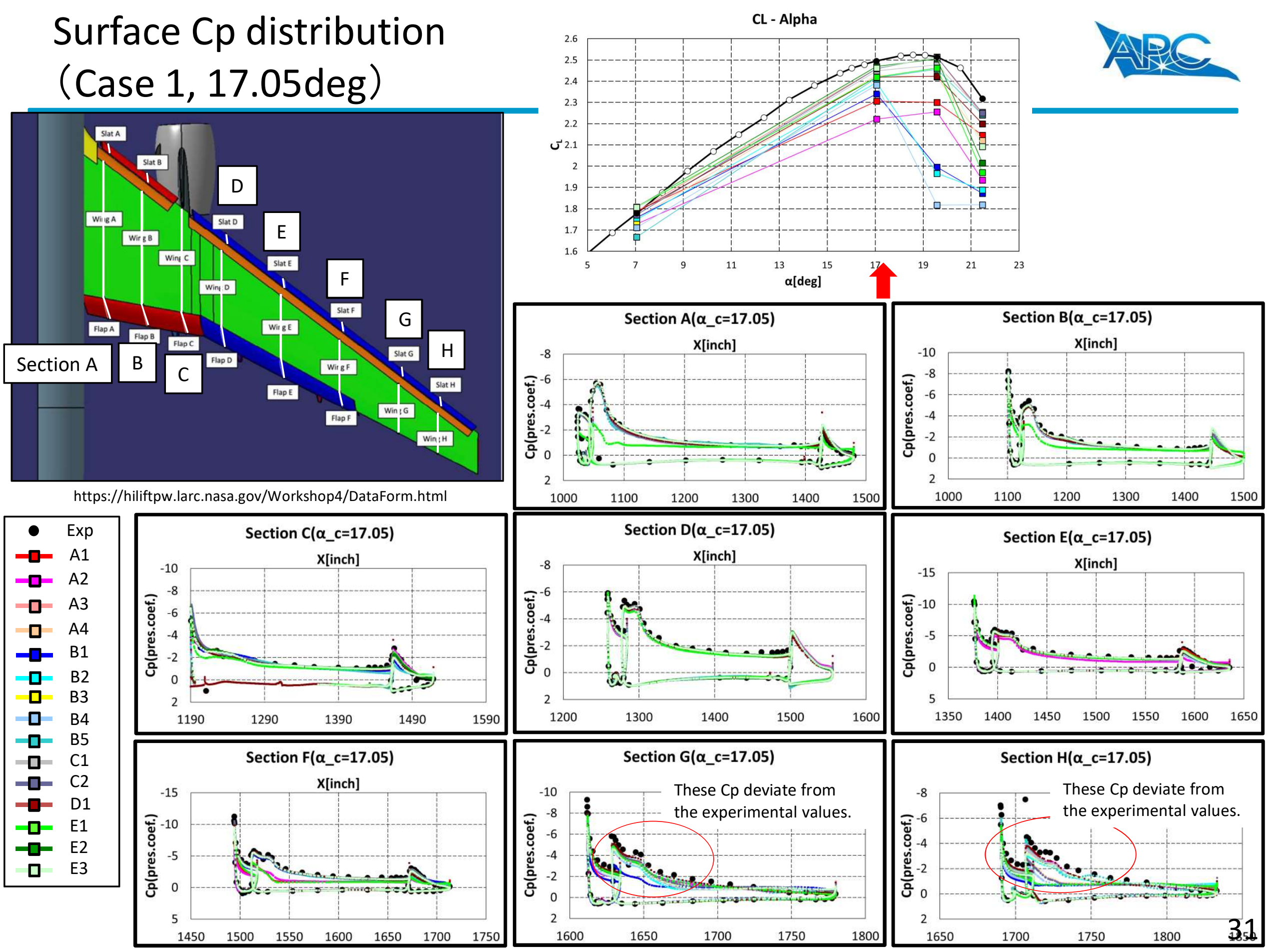
Surface Cp distribution
(Case 1, 17.05deg)
CL - Alpha
α[deg]
Section A
B
C
D
E
F
G
H
https://hiliftpw.larc.nasa.gov/Workshop4/DataForm.html
Exp
A1
A2
A3
A4
B1
B2
B3
B4
B5
C1
C2
D1
E1
E2
E3
Section A(α_c=17.05)
Section B(α_c=17.05)
Section C(α_c=17.05)
Section D(α_c=17.05)
Section E(α_c=17.05)
Section F(α_c=17.05)
Section G(α_c=17.05)
Section H(α_c=17.05)
X[inch]
Cp(pres.coef.)
These Cp deviate from the experimental values.
These Cp deviate from the experimental values.
31

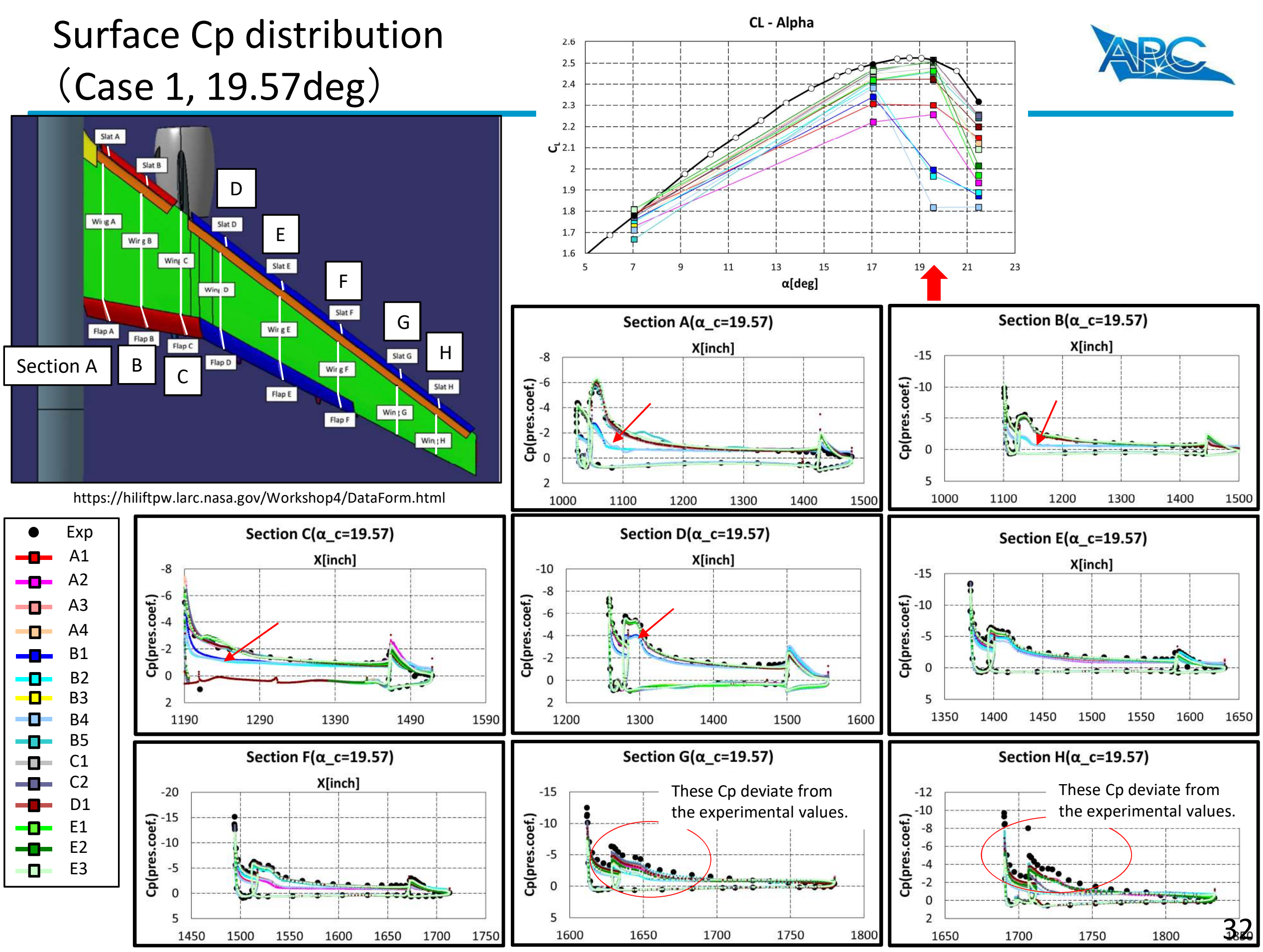
Surface Cp distribution
(Case 1, 19.57deg)
CL - Alpha
α[deg]
Section A
B
C
D
E
F
G
H
https://hiliftpw.larc.nasa.gov/Workshop4/DataForm.html
Exp
A1
A2
A3
A4
B1
B2
B3
B4
B5
C1
C2
D1
E1
E2
E3
Section A(α_c=19.57)
Section B(α_c=19.57)
Section C(α_c=19.57)
Section D(α_c=19.57)
Section E(α_c=19.57)
Section F(α_c=19.57)
Section G(α_c=19.57)
Section H(α_c=19.57)
X[inch]
Cp(pres.coef.)
These Cp deviate from the experimental values.
These Cp deviate from the experimental values.
32

Surface Cp distribution (Case 1, 21.47deg)

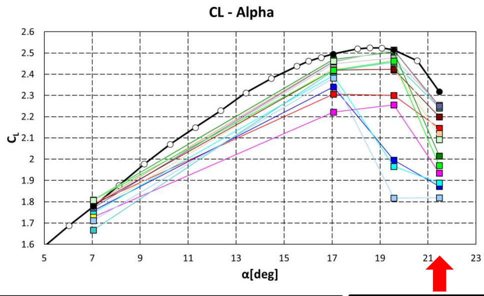

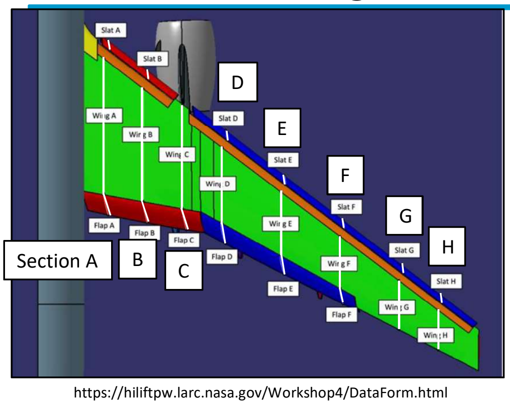

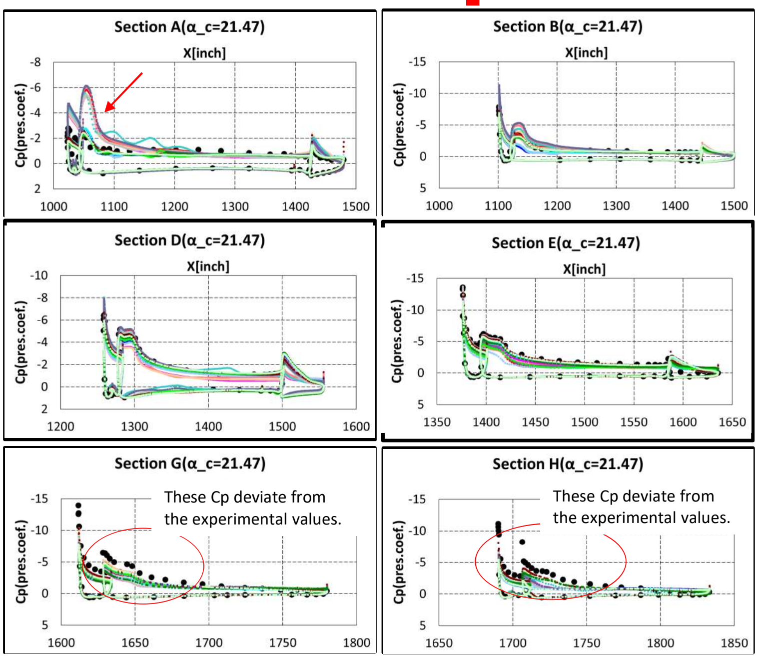

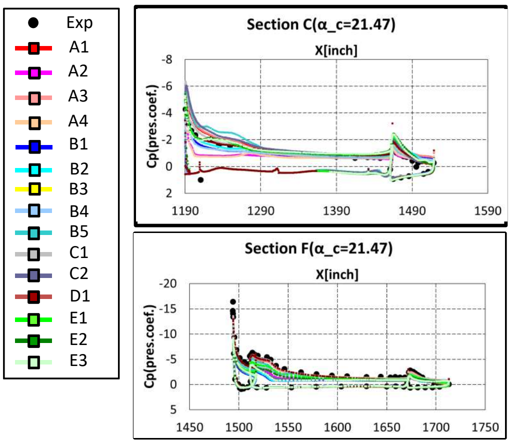

Case 3 : Steady computation

- Conditions
  - 3D CRM-HL flap angle : 43°/40°(inboard/outboard)
  - M = 0.2, Re = 5.49 x 10^6 (C_{ref} = 275.8inches), T_{ref} = 521°R
  - AoA = 7.05, 17.05deg

CL, CD, and Cm - Alpha, Case 3

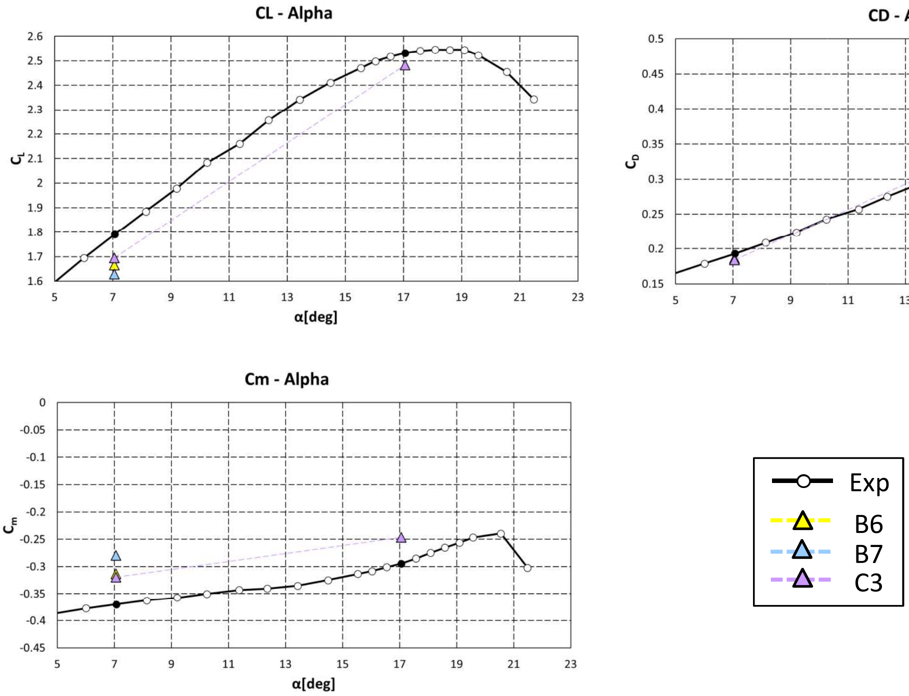

35

Lift, Drag, and Moment Increments

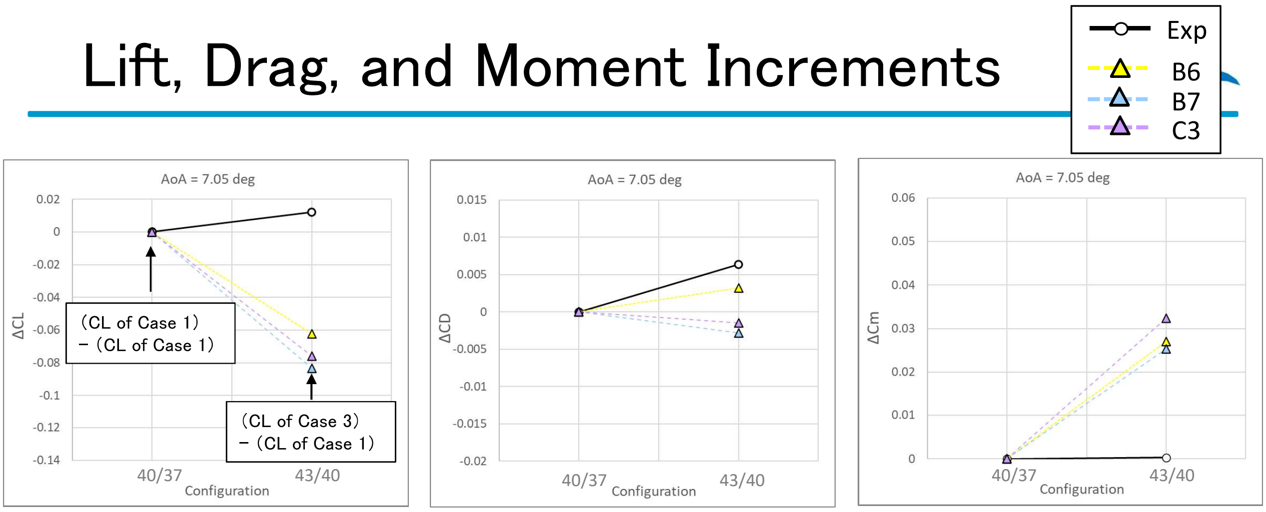

HLPW4（03_GMGW3_HLPW4_RANS.pdf,p.13 - 15）

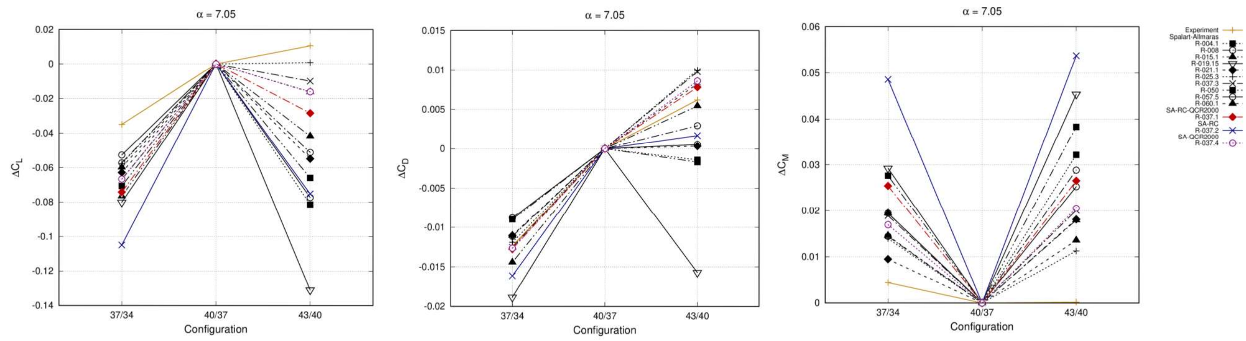

36

Surface Cf Contours (Case 3, 7.05deg)

ID-Grid(generated by)

40°/37° (inboard/outboard)

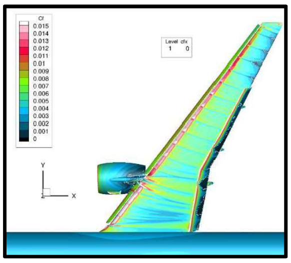

B3-HLWP4(ANSA)

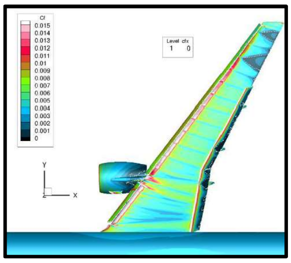

B4-Custom

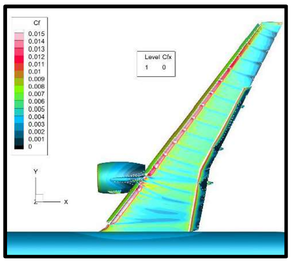

C2-HLWP4(MEGG3D)

43°/40° (inboard/outboard)

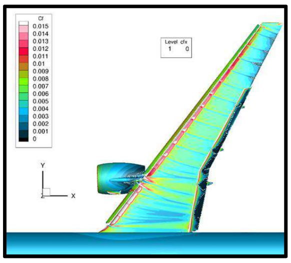

B6-HLWP4(ANSA)

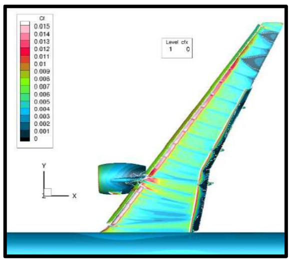

B7-Custom

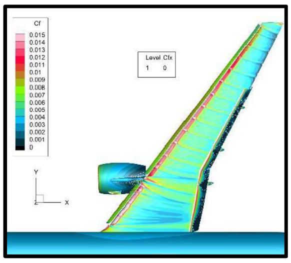

C3-HLWP4(Pointwise)

37

Surface Cf Contours (Case 3, 7.05deg)

ID-Grid(generated by)

40°/37° (inboard/outboard)

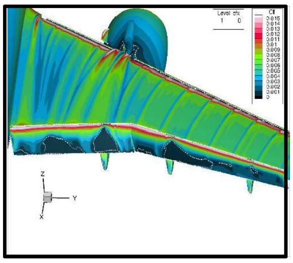

B3-HLWP4(ANSA)

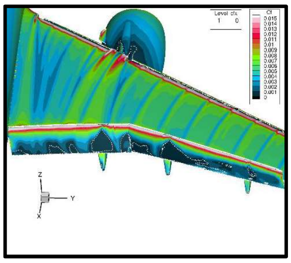

B4-Custom

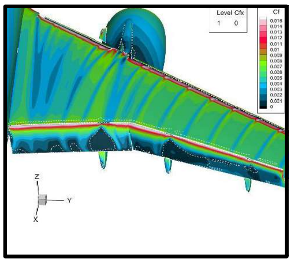

C2-HLWP4(MEGG3D)

43°/40° (inboard/outboard)

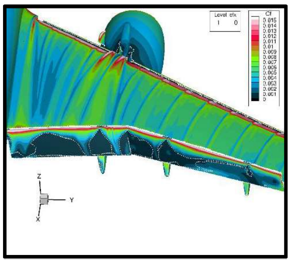

B6-HLWP4(ANSA)

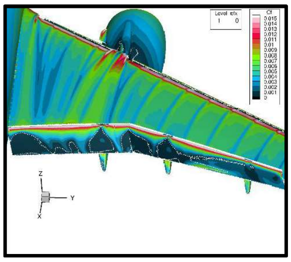

B7-Custom

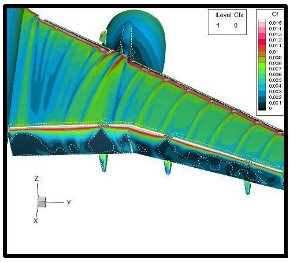

C3-HLWP4(Pointwise)

38

Surface Cf Contours（Case 3, 7.05deg）

ID-Grid(generated by)

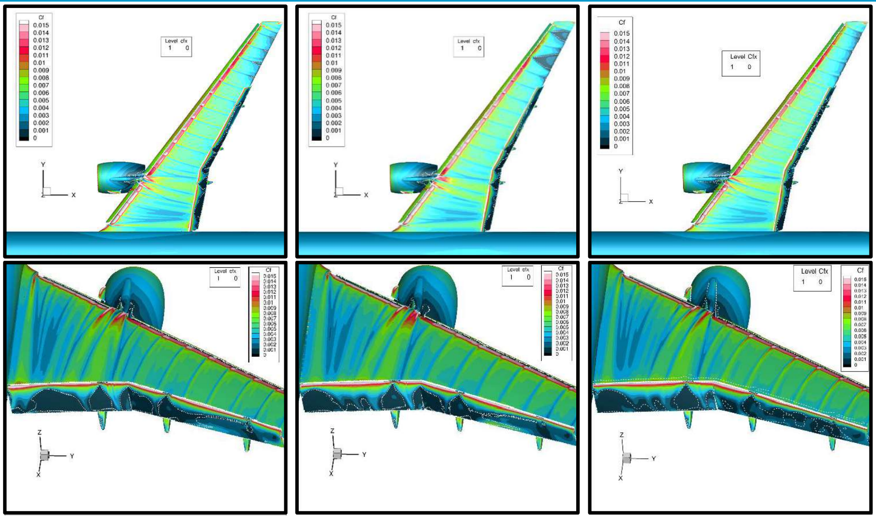

B6-HLWP4(ANSA) B7-Custom C3-HLWP4(Pointwise)

Exp
B6
B7
C3

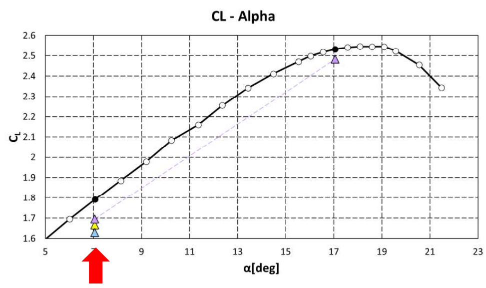

39

Surface Cf Contours（Case 3, 17.05deg）

ID-Grid(generated by)

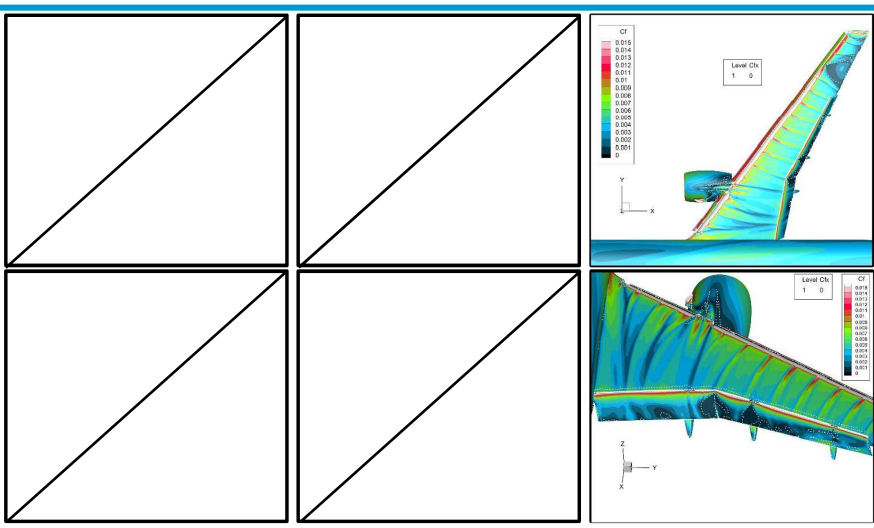

B6-HLWP4(ANSA) B7-Custom C3-HLWP4(Pointwise)

Exp
B6
B7
C3

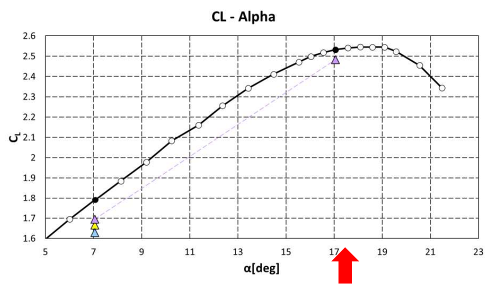

40

Surface Cp distribution (Case 3, 7.05deg)

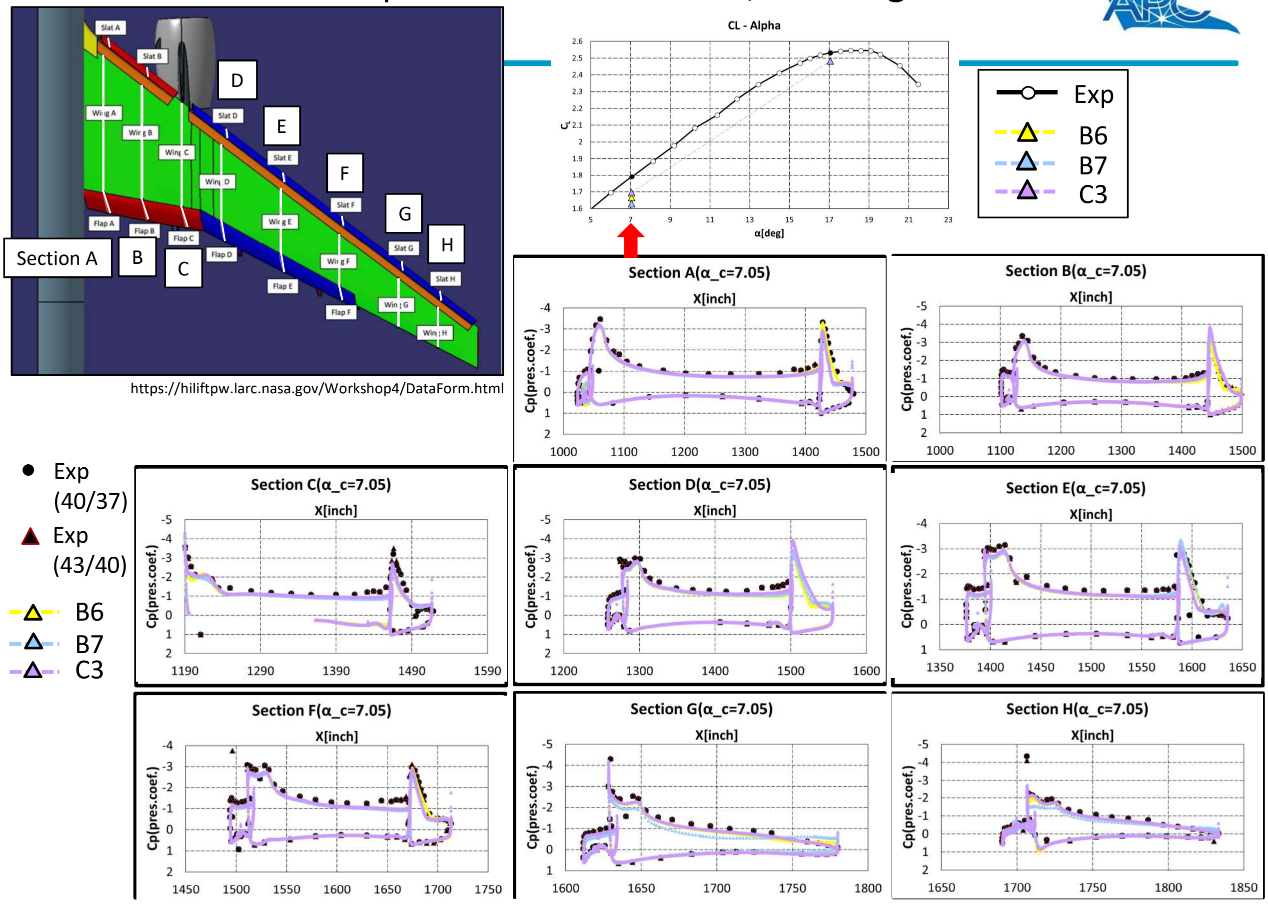

Surface Cp distribution (Case 3, 17.05deg)

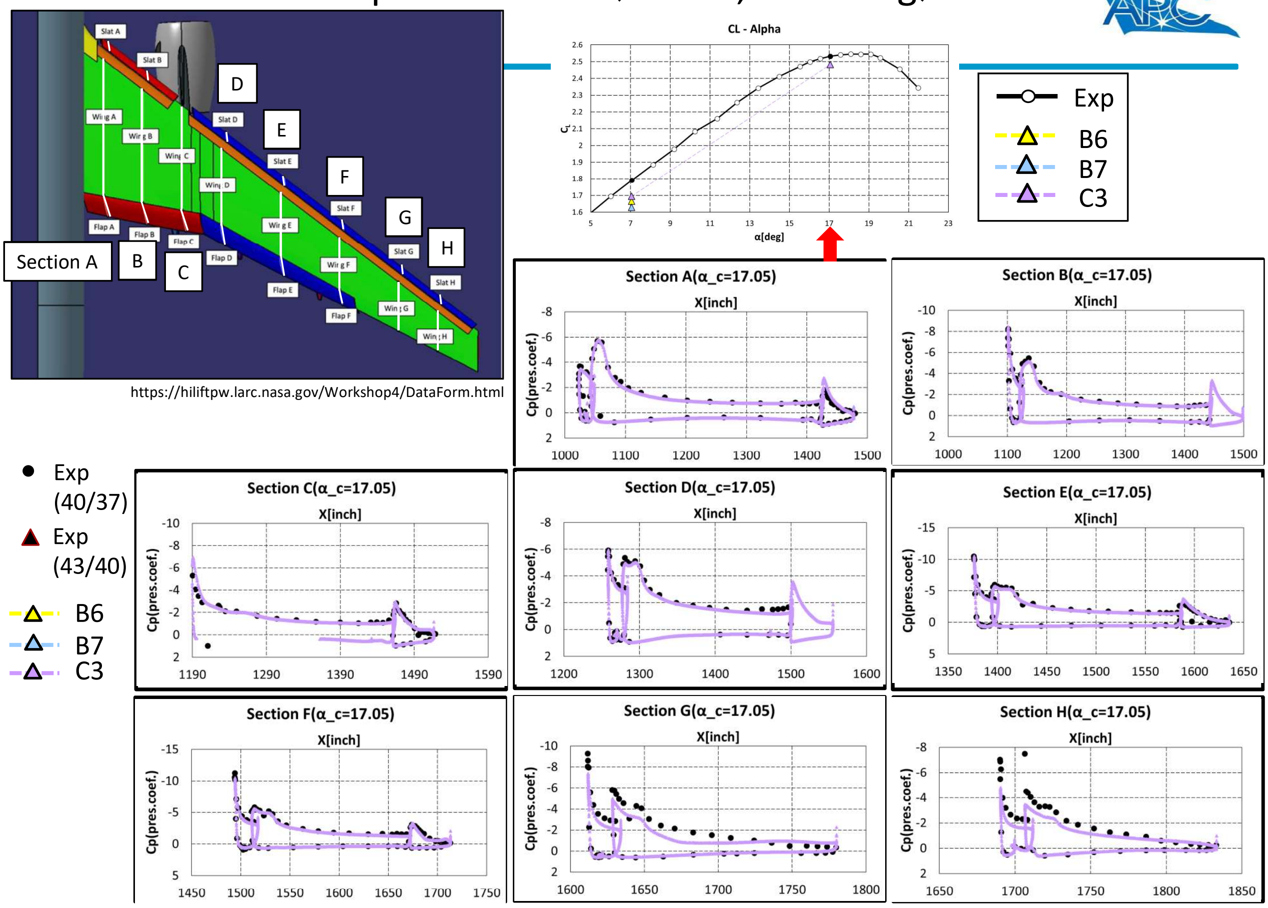

Case 4 : Steady computation

- Conditions
  - M = 0.2, Re = 5.00 x 10^6 (C_{ref} = 1), T_{ref} = 272.1K
  - AoA = 16.0deg

TMR提供格子（FAMILY1）

Grid Level	面あたりのノード数N
L1 (coarsest)	173958
L2	294161
L3	508099
L4	930671
L5	1679982
L6	3227904
L7 (finest)	5980721

Participants of Case 4

ID	Name	Organization	Code	Grid	Turbulence Model	Initial Condition
A5	Zauner Markus	JAXA	FaSTAR (Unstructured solver)	TMR提供格子(FAMILY1)	SA-noft2	Uniform flow （L7格子の計算のみL6格子の収束値をL7格子にマッピングし、この値を初期値にしてGlobal time stepを用いて計算）
A6	Zauner Markus	JAXA	FaSTAR (Unstructured solver)	TMR提供格子(FAMILY1)	SA-noft2	Uniform flow (L7格子の計算のみLocal time stepの未収束値を初期値にしてGlobal time stepを用いて計算)
B8	山内優果	KHI	Cflow (Unstructured solver)	TMR提供格子(FAMILY1)	SA-neg	Uniform flow
C4	古谷龍太郎	JAXA	TAS (Unstructured solver)	TMR提供格子(FAMILY1)	SA-noft2-R(Crot=1)	Uniform flow
C5					SA	

Grid Convergence（1/2）

- A5
- A6
- B8
- C4
- C5
- F1
- F2

F1：FUN3D, Family 1, SA-neg
F2：FUN3D, Family 1, SA-neg, 2nd order turbulence

A5とA6は重なっている
L1～L6格子のデータは同じもの
L7格子のデータは初期条件が異なる

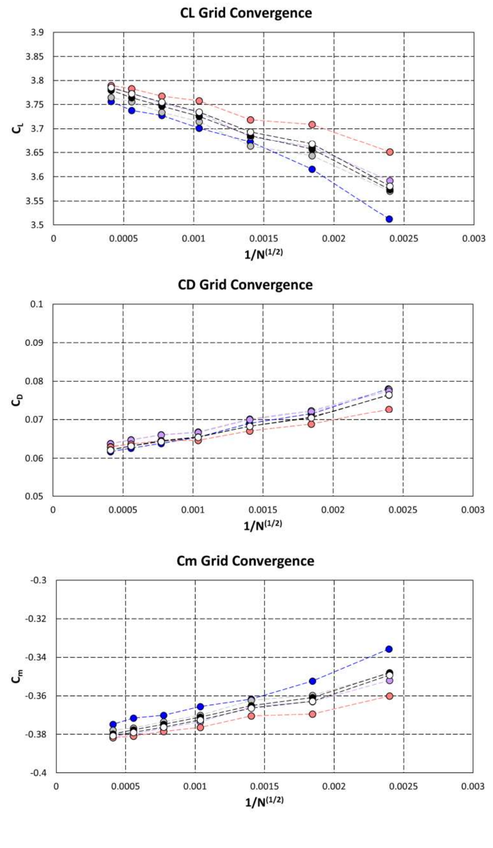

Turbulence Modeling Resource

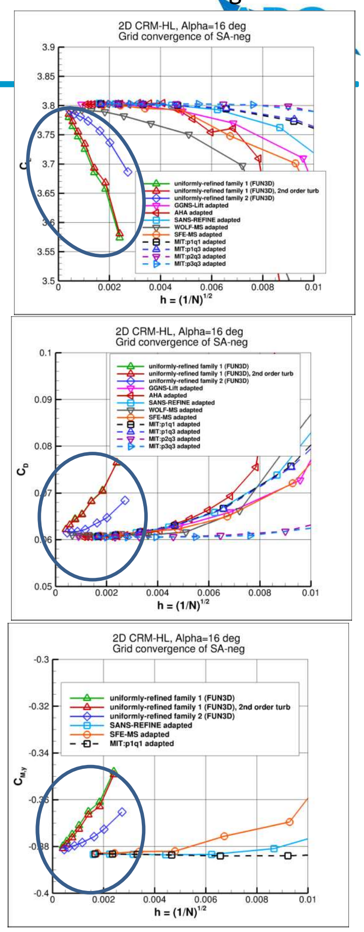

Grid Convergence（2/2）

A5
A6
B8
C4
C5
F1
F2

F1 : FUN3D, Family 1, SA-neg
F2 : FUN3D, Family 1, SA-neg,
2nd order turbulence

A5とA6は重なっている
L1～L6格子のデータは
同じもの
L7格子のデータは
初期条件が異なる

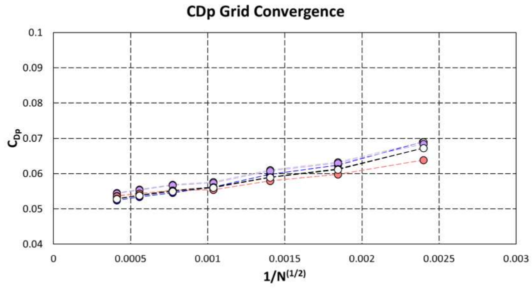

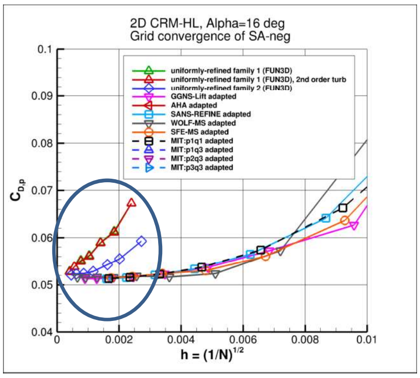

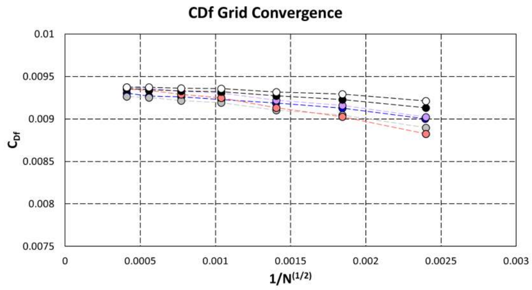

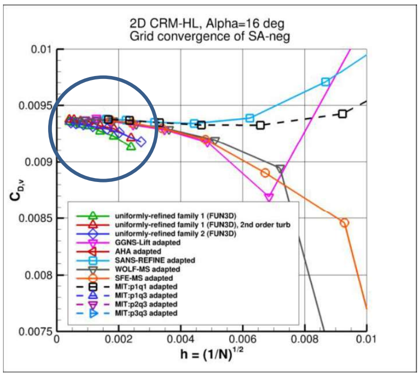

Surface Cp distribution

A5
A6
B8
C4
C5

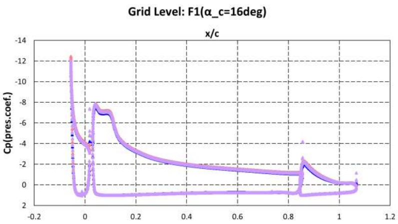

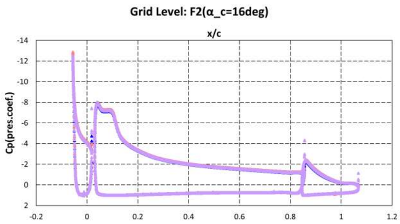

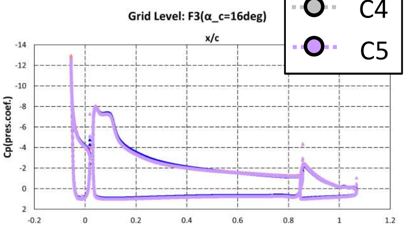

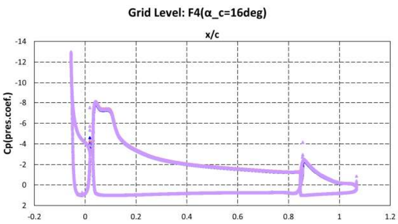

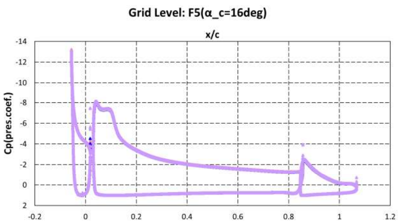

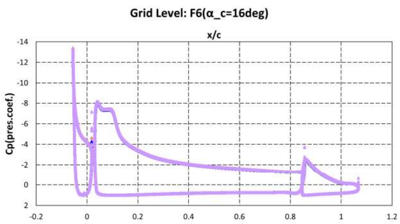

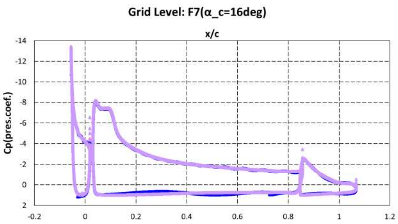

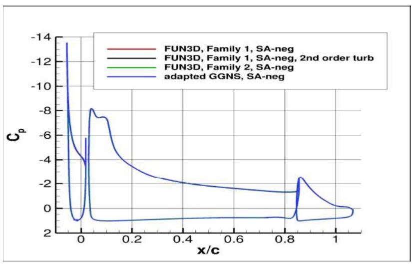

Turbulence Modeling
Resource

Summary

- Case1
  - 空力係数はHLPW4と同じ傾向、ばらつき。
  - CFDの方が剥離を大きめに予測しておりCLが小さい。オイルフローとの比較や圧力分布の比較でも、剥離を大きく予測していることを確認。
  - 正しい剥離パターンで、空力係数(CLmax)を予測できた参加者はいない。外翼側のスラットトラックからの剥離が過大。内翼側からの失速にならない場合がある。
  - 初期値依存性がある(cold start vs warm start)。

49

Summary

- Case2
  - 参加者なし
- Case3
  - フラップ舵角効果の影響は困難。
- Case4
  - NASA TMRの結果と同様の結果であり、Verificationとして良好な結果。

50

謝辞

- 本資料を作成するにあたり、APC-8の参加者には、計算結果データを提出していただきました。また、APC有識者会議の皆様には、集計結果に関するご助言をいただきました。FMIC R&Dの松崎智明氏、菱友システムズの林謙司氏には集計作業のご支援をいただきました。上記の関係者の皆様に、ここに感謝の意を表します。

51

Discussion

- 今後（APC-9）では、どこに着目すべきか？
- どんな風洞試験データが必要か？（例：全機と半裁の比較、ラフネス有無、境界層プロファイル、PIVによる空間速度分布など）
- CFDのばらつきを減らすにはどうしたら良いか？
- 定常RANS解析で改善する見込みはあるのか？
- Trackからの剥離が過大になる要因は？対策は？
- 床面境界層/風洞壁を模擬した解析を実施すべきか？
- 定常解析における解の収束性は？
- 最適な格子、乱流モデルは？あるいは、非定常計算？

52

APC-8のフォローアップの集計結果

Summary of APC-8 follow-up

橋本 敦 (JAXA)
Hashimoto Atsushi(JAXA)

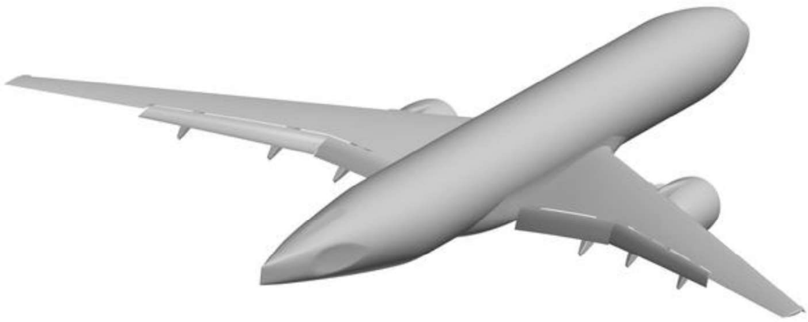

Participants of Case 1

ID	Name	Organization	Code	Grid (generated by)	Description of the grid	Turbulence Model	Initial Condition
A1	Zauner Markus	JAXA	FaSTAR (Unstructured solver)	HLPW4(MEGG3D)		SA-noft2	Cold start
A2						SA-noft2-R-QCR2000	
A3						SA-noft2	Warm start
A4						SA-noft2-R-QCR2000	
B1	山内優果	KHI	Cflow (Unstructured solver)	HLPW4(MEGG3D)		SA-neg	Uniform flow
B2				HLPW4(Pointwise)	Pointwise grid(1.3.C)		
B3				HLPW4(ANSA)	ANSA(101.C)		
B4				Custom	Orthogonal octree + Body-Fitted layer grid	SA-neg	
B5						SA-R-QCR	
C1	古谷龍太郎	JAXA	TAS (Unstructured solver)	HLPW4(MEGG3D)		SA-noft2-R(Crot=1)	Uniform flow
C2							Low angle of attack
D1	中島吉隆	Hexagon	scFLOW (Unstructured solver)	Custom	Polyhedral mesh generated by scFLOW	SA-neg	Uniform flow
E1	船田雅也	Univ. of Tokyo	UTCart (Unstructured Cartesian solver)	Custom	Hierarchical orthogonal grid(100M)	SA-noft2 +Wall function	Uniform flow
E2					Hierarchical orthogonal grid(200M)		
E3					Hierarchical orthogonal grid(400M)		

54

Case 1 : Steady computation

- Conditions
  - 3D CRM-HL flap angle : 40°/37°(inboard/outboard)
  - M = 0.2, Re = 5.49 x 10^6 (C_{ref} = 275.8inches), T_{ref} = 521°R
  - AoA = 7.05, 17.05, 19.57, 21.47deg

Q-Criterion Surface, X-Vorticity（Case 1, 7.05deg, Viewpoint 5）

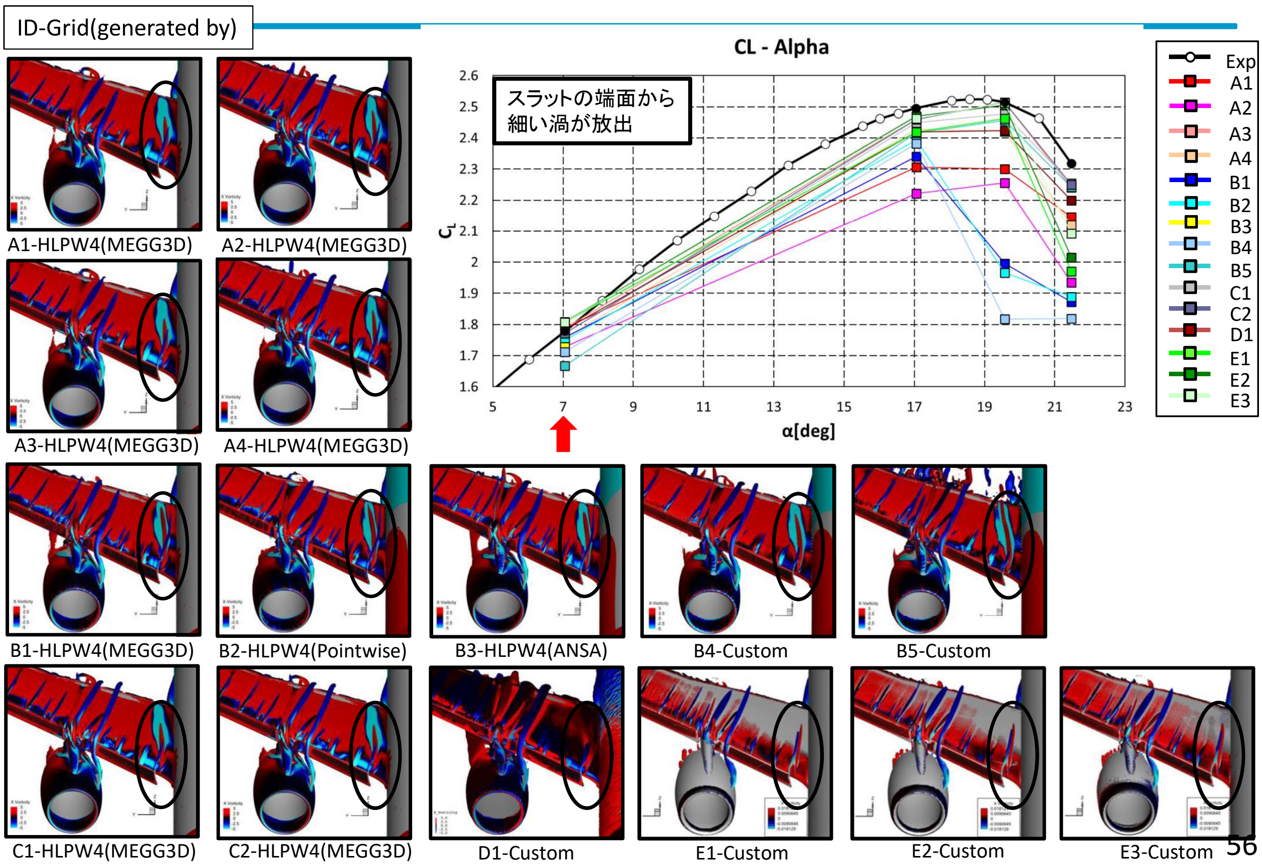

Q-Criterion Surface, X-Vorticity（Case 1, 17.05deg, Viewpoint 5）

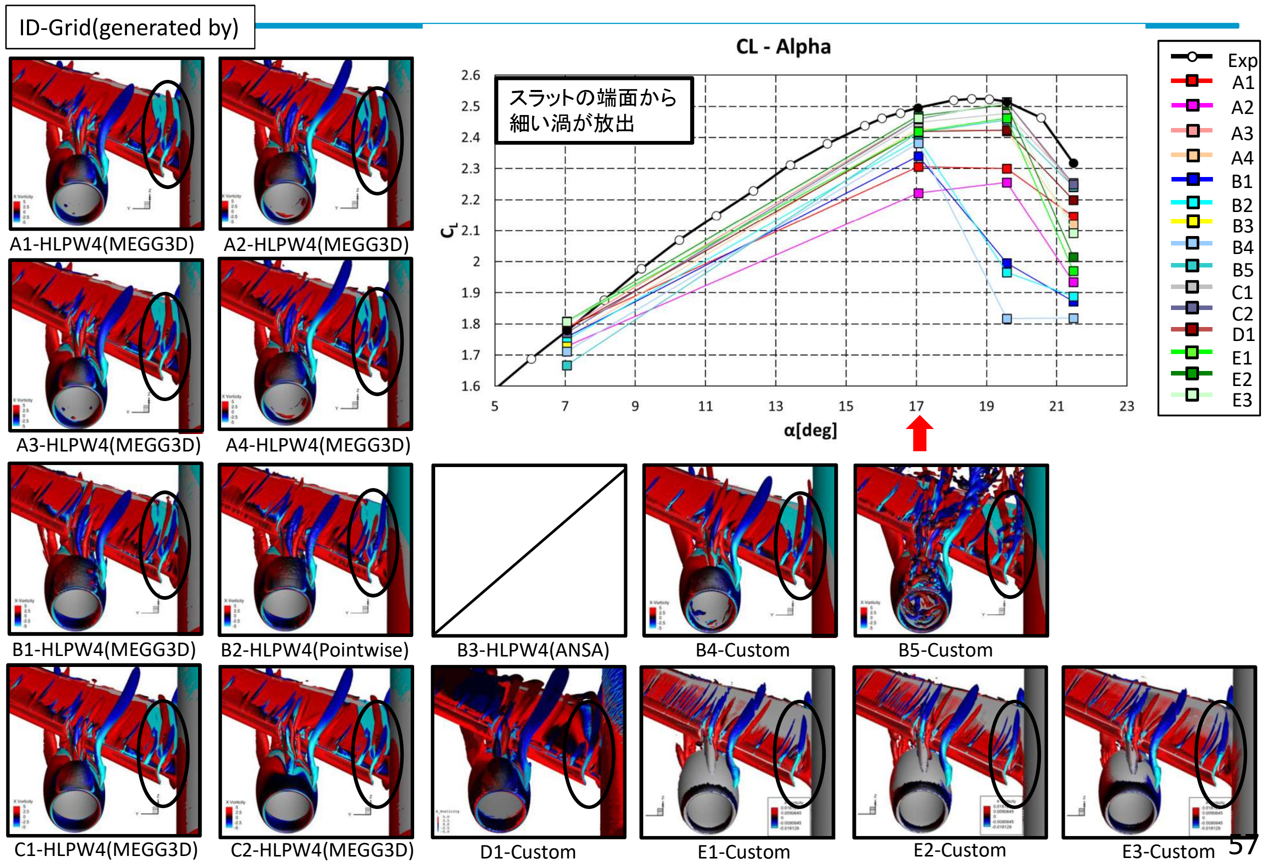

Q-Criterion Surface, X-Vorticity（Case 1, 19.57deg, Viewpoint 5）

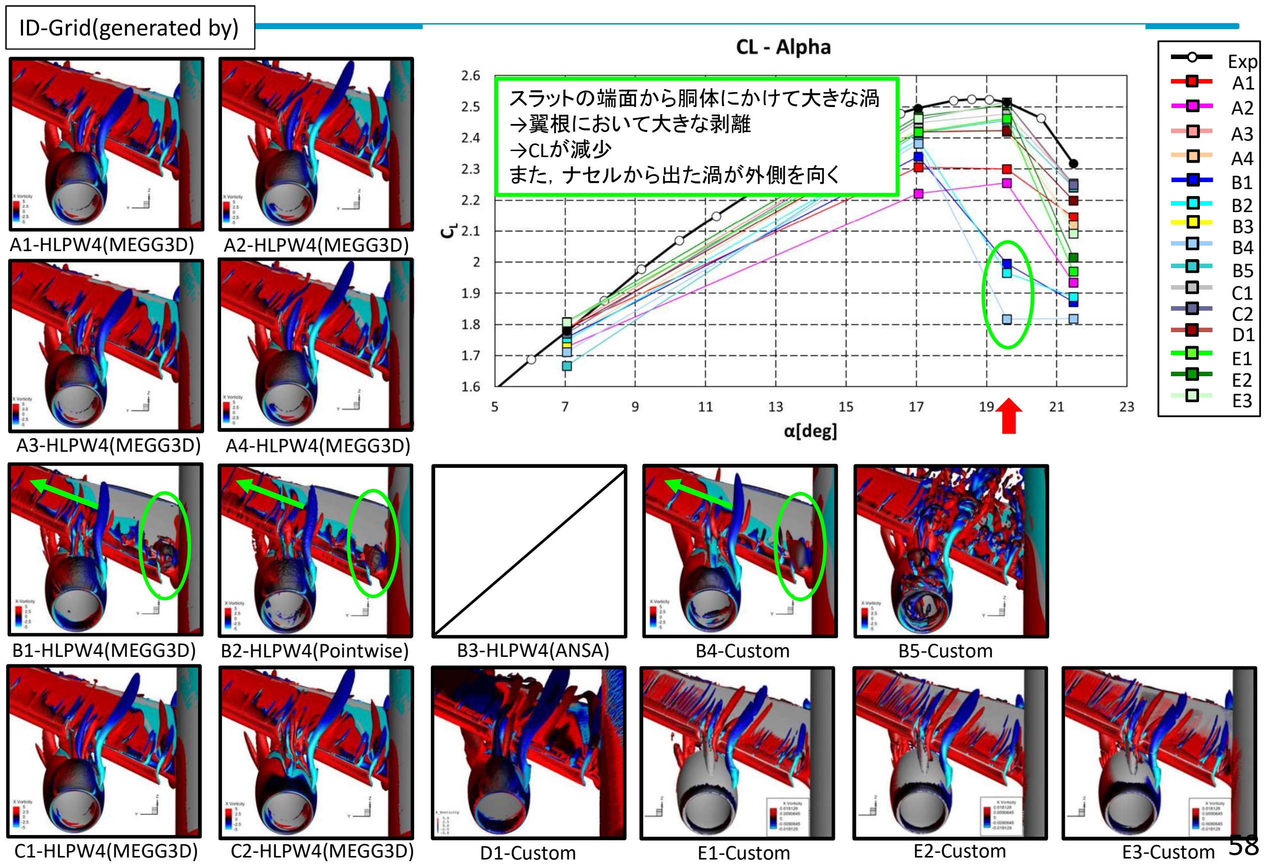

Q-Criterion Surface, X-Vorticity（Case 1, 21.47deg, Viewpoint 5）

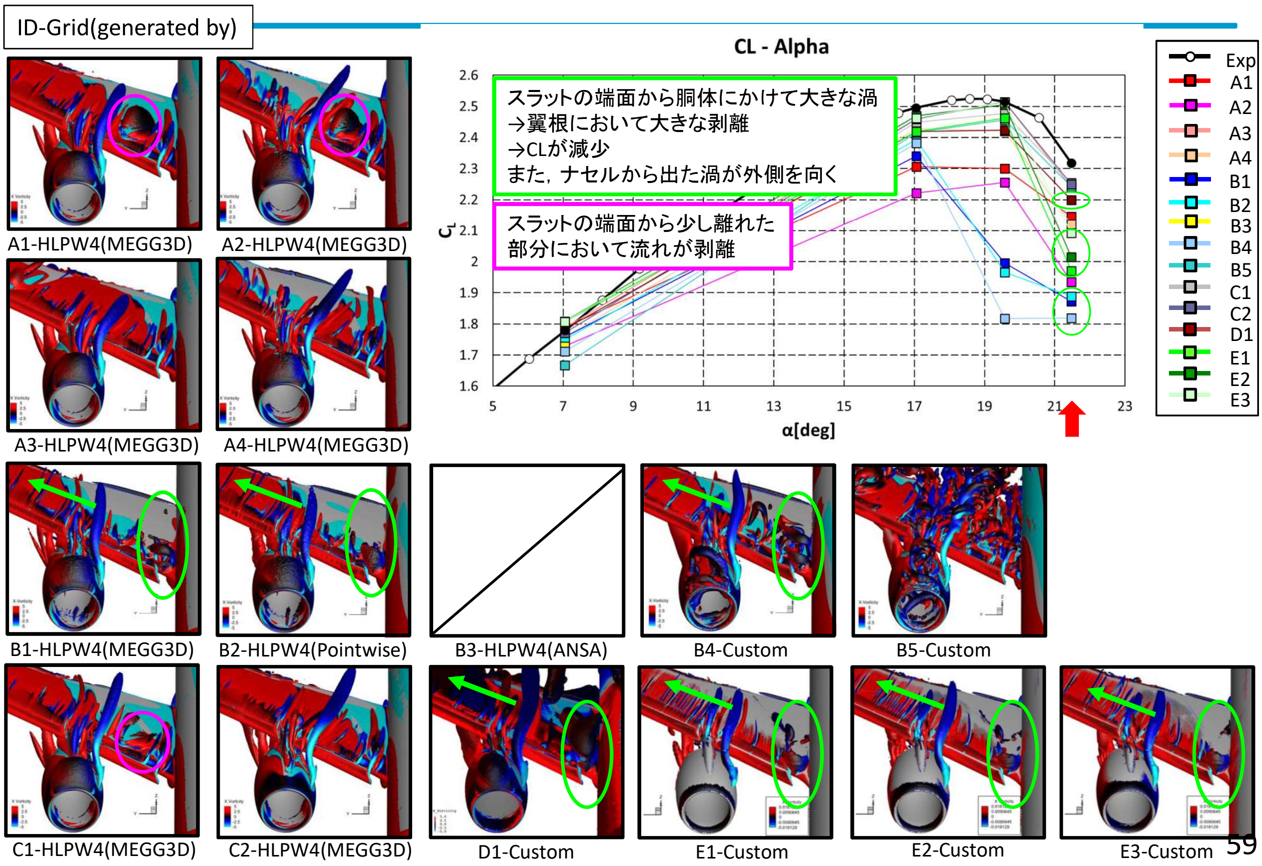

Wall-streamtraces, Cf（Case 1, 21.47deg, Viewpoint 6）

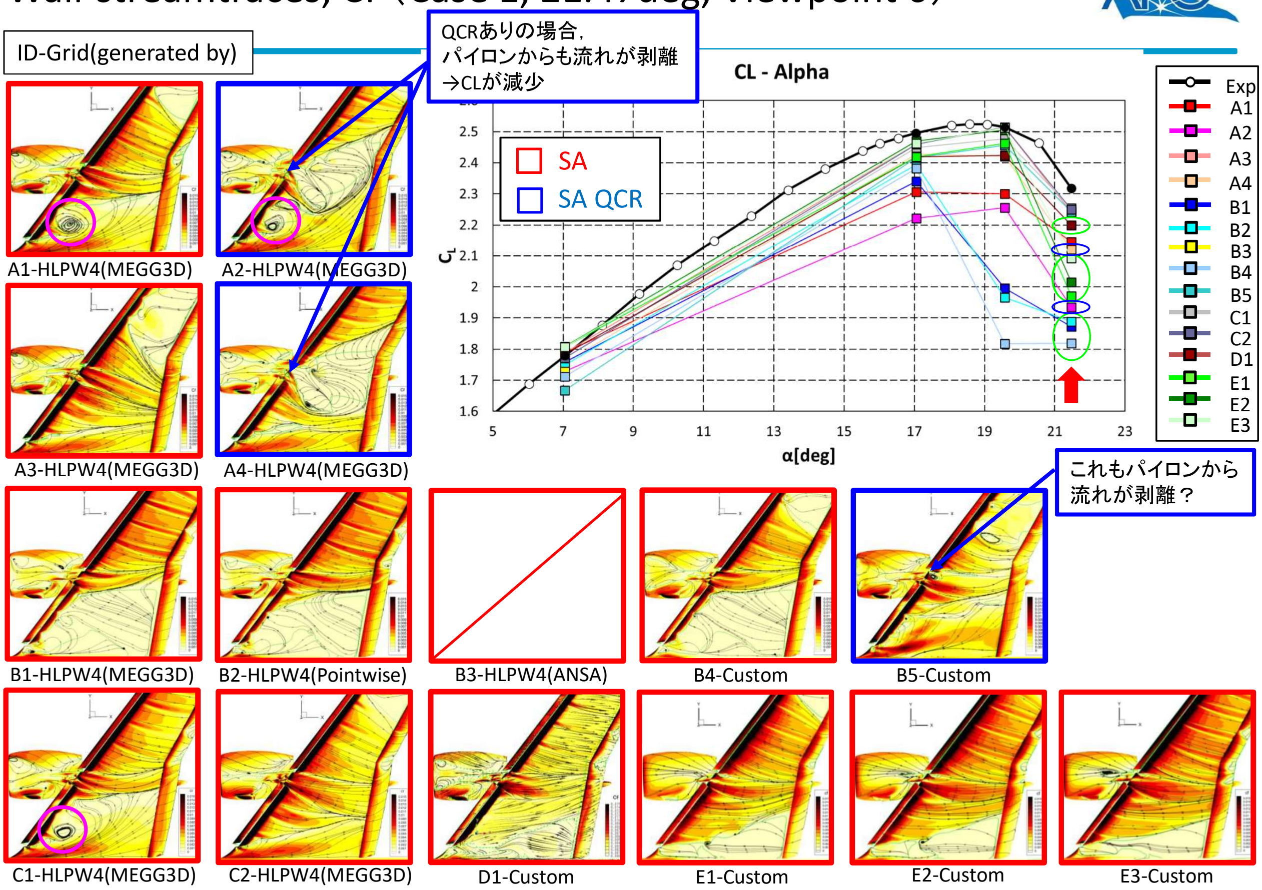

Classification by Participants

CL-Alpha, Case 1

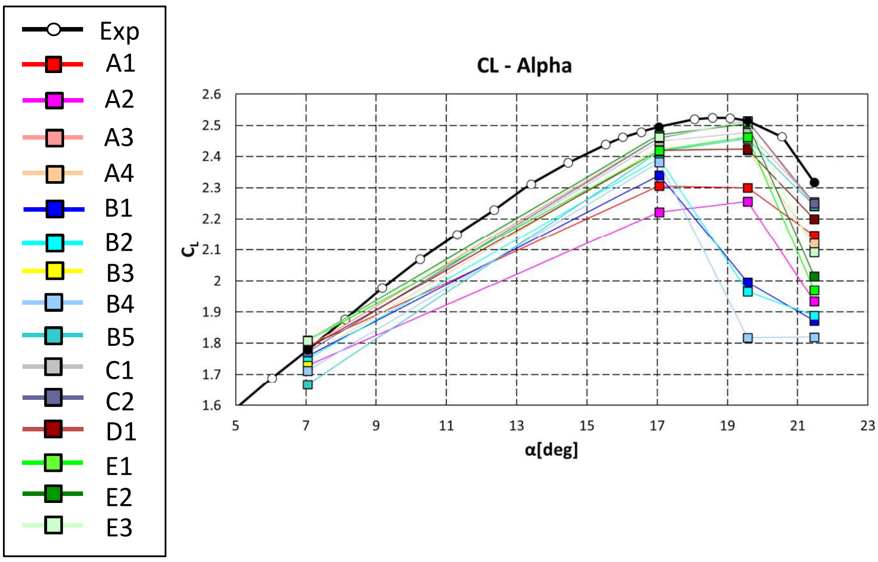

HLPW4
All Best-Practice Results
(03_GMGW3_HLPW4_RANS.pdf, p.17)

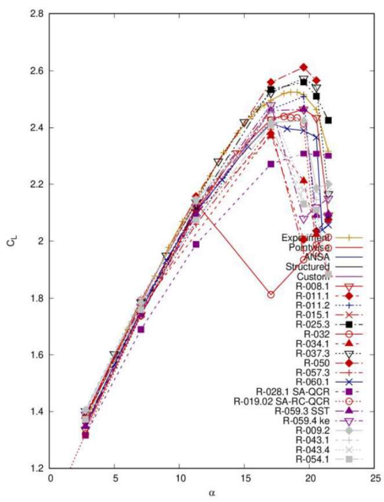

CD-Alpha, Case 1

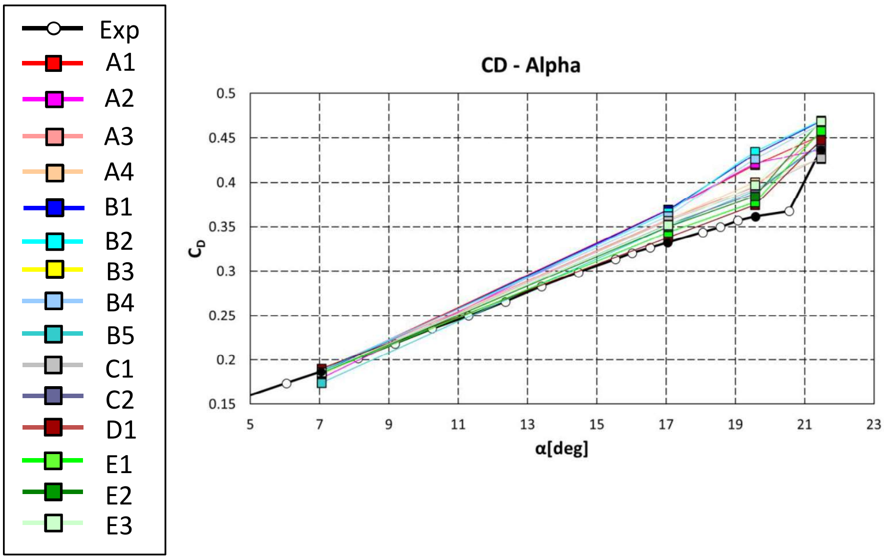

HLPW4
All Best-Practice Results
(03_GMGW3_HLPW4_RANS.pdf, p.17)

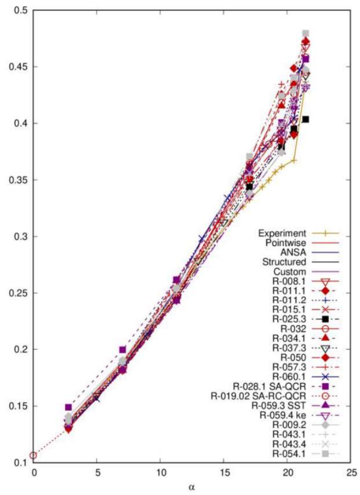

63

Cm-Alpha, Case 1

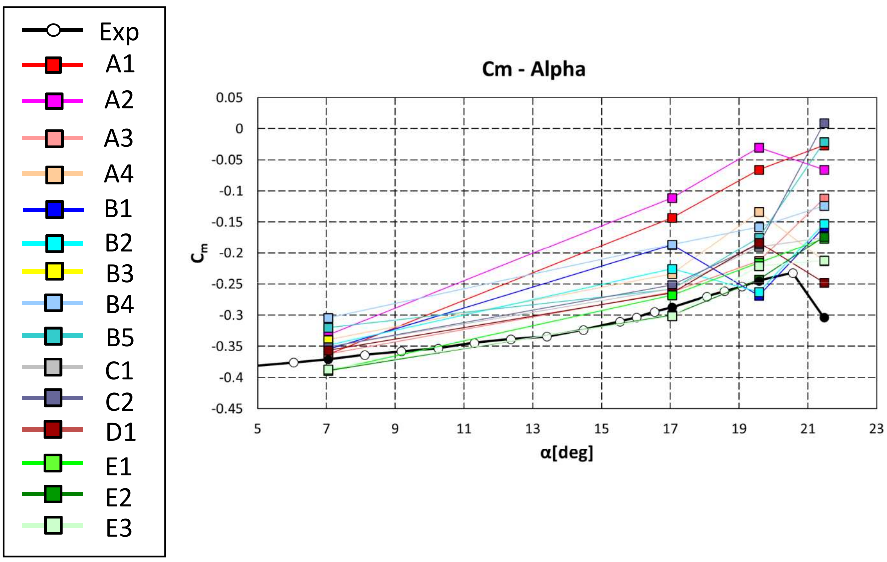

HLPW4
All Best-Practice Results
(03_GMGW3_HLPW4_RANS.pdf, p.17)

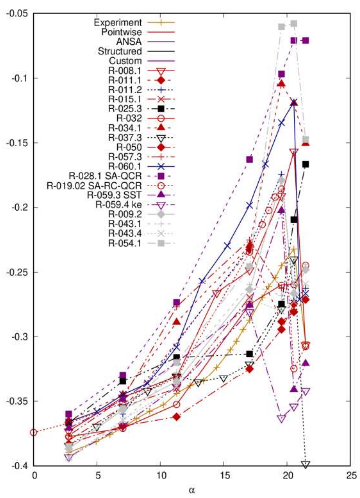

64

Q-Criterion Surface, X-Vorticity (Case 1, 7.05deg, Viewpoint 3)

ID-Grid(generated by)

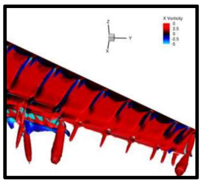
A1-HLPW4(MEGG3D)

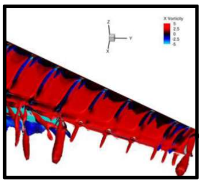
A2-HLPW4(MEGG3D)

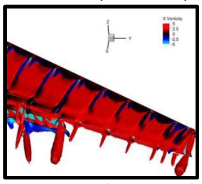
A3-HLPW4(MEGG3D)

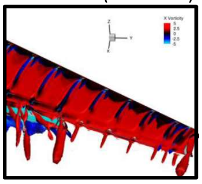
A4-HLPW4(MEGG3D)

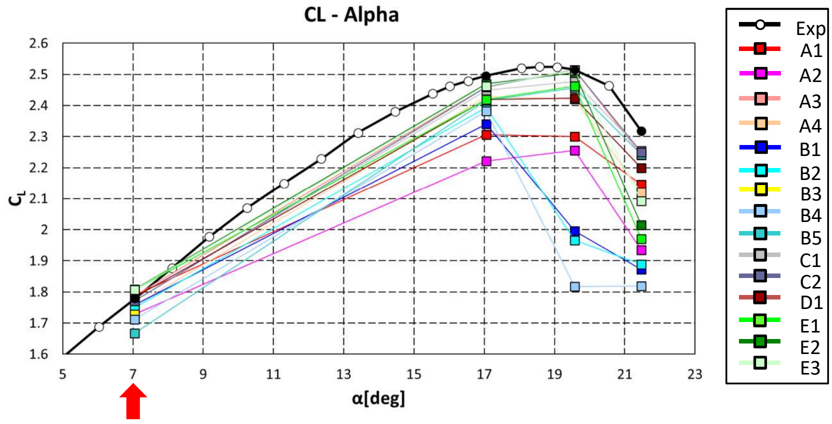

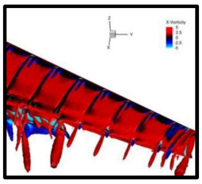
B1-HLPW4(MEGG3D)

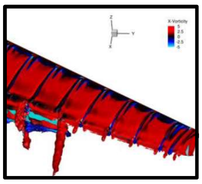
B2-HLPW4(Pointwise)

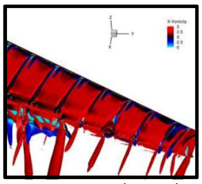
B3-HLPW4(ANSA)

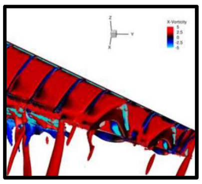
B4-Custom

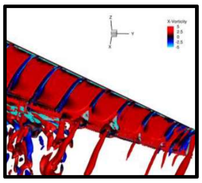
B5-Custom

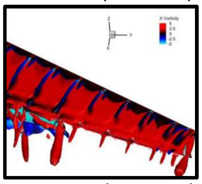
C1-HLPW4(MEGG3D)

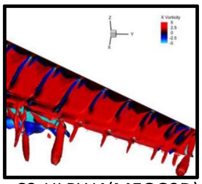
C2-HLPW4(MEGG3D)

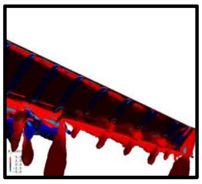
D1-Custom

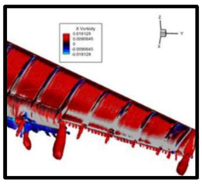
E1-Custom

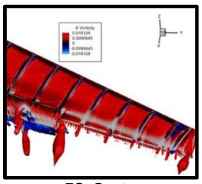
E2-Custom

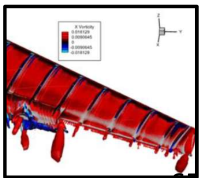
E3-Custom

65

Q-Criterion Surface, X-Vorticity (Case 1, 17.05deg, Viewpoint 3)

ID-Grid(generated by)

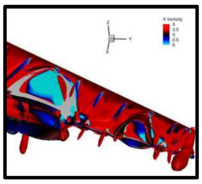
A1-HLPW4(MEGG3D)

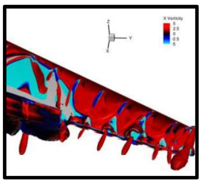
A2-HLPW4(MEGG3D)

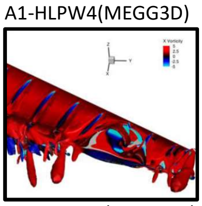
A3-HLPW4(MEGG3D)

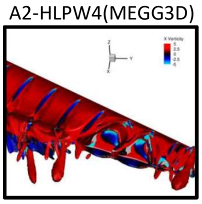
A4-HLPW4(MEGG3D)

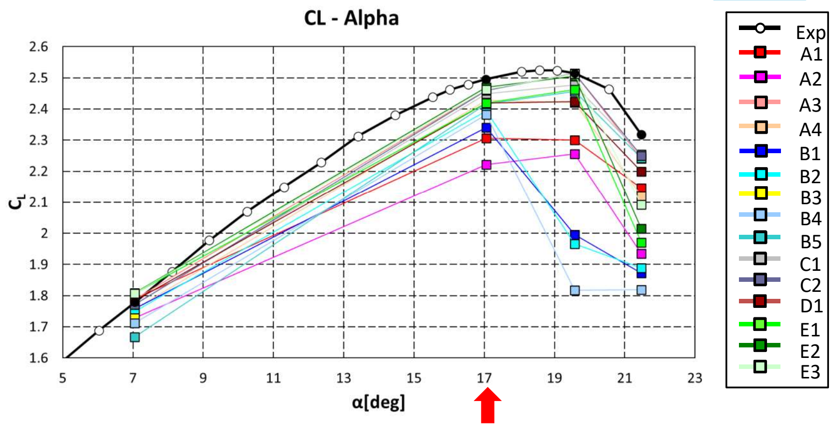

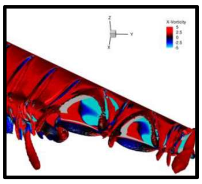
B1-HLPW4(MEGG3D)

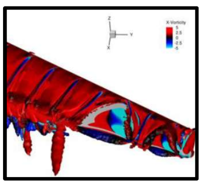
B2-HLPW4(Pointwise)

B3-HLPW4(ANSA)

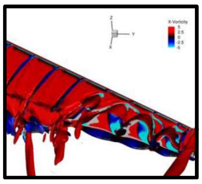
B4-Custom

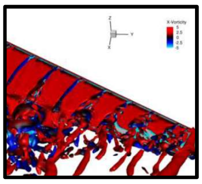
B5-Custom

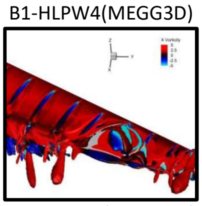
C1-HLPW4(MEGG3D)

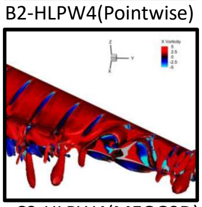
C2-HLPW4(MEGG3D)

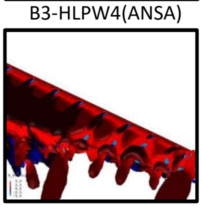
D1-Custom

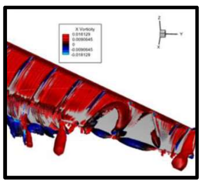
E1-Custom

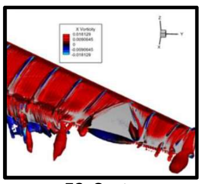
E2-Custom

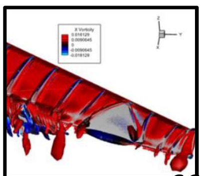
E3-Custom

66

Q-Criterion Surface, X-Vorticity（Case 1, 19.57deg, Viewpoint 3）

ID-Grid(generated by)

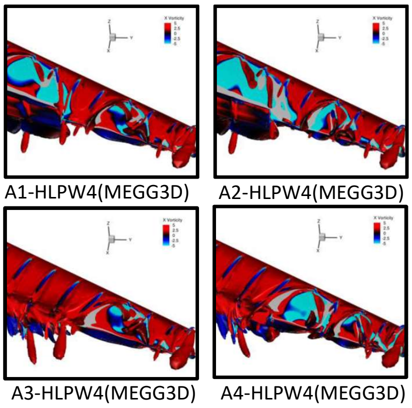

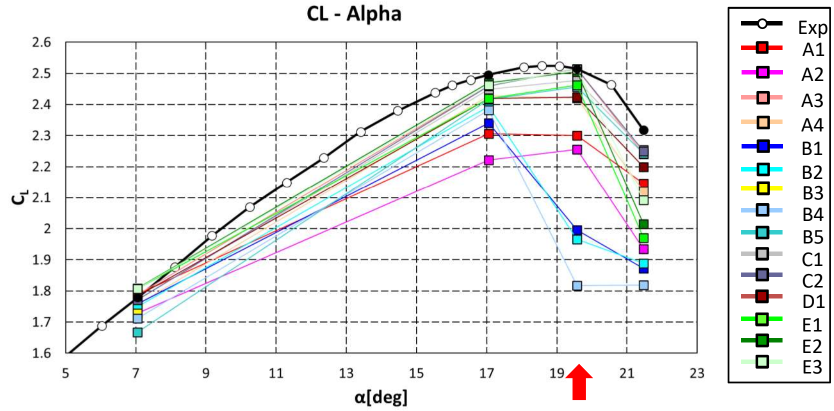

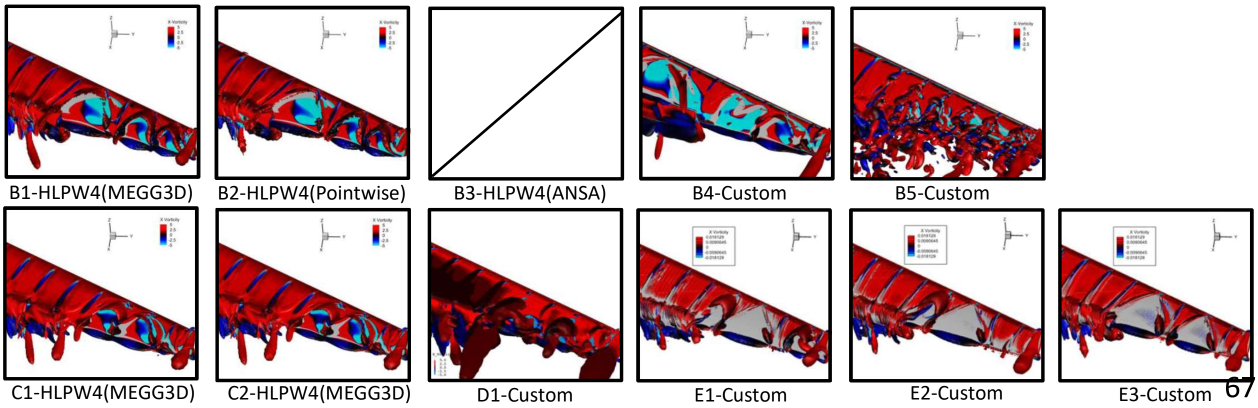

67

Q-Criterion Surface, X-Vorticity（Case 1, 21.47deg, Viewpoint 3）

ID-Grid(generated by)

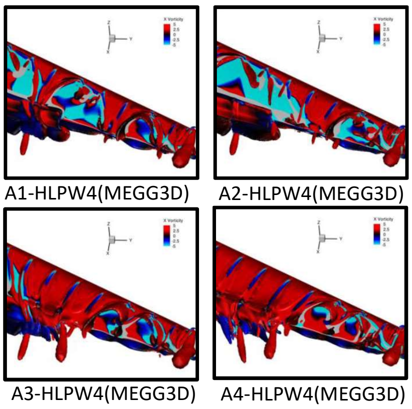

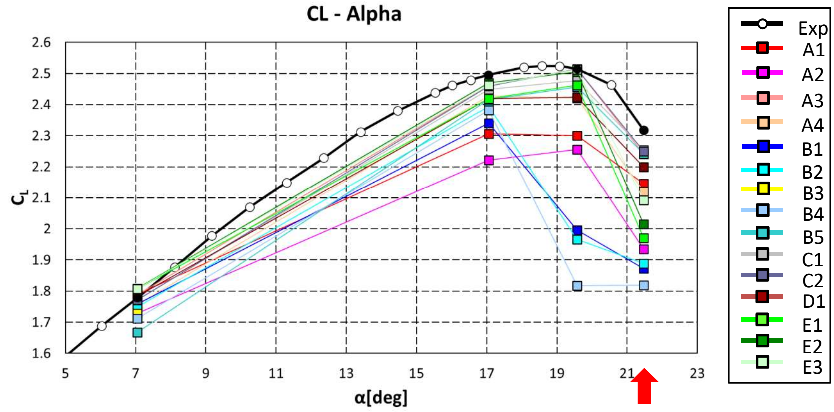

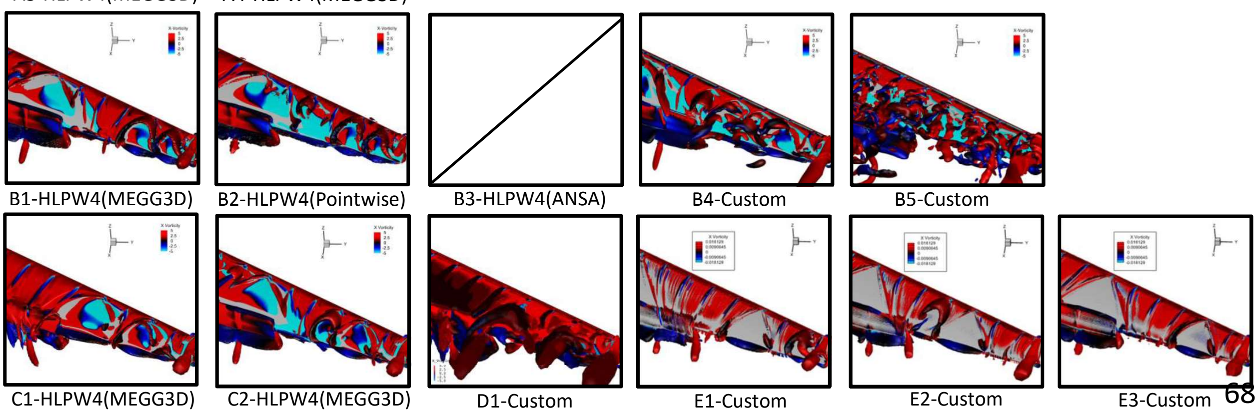

68

Q-Criterion Surface, Lscale (Case 1, 7.05deg, Viewpoint 3)

ID-Grid(generated by)

Lscale = $\sqrt[3]{\text{Cell-Volume}}$ [m]

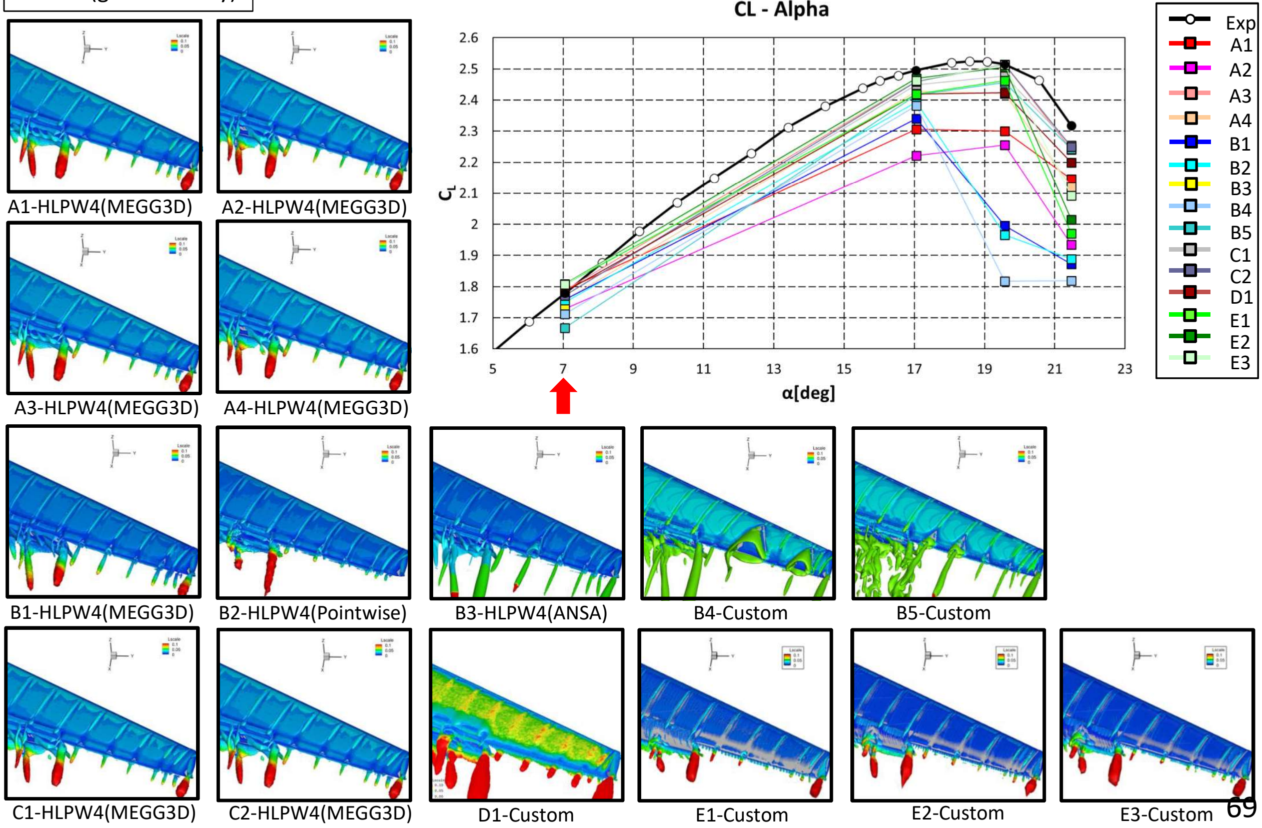

69

Q-Criterion Surface, Lscale (Case 1, 17.05deg, Viewpoint 3)

ID-Grid(generated by)

Lscale = $\sqrt[3]{\text{Cell-Volume}}$ [m]

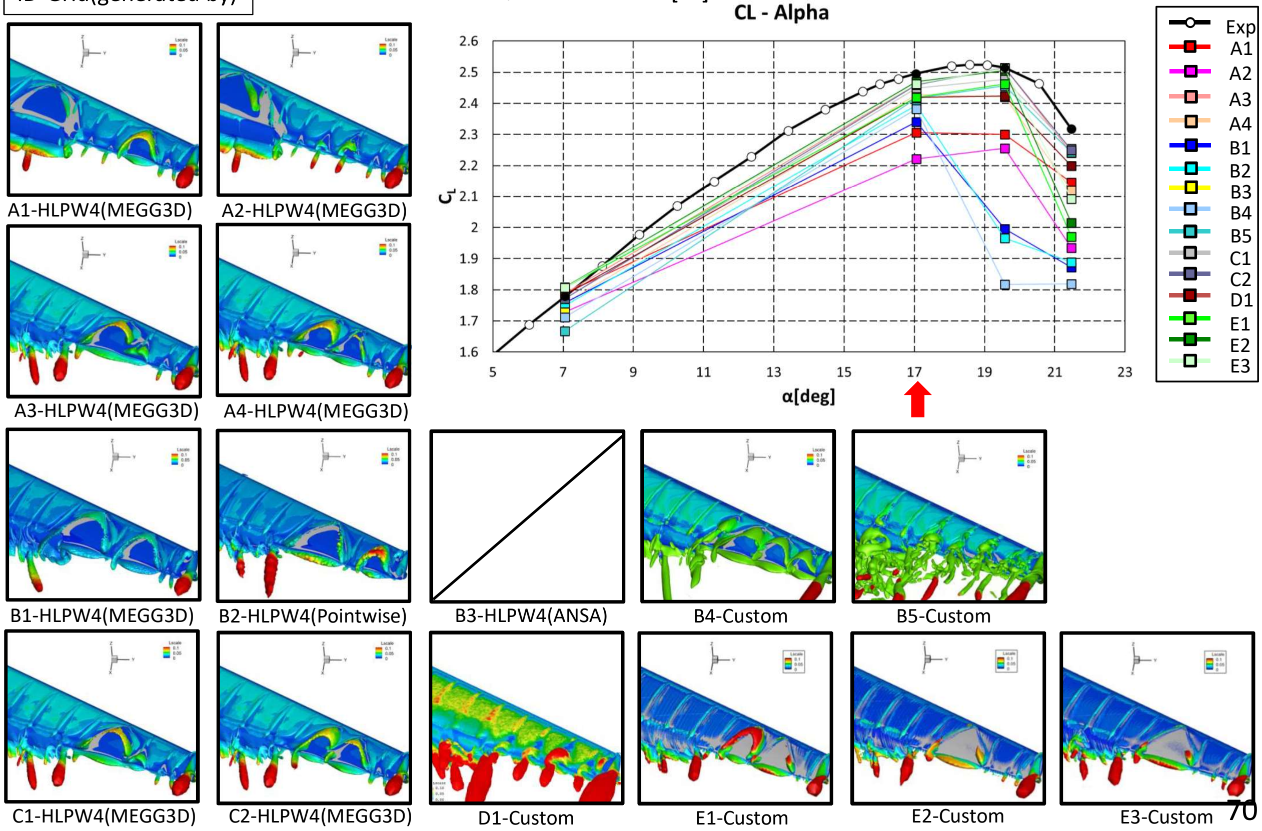

70

Q-Criterion Surface, Lscale（Case 1, 19.57deg, Viewpoint 3）

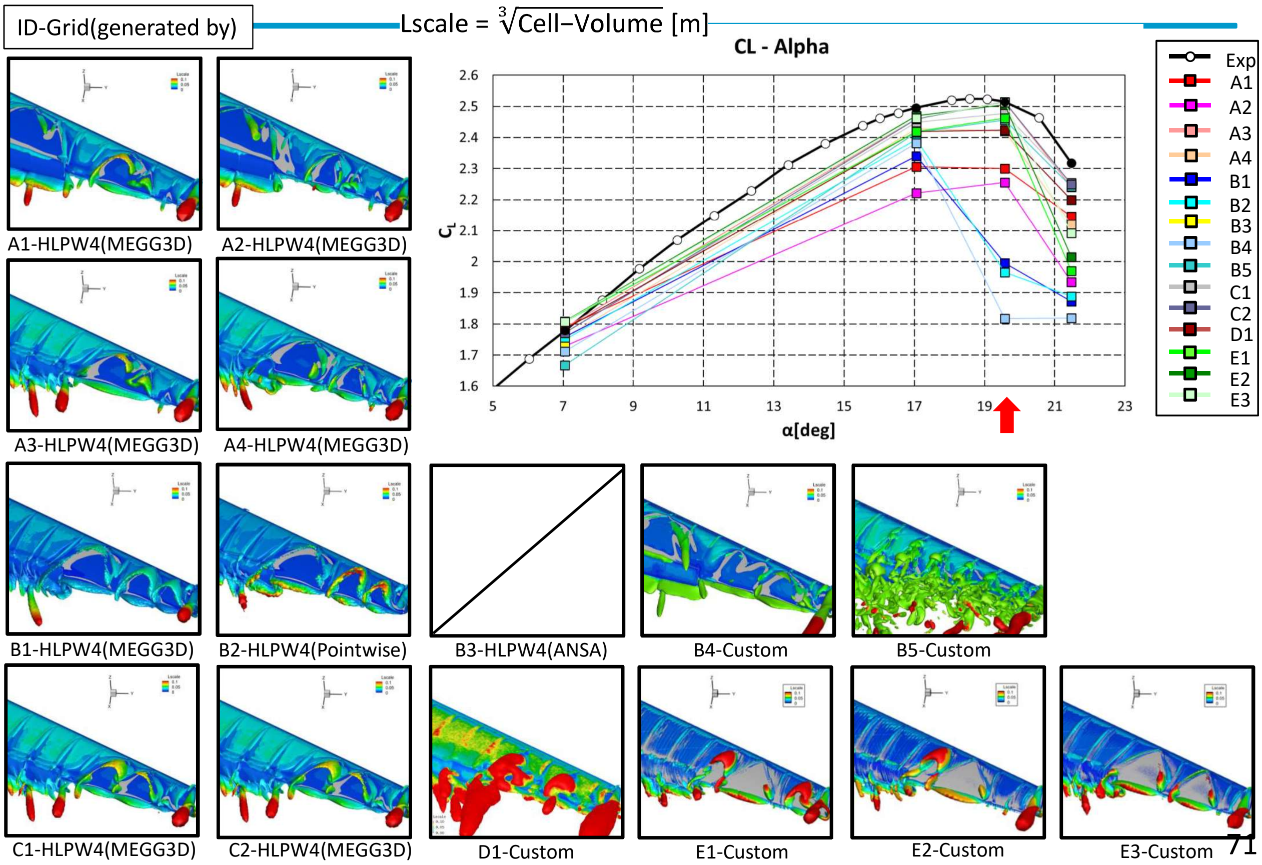

Q-Criterion Surface, Lscale（Case 1, 21.47deg, Viewpoint 3）

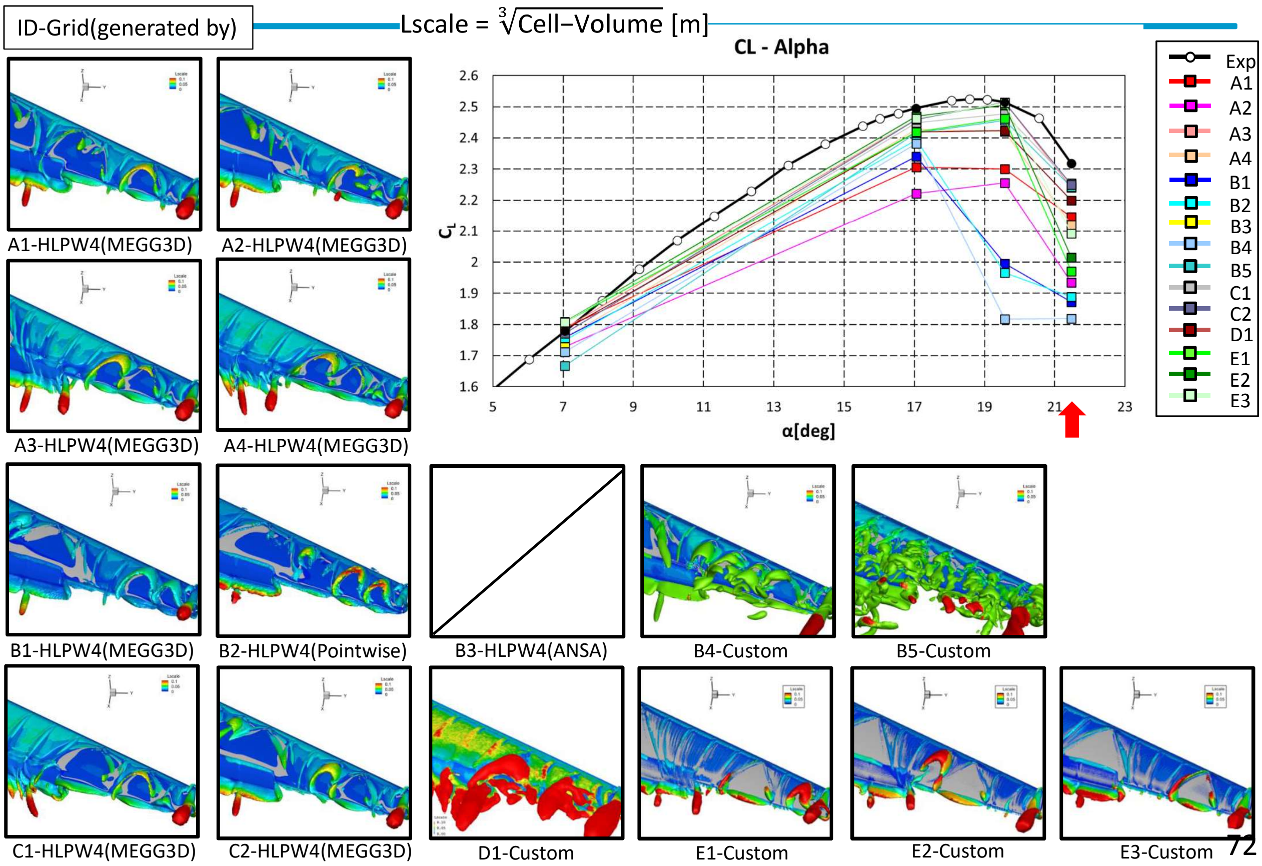

Q-Criterion Surface, X-Vorticity (Case 1, 7.05deg, Viewpoint 4)

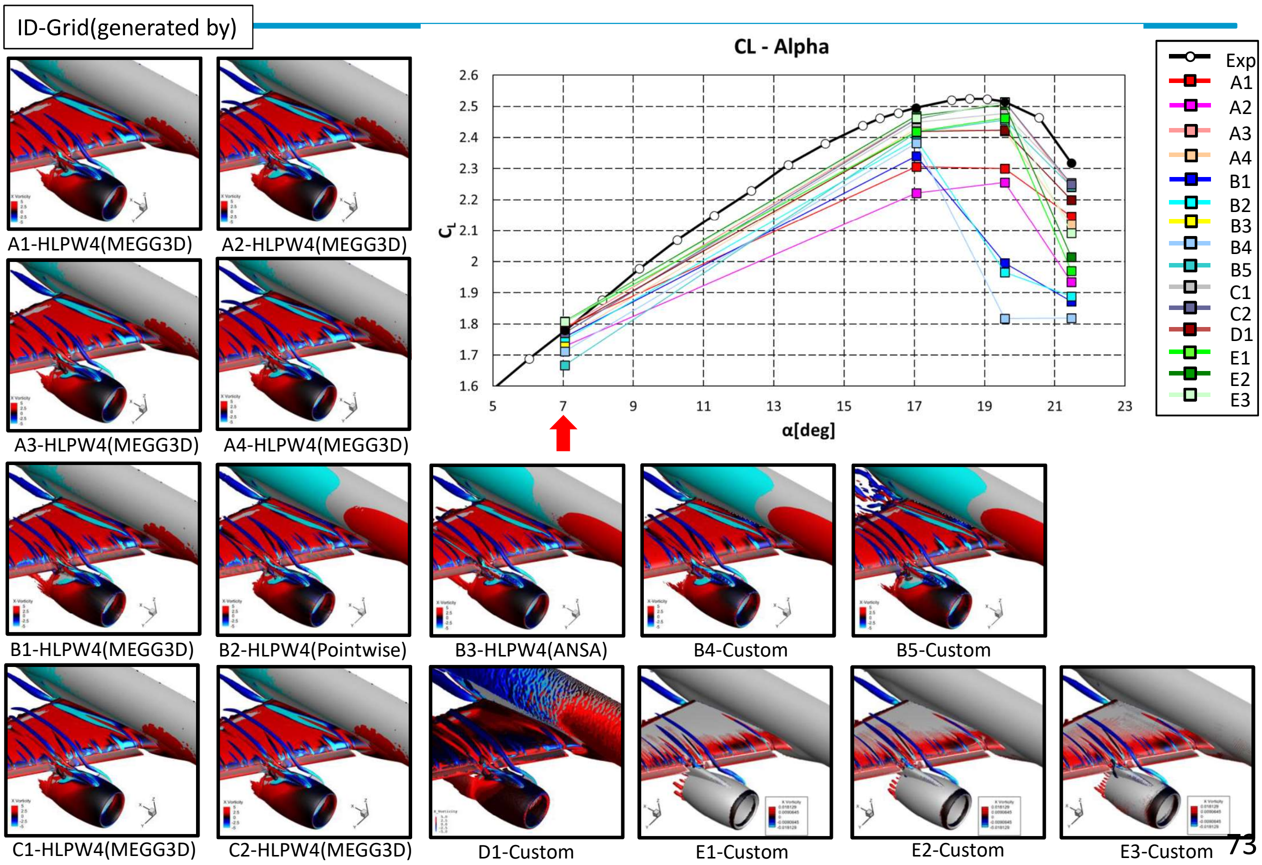

Q-Criterion Surface, X-Vorticity (Case 1, 17.05deg, Viewpoint 4)

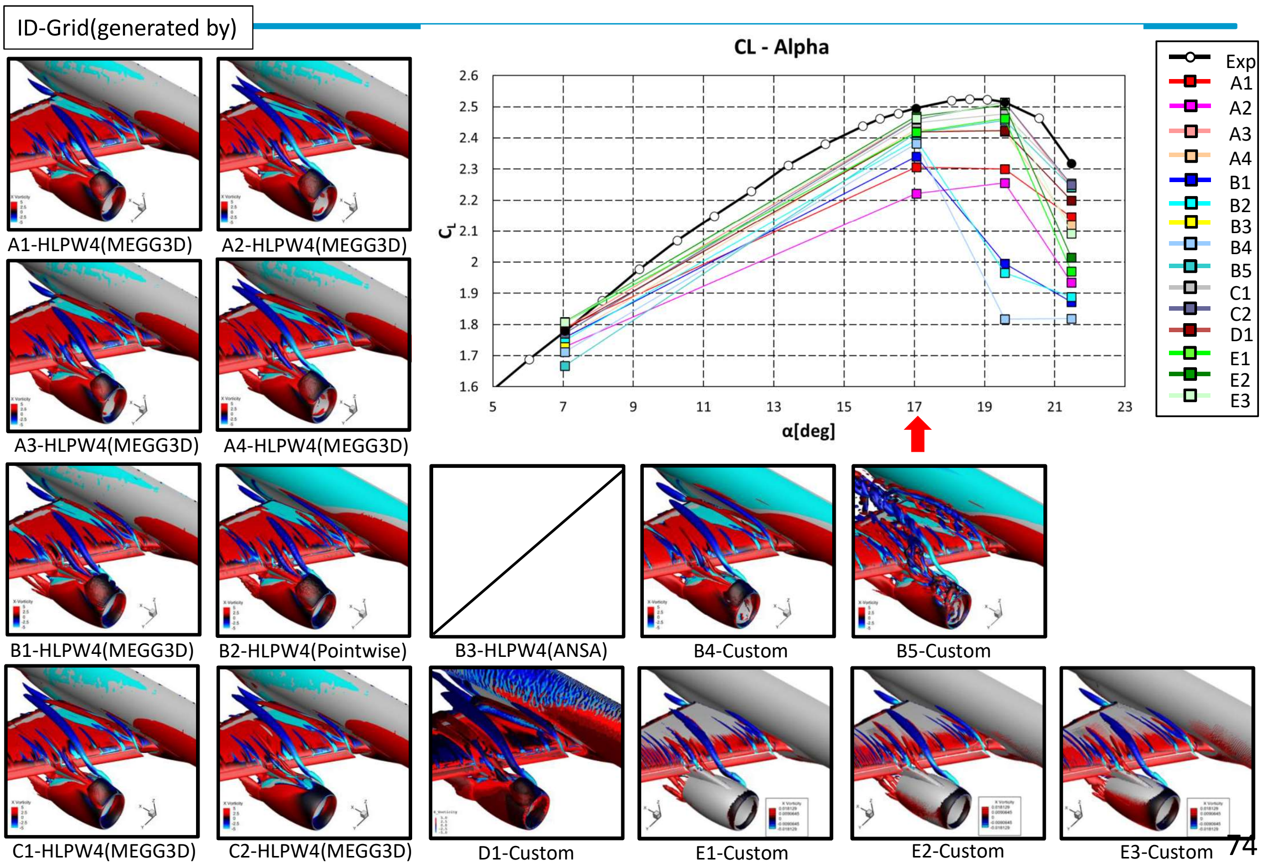

Q-Criterion Surface, X-Vorticity（Case 1, 19.57deg, Viewpoint 4）

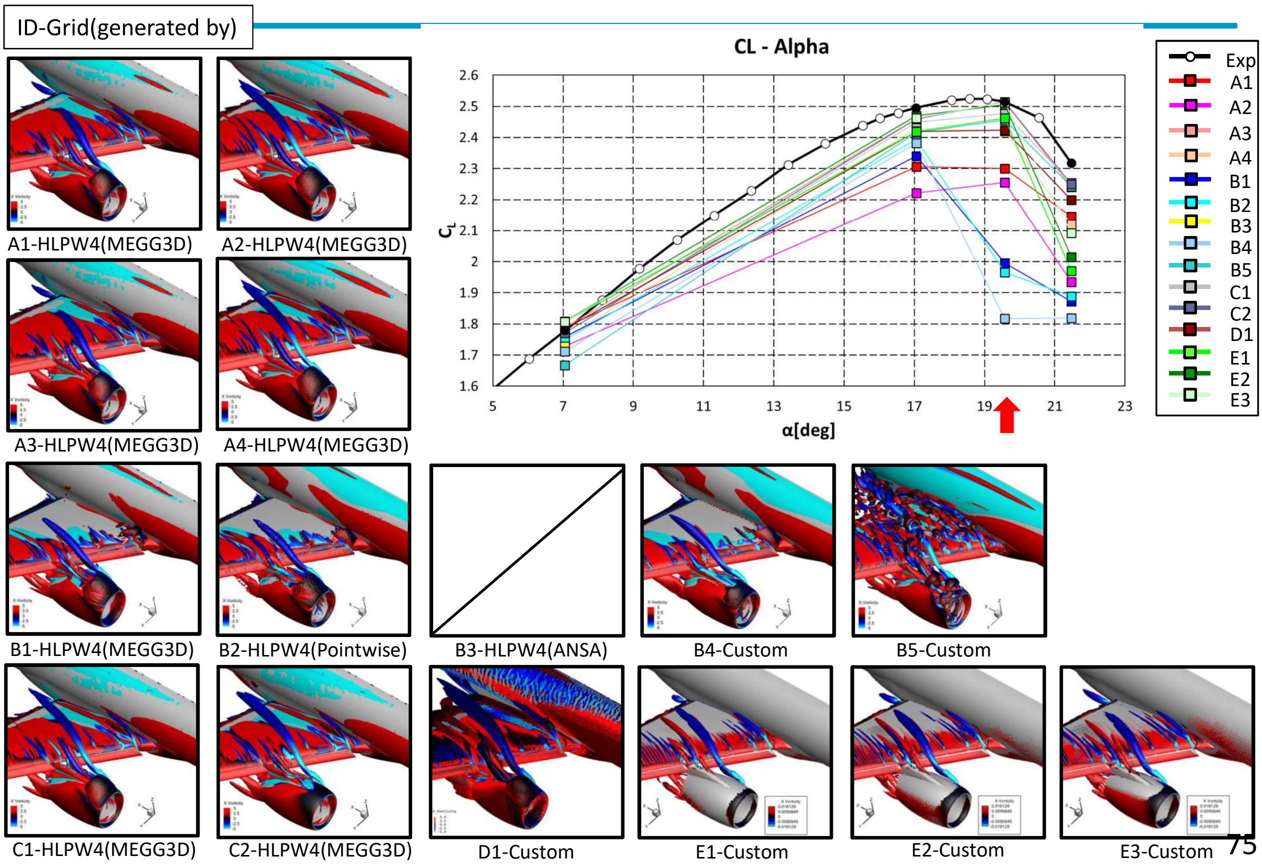

75

Q-Criterion Surface, X-Vorticity（Case 1, 21.47deg, Viewpoint 4）

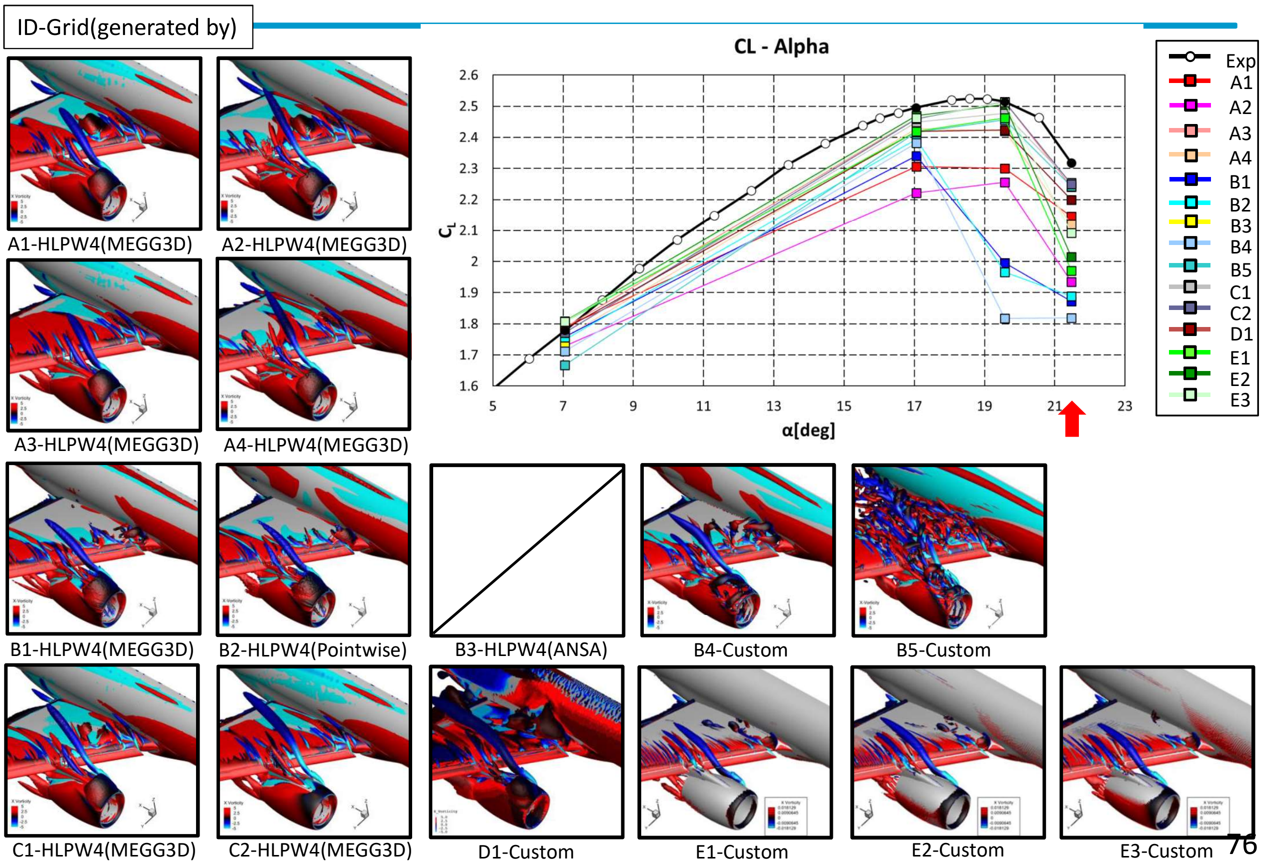

76

Q-Criterion Surface, Lscale（Case 1, 7.05deg, Viewpoint 4）

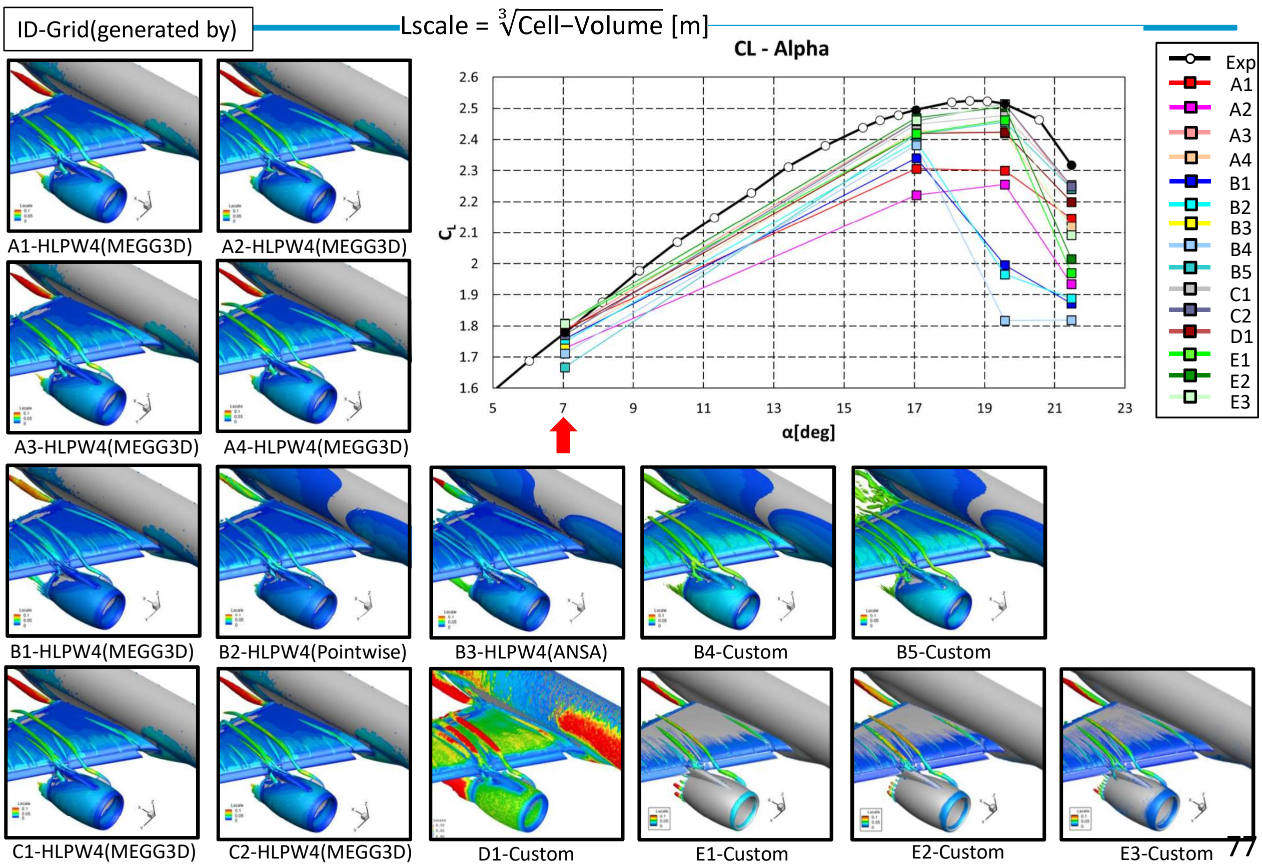

Q-Criterion Surface, Lscale（Case 1, 17.05deg, Viewpoint 4）

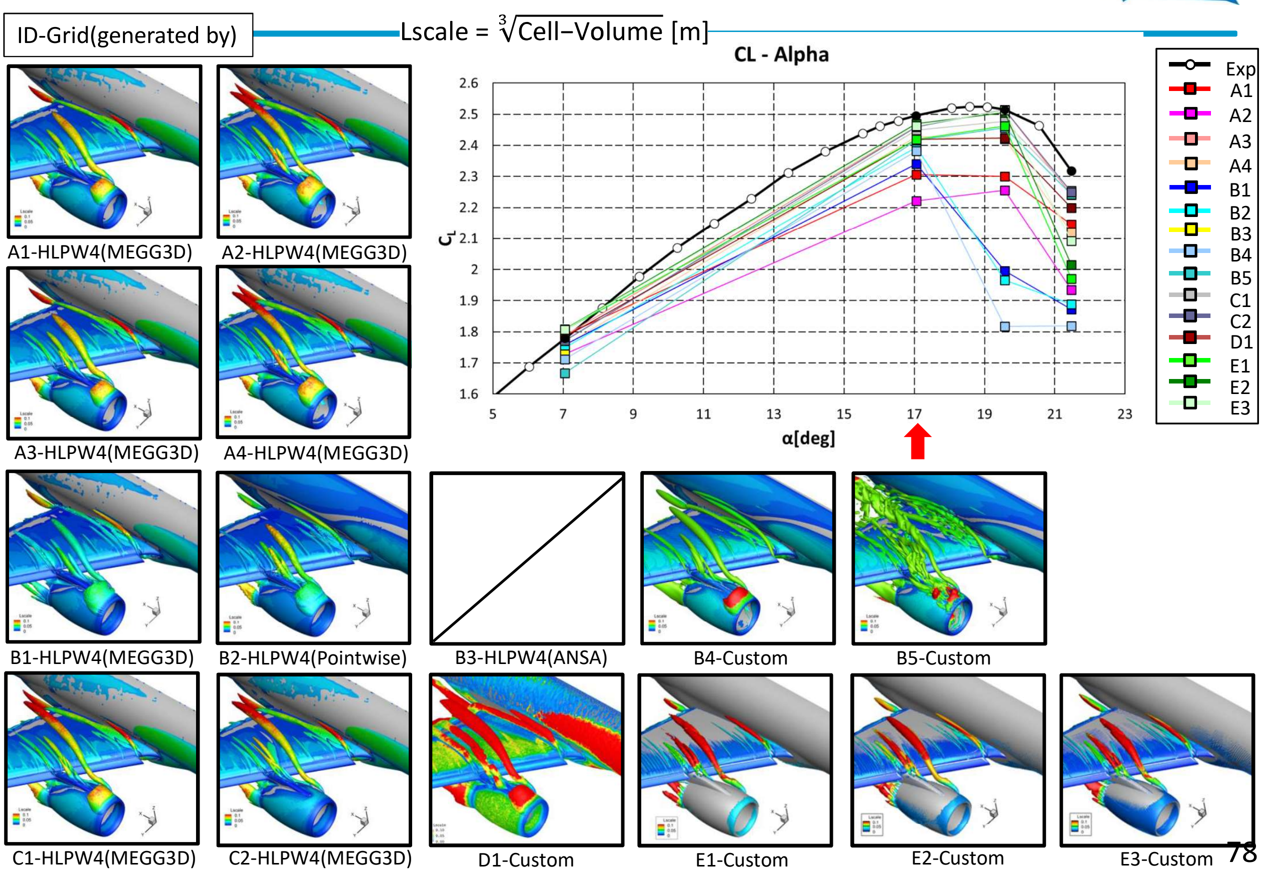

Q-Criterion Surface, Lscale（Case 1, 19.57deg, Viewpoint 4）

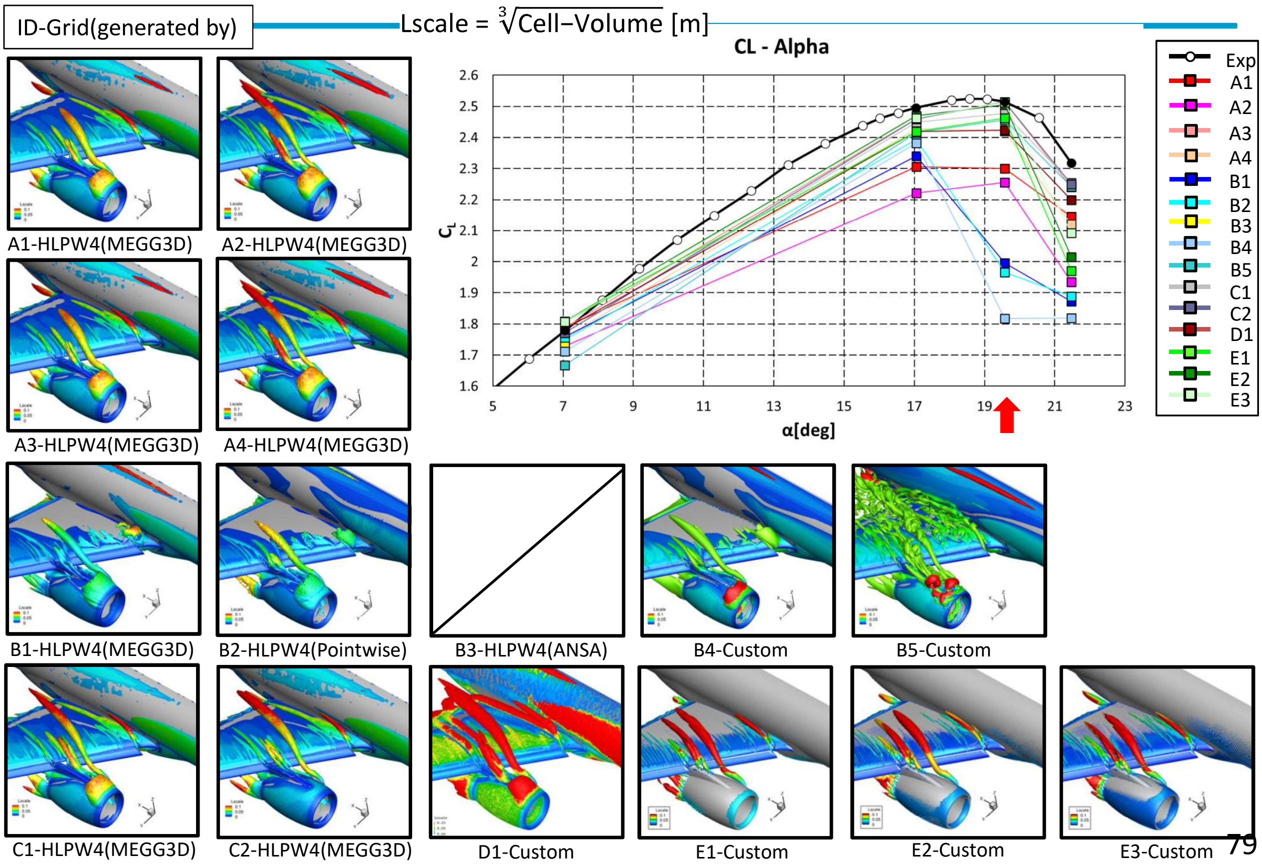

Q-Criterion Surface, Lscale（Case 1, 21.47deg, Viewpoint 4）

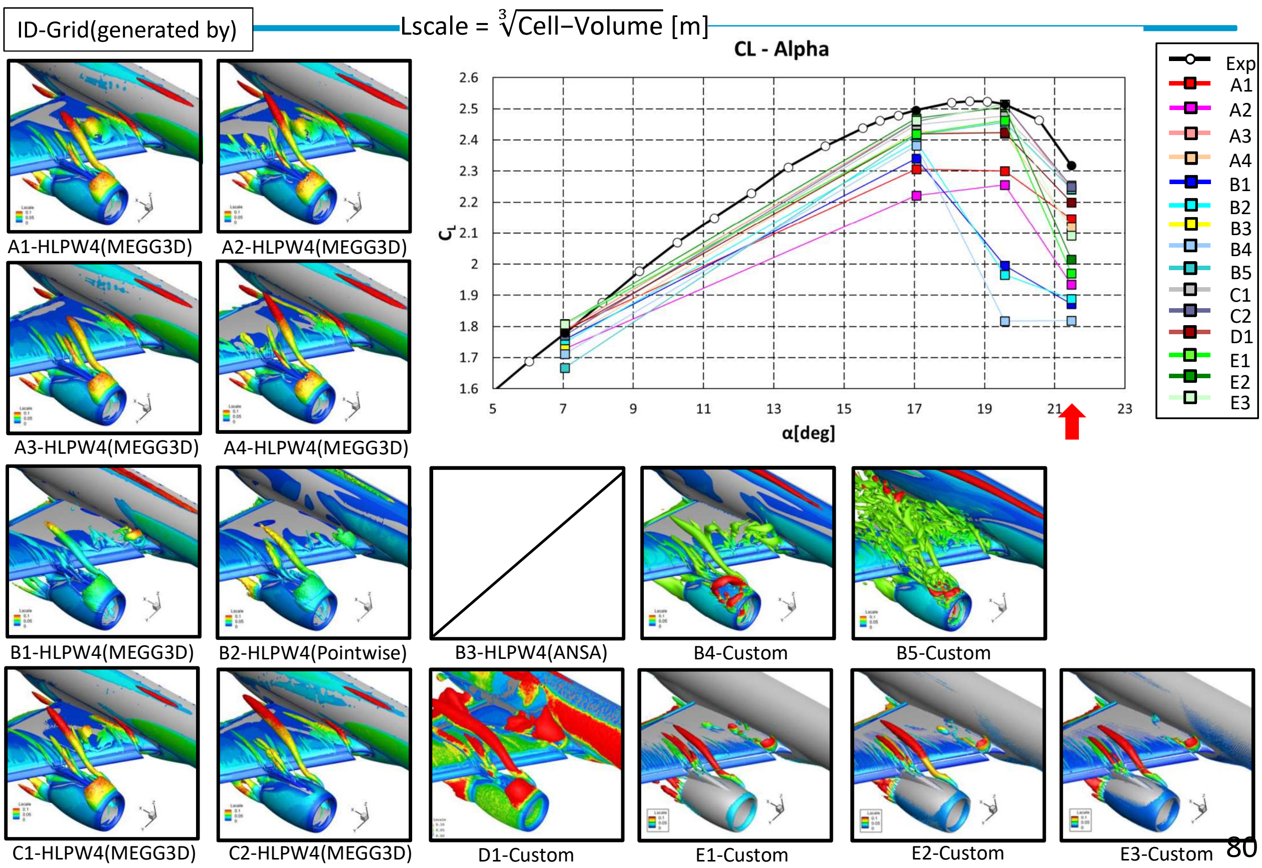

Q-Criterion Surface, X-Vorticity（Case 1, 7.05deg, Viewpoint 5）

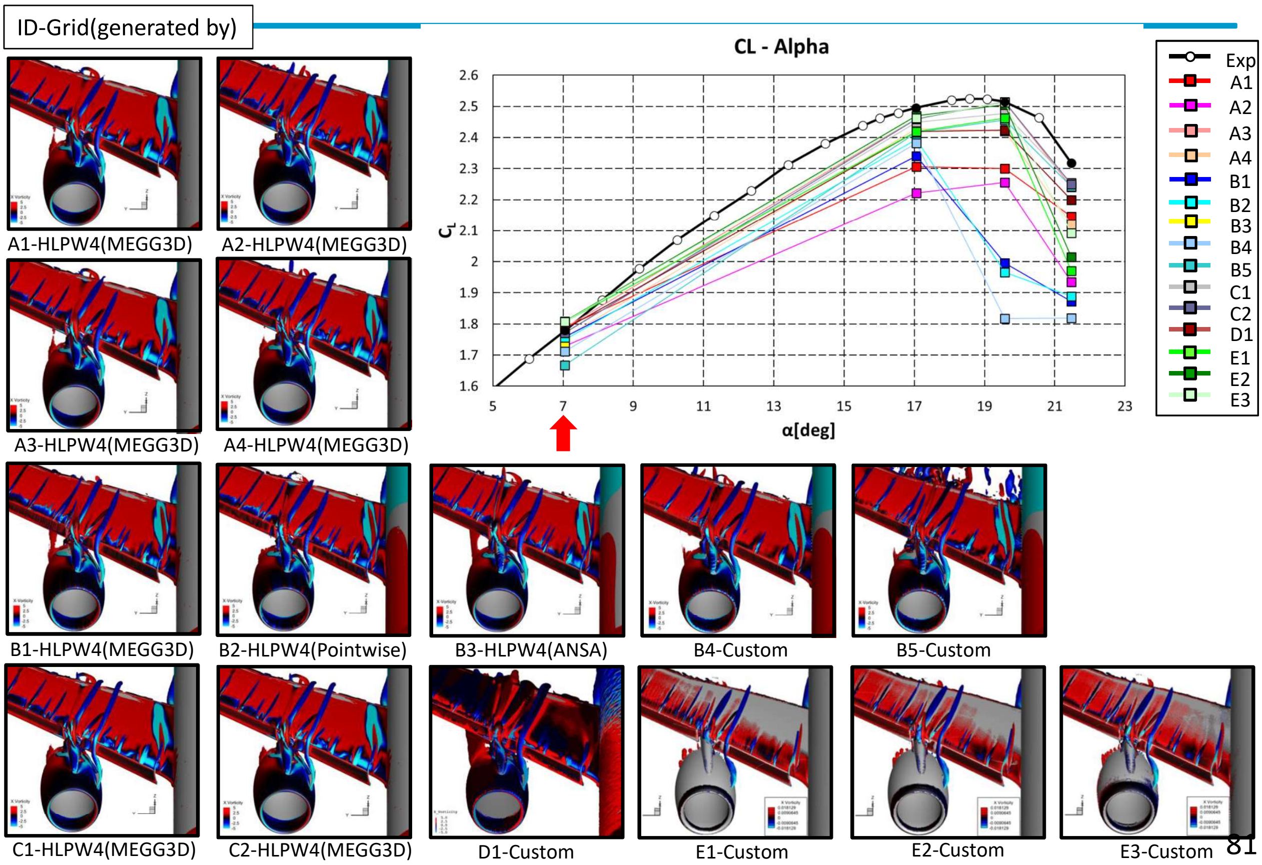

Q-Criterion Surface, X-Vorticity（Case 1, 17.05deg, Viewpoint 5）

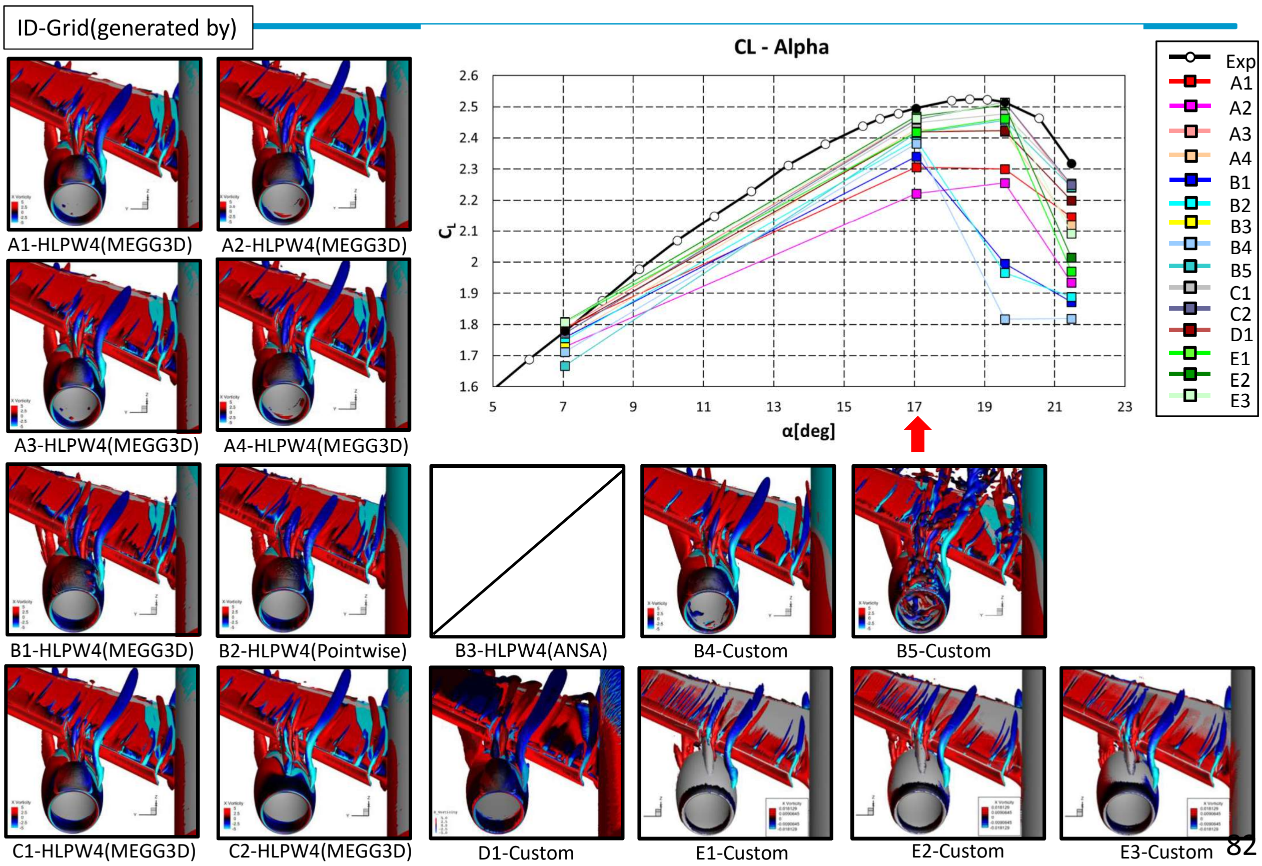

Q-Criterion Surface, X-Vorticity（Case 1, 19.57deg, Viewpoint 5）

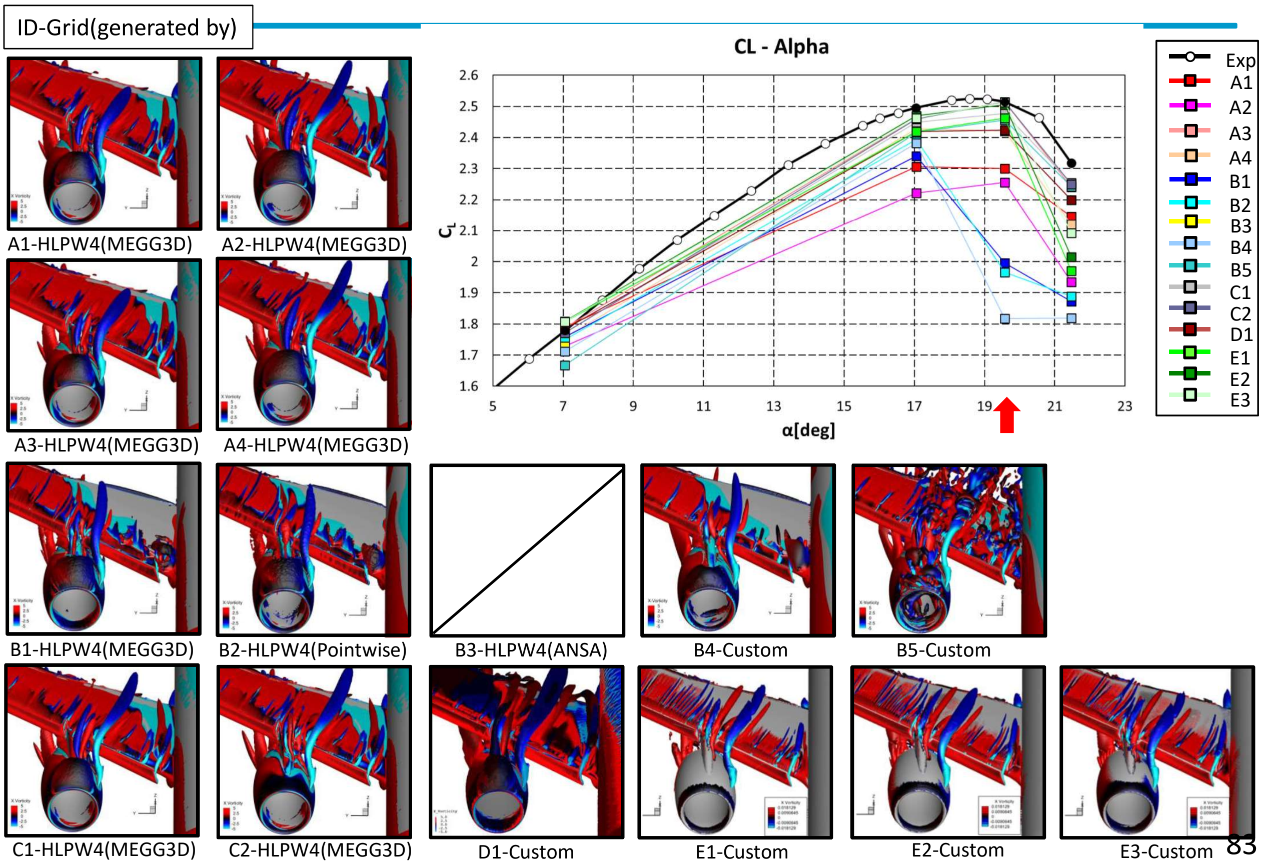

Q-Criterion Surface, X-Vorticity（Case 1, 21.47deg, Viewpoint 5）

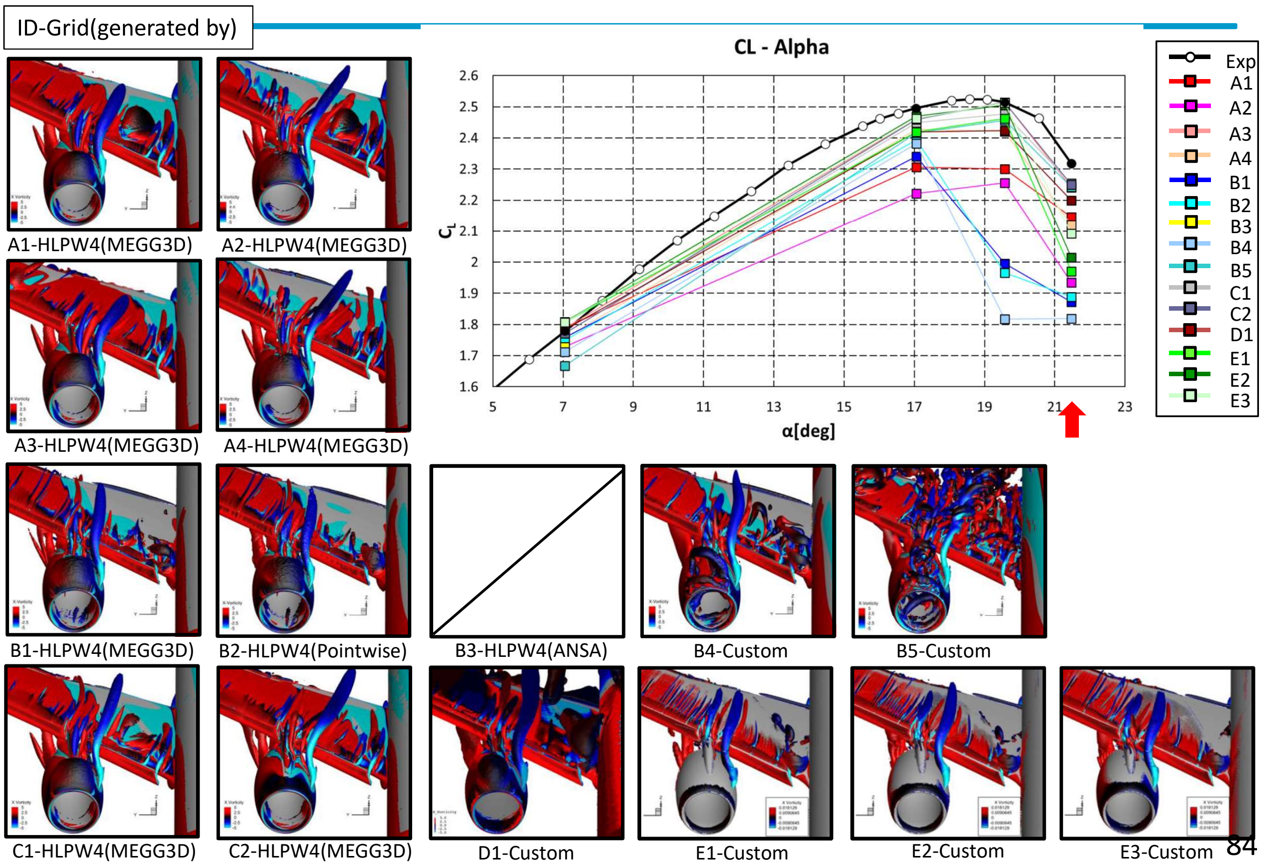

Q-Criterion Surface, Lscale（Case 1, 7.05deg, Viewpoint 5）

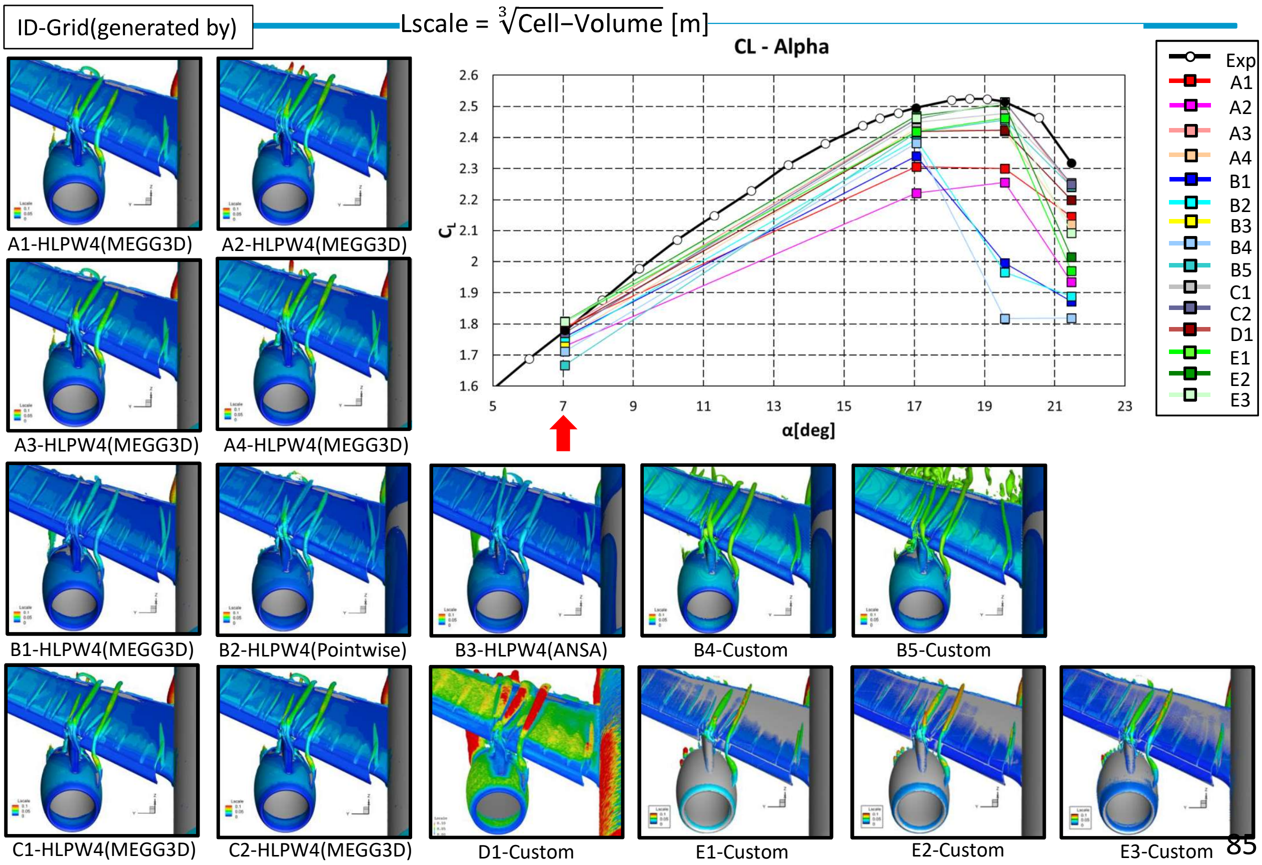

Q-Criterion Surface, Lscale（Case 1, 17.05deg, Viewpoint 5）

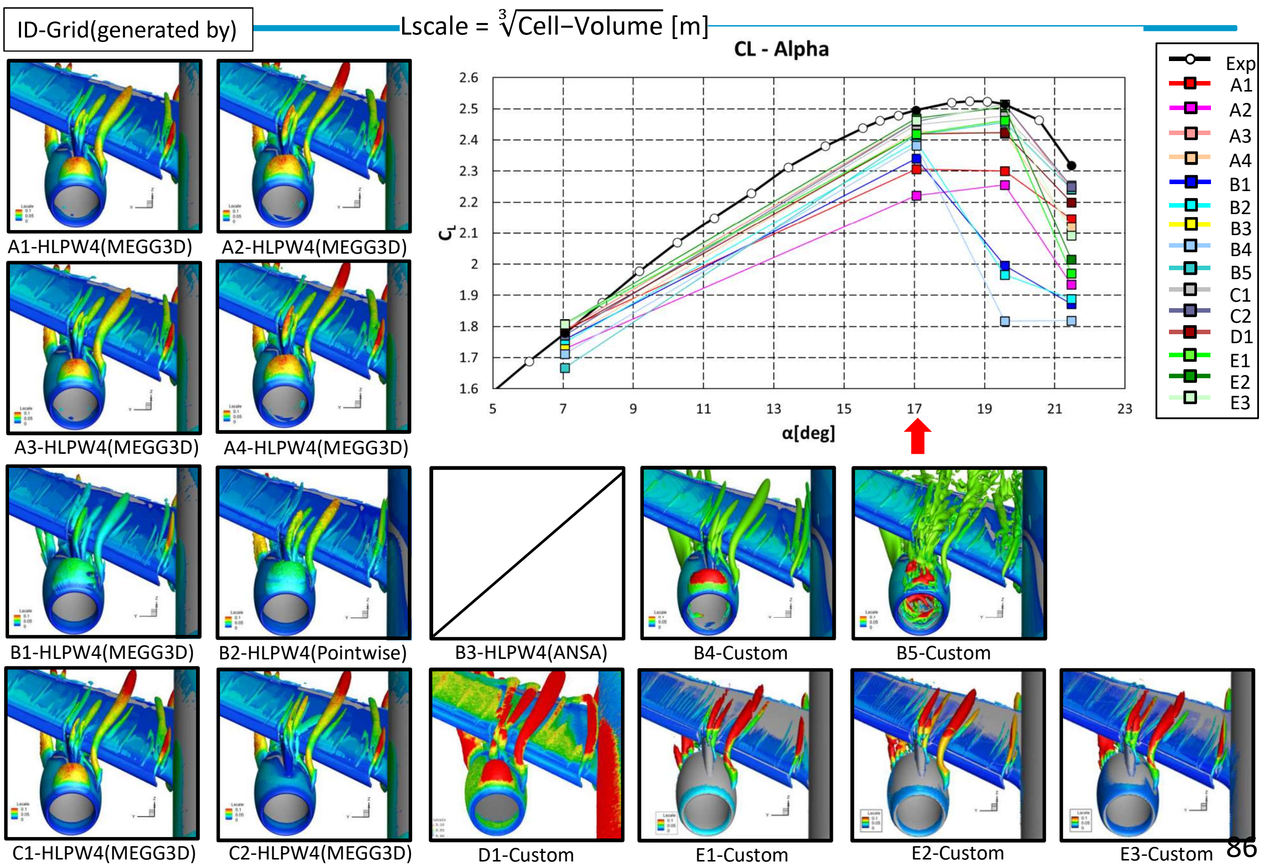

Q-Criterion Surface, Lscale（Case 1, 19.57deg, Viewpoint 5）

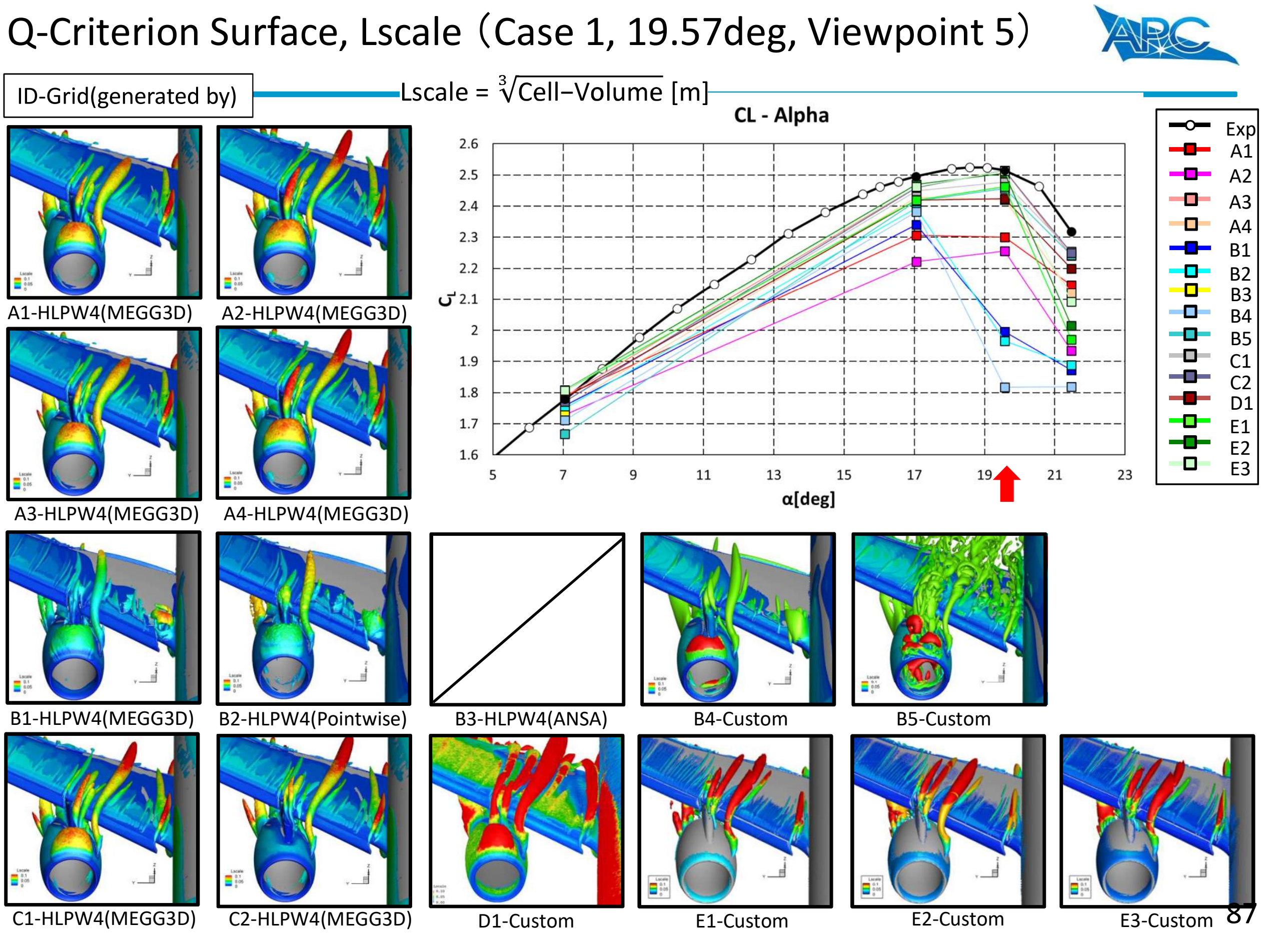

87

Q-Criterion Surface, Lscale（Case 1, 21.47deg, Viewpoint 5）

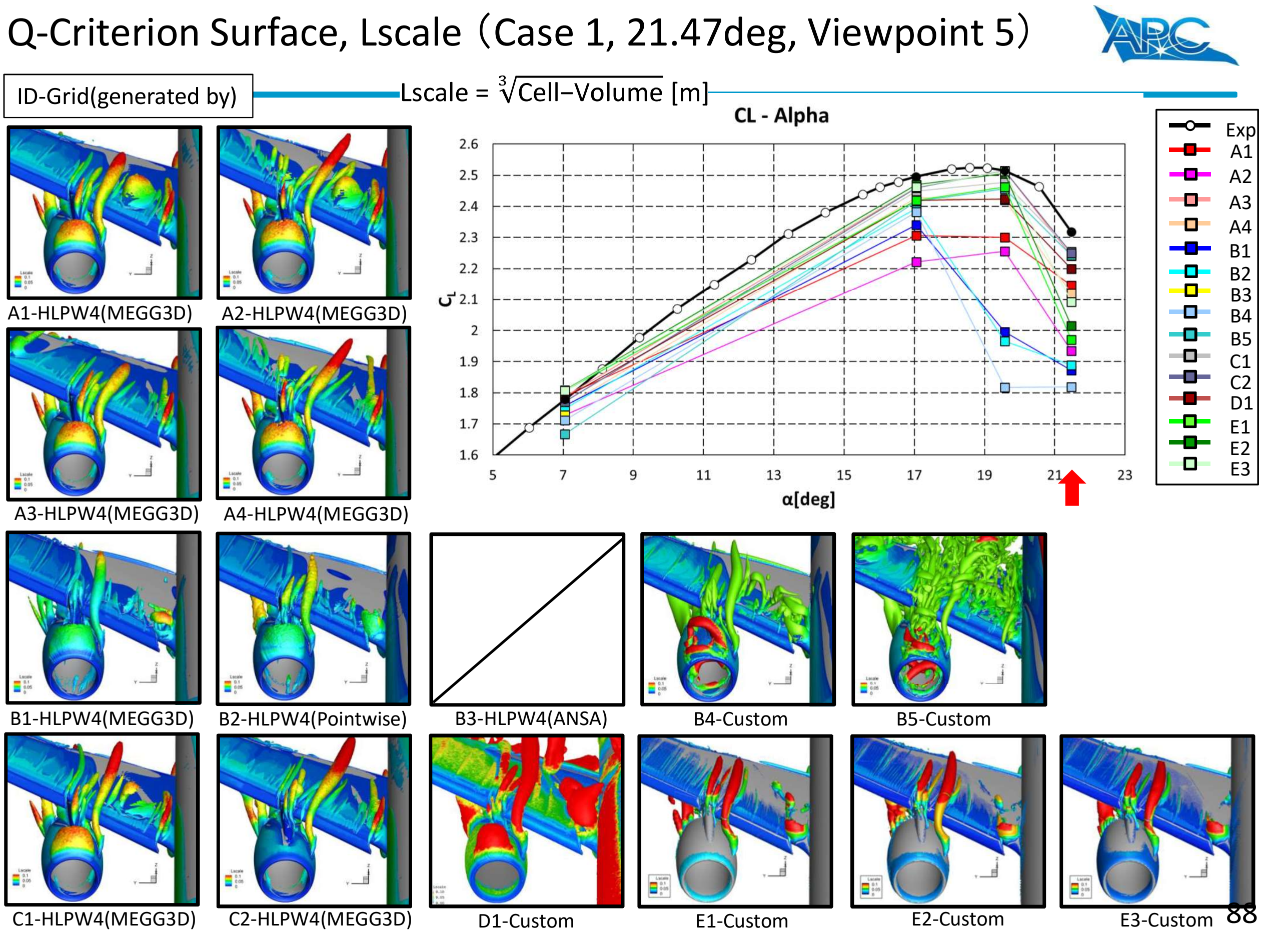

88

Wall-streamtraces, Cf (Case 1, 7.05deg, Viewpoint 6)

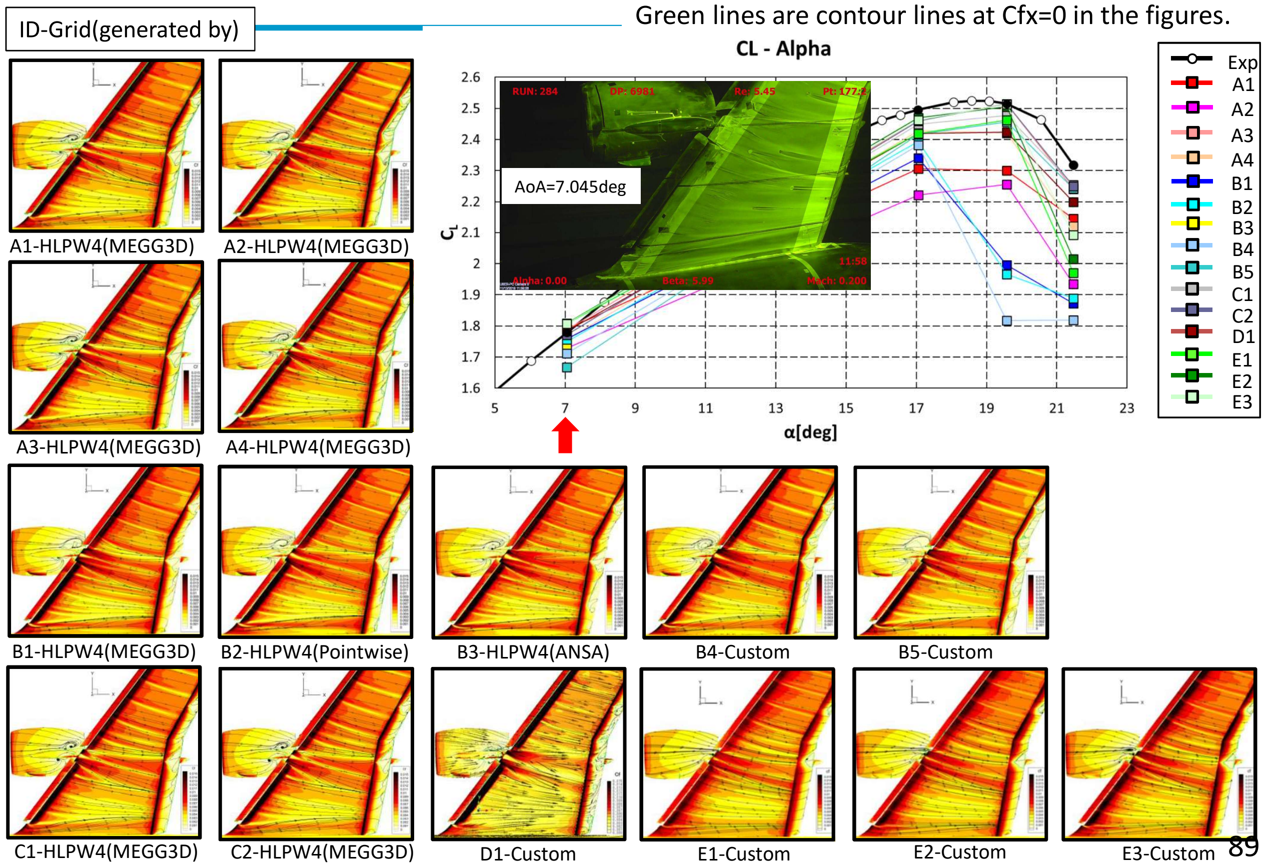

89

Wall-streamtraces, Cf (Case 1, 17.05deg, Viewpoint 6)

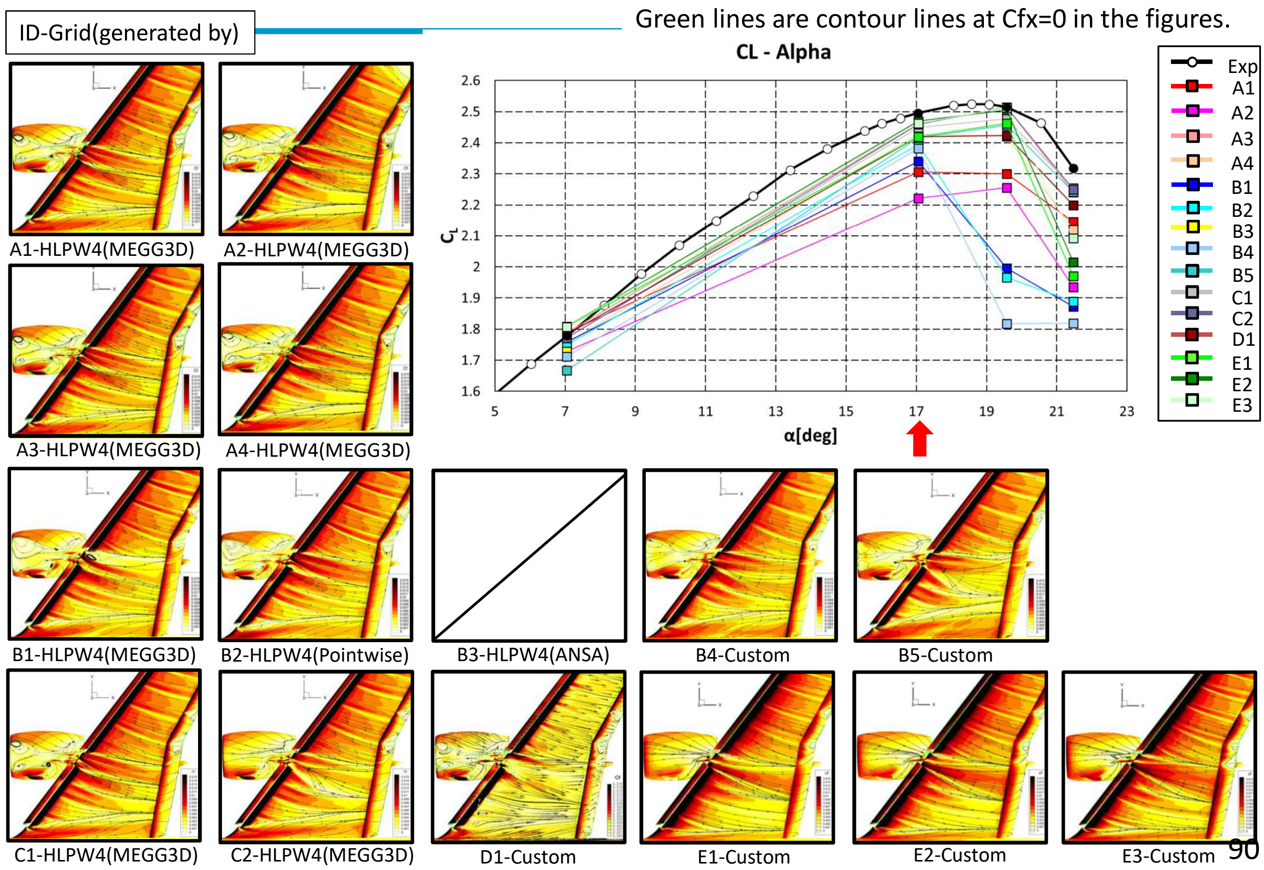

90

Wall-streamtraces, Cf（Case 1, 19.57deg, Viewpoint 6）

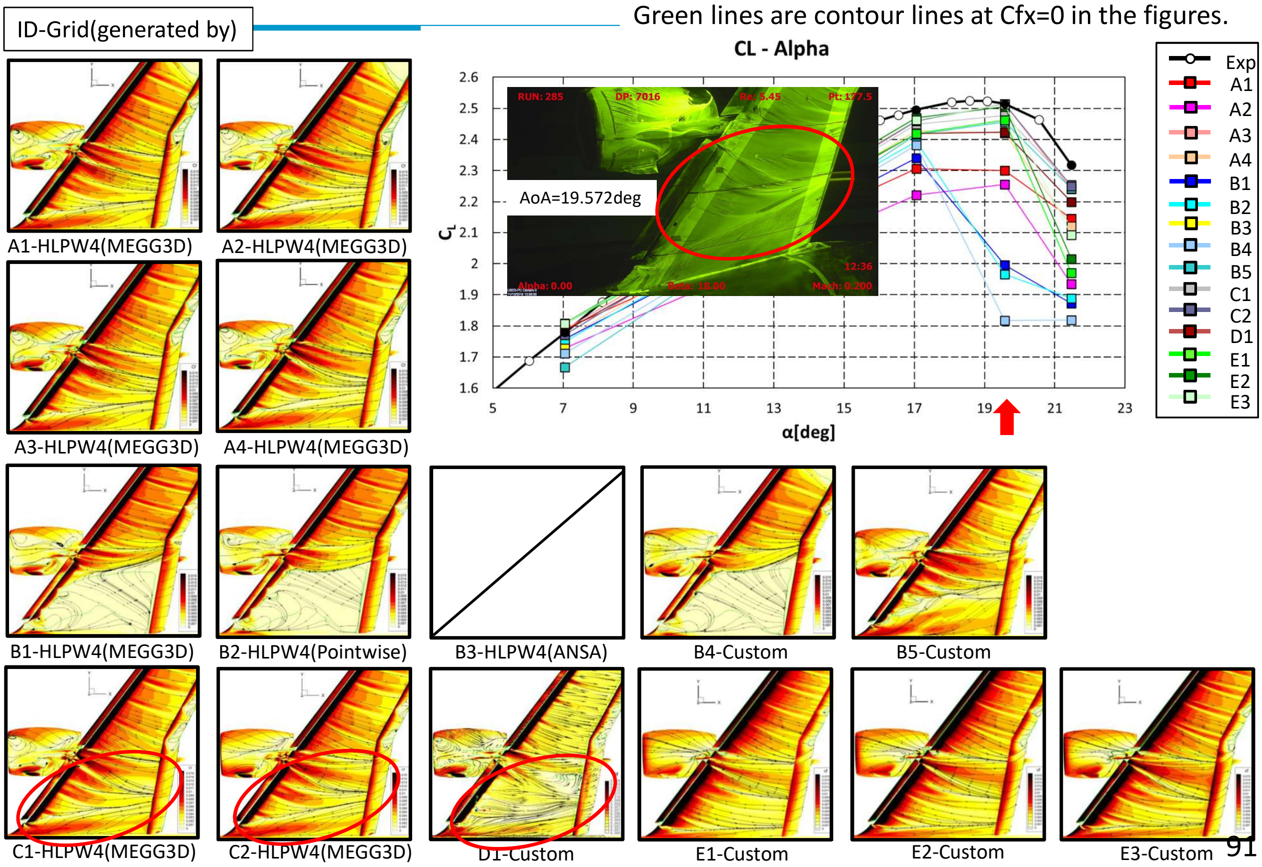

Wall-streamtraces, Cf（Case 1, 21.47deg, Viewpoint 6）

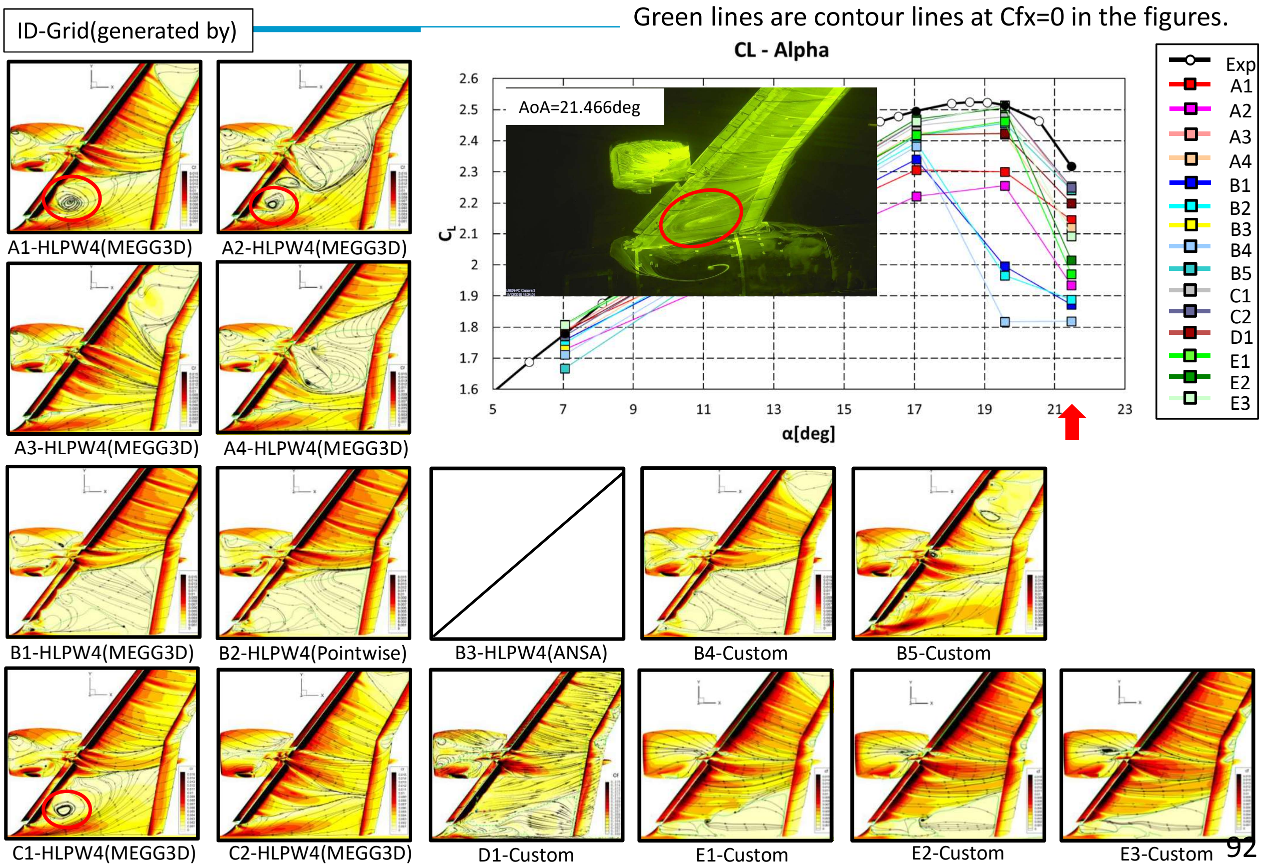

宇宙航空研究開発機構特別資料　JAXA-SP-22-003
JAXA Special Publication

Eighth Aerodynamics Prediction Challenge（APC-8）

発　　　　行　国立研究開発法人宇宙航空研究開発機構（JAXA）
〒182-8522　東京都調布市深大寺東町7-44-1
URL: https://www.jaxa.jp/
発　行　日　2022年12月23日
電子出版制作　松枝印刷株式会社

宇宙航空研究開発機構
Japan Aerospace Exploration Agency